NASA Contractor Report 3402

Determination of Physical and Chemical States of Lubricants in Concentrated Contacts - Part 2

James L. Lauer

GRANT NSG-3170
FEBRUARY 1981

NASA

NASA Contractor Report 3402

Determination of Physical and Chemical States of Lubricants in Concentrated Contacts - Part 2

James L. Lauer
Rensselaer Polytechnic Institute
Troy, New York

Prepared for
Lewis Research Center
under Grant NSG-3170

National Aeronautics
and Space Administration

**Scientific and Technical
Information Branch**

1981

TABLE OF CONTENTS

1. INTRODUCTION

The project whose setup phase was described in the earlier report [1] proceeded in two main directions: (i) correlation of fluid, especially traction fluid, behavior with spectroscopic properties, related, in turn, to molecular structure, and (ii) determination of at least one mechanism of lubricant failure in concentrated contacts. Data collection and interpretation constituted the bulk of the work.

It turned out that the most important experiments involved both traction and failure, for addition of substantial concentrations (5-20% by weight) of 1,1,2-trichlorethane to a traction fluid rapidly induced chemical changes followed by failure in a heavily stressed operating elastohydrodynamic contact. With smaller concentrations (~2%) chemical changes were not immediately noticeable, but significant physical changes--loss of traction, molecular orientation, changes of surface temperature were observed. The chemical changes agreed perfectly with a scheme proposed almost 20 years ago by Kovacic [2] and coworkers, i.e. ionically promoted and catalyzed unsaturation, aromatization, and polymerization by ferric chloride. An aromatic fluid, 5P4E polyphenyl ether, was rapidly attacked by chloride in lightly stressed contacts at freshly abraded surfaces and formed polymeric carbons by cross-linking, presumably as a consequence of aromatic anion formation, as visualized by Goldblatt [3]. Here too significant physical changes preceded catastrophic failure, when the chloride concentration was lower and the operating conditions less severe. These changes could be observed only with operating contacts--analogous experiments under stationary conditions could show similar chemical changes but might not provide realistic information on the parameters necessary for reaction, since the mechanical stresses, molecular orientations, very

large temperature gradients, etc., which occur in bearing contacts, could not be easily simulated. A series of experiments with different surfaces and conditions was therefore started and significant effects have already been found.

An interesting correlation was found between dichroic ratio (ratio of infrared band intensity emitted parallel and perpendicular to the direction of flow in a concentrated contact) and traction for a traction fluid. It would seem that in a heavily stressed contact the traction fluid could behave analogously to a stretched rubbery solid. Further work now in progress could provide useful clues on improved traction fluids.

A separate unit was built to measure traction under essentially the same conditions as those prevailing in the ball/plate apparatus coupled to the infrared emission spectrophotometer. Furthermore, thanks to the generosity of the Central Research Department of the Du Pont Company, Wilmington, Delaware, it was possible to begin setting up another Fourier emission spectrophotometer with a step drive and a rotating polarizing filter. It is expected that this unit will provide greater sensitivity and faster data-generating capability.

As in the past, some of the work reported here was also supported by a grant from the Air Force Office of Scientific Research (AFOSR-78-3473).

2. APPARATUS

2.1 New Ball/Plate Apparatus

The apparatus shown in Figure 1 used the geometry of Winer [4] and co-workers, i.e. the plate (window) is in a horizontal plane above and tangential to the ball rotating about a horizontal axis, rather than the geometry of the contact interfaced with our spectrometer, in which the plate (window) is in a horizontal plane below the axis of rotation. The reason for the difference is the need to provide ready optical access through a large (two-inch) diameter sapphire window to read and photograph through a microscope Newton's rings for film thickness measurements, to photograph the fluorescence of the contact region for the generation of a temperature map (the fluorescence decreases with increased temperature) and to record fluorescence spectra. Especially for fluorescence work a large window is necessary, since ready access must be available to the exciting radiation.

However, one of the main design considerations for this apparatus involved the measurement of traction. Since facilities for heating or cooling were incorporated into the rectangular box under the ball, from which the lubricant is dragged into the contact region by the rotating ball, it appeared to be more practical to allow the plate holding the sapphire window to slide rather than the entire reservoir, as in Winer's design. Since the plate must also be loaded, the present design features a sliding plate within the loading plate; in other words, the window can slide tangentially to the ball and in a horizontal plane, since it is mounted on tracks attached to the larger loading plate. Motion along the tracks is essentially without friction since sliding bearings ("super" ball bushings) are used as intermediates. The window motion is restrained by a sheet-metal leaf spring to which a strain gauge is attached which, in turn, is connected to another gauge (the reference gauge attached

to the platform) so that only the output difference is read by a meter. The meter readings were calibrated for known conditions and constitute our "tractions".

Other features of the apparatus are the belt drive--to avoid vibrations in the contact region--, two adjustable rollers under the ball--to avoid run-out and a toothed gear with an electronic pickup near the perimeter--to read ball speed with an electronic counter.

The microscope used for the measurements was built partly with available and partly with purchased parts. Its heart is the Ealing Tetravar unit, a housing containing a beamsplitter to which an objective lens, a camera, an illuminator, and a binocular eyepiece can be attached simultaneously. The objectives most useful to us are the reflecting 15x and 36x Ealing-Beck all-mirror Cassegrainians, which have working distances of 22 and 8 mm, respectively. These long working distances are essential for reading through the half-inch thich sapphire window.

The unit took longer to build than expected because of slow parts deliveries. The camera adapter is still on order. However, most of the unit is now in excellent working condition. We believe its flexibility is remarkable.

2.2 New Blackbody Reference

Most of our emission spectroscopy requires a blackbody reference source: a mechanical chopper alternatingly introduces source and reference radiation into the spectrometer-interferometer and the phase-locked amplifier brings only the difference signal to the recording device. For high-quality spectra of lubricant films, the background (i.e. the blackbody radiation from the bounding surfaces) must be almost totally balanced by the reference source. Since our sample is the thin lubricant film of an ehd contact and since the heat generated in the contact depends on load, ball speed, and

of course, the nature of the fluid itself, it is necessary to vary the reference temperature frequently to match the changed conditions. This is a very slow process. To be stable, a reference heat source or blackbody source must be massive to present much thermal inertia, but to be readily changed with respect to temperature, it should be light and small. Furthermore the blackbody radiation from the reference source should be directed toward the chopper and controllable only by a temperature change; in other words, the body or shield of the reference should not contribute to the reference radiation. And lastly, the reference source must fit physically into the interferometer-spectrometer source unit.

Such a source was built over a period of time and is shown in Figure 2. The blackbody part is merely a hole, one millimeter in diameter, drilled three-quarters down along the axis of a brass cylinder, one inch in diameter and three inches long. A V-shaped mask in front of the hole permits changes of aperture. The cylinder is wrapped with copper tubing through which water can be circulated to provide cooling. Conversely, the cylinder can be heated by three small electric cartridge heaters surrounding the central hole. Around the cooling coils a narrow air space is provided and beyond that is a shield of aluminum. Thermocouples are provided at various locations to monitor the performance. Testing has shown that the blackbody can be brought to near 200°C in a few minutes and maintained there by thermostatic switches. Even at that high temperature no radiation would be detected from the shield; it remained at ambient temperature. In a few minutes of water-cooling the temperature was brought down to 100° and could be maintained there.

Since the blackbody is completely enclosed in the source section of our interferometer, all controls, including the slit control, had to be made accessible from the outside.

Strange as it may seem, such a blackbody is not a trivial development. Our tests showed that its radiance closely matches the theoretical. Commercial blackbodies are very much bulkier and very expensive. Our blackbody could find use in radiometers other than ours. We have had a number of inquiries about it from commercial instrument makers.

2.3 Polarizing Chopper, Second Interferometer

Our work has shown that some infrared emission bands of lubricants in operating ehd contacts are dichroic; i.e. their intensity depends on whether a plane polarizing filter is oriented about the optic exis of the objective in such a way as to transmit radiation polarized in the conjunction plane (plane containing the center of bearing ball and the perimeter contacting the diamond window) or whether the filter is oriented so as to transmit radiation polarized at right angles to the conjunction plane.* Hence most of the work reported here required three separate runs to provide three independently recorded spectra (not polarized, or N, then V and H). Everyone of these spectra had to be run against a blackbody reference source at an appropriate temperature. Why not make use of the polarization?

A chopper was therefore built in the form of a rotating polarizer, i.e. a polarizing filter for the infrared rotating about the optic axis of the instrumentation. Every quarter revolution, the plane of polarization changes from V to H and the phase-locked amplifier allows only the difference between V and H to be detected. This procedure automatically removes the blackbody background--being randomly polarized, it is substracted out--and reduces the number of spectral runs needed to obtain spectral and polarization data from three

---

*For convenience, the first mentioned orientation will be referred to as V-polarized, the latter as H-polarized.

to two. The sensitivity is increased because of the greater signal/noise ratio. However, the drawback is that only polarized spectral bands, i.e. dichroic bands, are detected. For general use the reference source is therefore still needed. Figure 3 shows the rotating polarizer.

This chopper was designed and built as part of a new interface for emission Fourier infrared spectroscopy. The new reference source constitutes another element of this interface. Fortunately, it was possible to design, build, and test the new parts without disrupting data acquisition with the old interferometer, because an almost identical FS-720 Fourier Interferometer was donated* to us by the Du Pont Company. The reason for the "almost" is the substitution of a step drive for the continuous drive of our old instrument. The step drive moves the mirror for a set distance (the smallest built-in step is 2.5 μm), stops, triggers the detector to read, and then moves the mirror another step.

The continuous drive keeps track of mirror displacement by counting Moiré fringes generated between two combs (Moiré gratings), one stationary and one moving with the mirror and recorded by a lamp/photocell arrangement. The advantages of the step drive over the Moiré system are (i) the possibility of placing the central fringe of the interferogram exactly at a "read" position, thus eliminating the need for phase corrections, (ii) greater accuracy in taking data since the triggering signal is independent of mirror speed, (iii) the relative ease with which step displacements can be altered by changing gear ratios, whereas the Moiré gratings are ruled at definite intervals (number of lines per mm), and (iv) the option of faster mirror speed--as long as the detector time constant is compatible with it. We have been able to divide the mirror displacements per triggering interval of the Moiré system by an electronic

*We want to thank the Du Pont Company, Experimental Station, Wilmington Deleware, for their magnificant gift.

signal shape detector (our Klinetics unit), but with some difficulty; the step drive can do this directly. The main disadvantage of the step drive, at the time our interferometer was bought, was its very much higher cost when compared to the Moiré drive. We are therefore grateful to Du Pont for their foresight in buying the step drive. New electronics had, however, to be provided for the step drive, as well as a new gear ratio.

The new polarizing chopper and the step drive are basically working, but are not yet fully functional. It will be possible to use all the new parts with our old interferometer or--and this appeals to us more--to run the new interferometer as a separate unit, sharing only the minicomputer.

The new reference, chopper, and the adaptations of the new interferometer were designed and built as said before, without interfering with the operation of the old one. We should soon be able to improve our rate and quality of data collection with the new instrumentation.

3. RESULTS

3.1 Traction Fluid Spectra and Related Data

For reference Figures 4 and 5 give the standard grating absorption spectra of Monsanto's Santotrac P-40 fluid and of 1,1,2-trichloroethane (containing some 1,1,1-isomer, which was distilled off before use). The latter material was used as an additive in our deterioration studies.

Figure 6 shows three EHD spectra in the 630-1230 cm^{-1} range of the P-40 fluid under moderately severe operating conditions. The temperatures of the fluid reservoir were somewhat different and this circumstance is reflected in spectral structure: the lower the temperature the more structure. However, the difference between these spectra and the absorption spectrum of Figure 4 is striking--most of the resolution has been lost and the peaks are barely standing out on a broad background. Figure 7 shows the spectrum of P-40 under similar operating conditions in the 1275-1850 cm^{-1} spectral range (for reasons connected with our Fourier interferometer these spectral ranges have to be scanned separately). This spectrum, though an emission spectrum, resembles the absorption spectrum of Figure 4 in its spectral region; in other words, the emission bands appear as absorption bands, but again only the peaks are discernable over a broad background.

This traction fluid is not the same as the one whose high pressure infrared absorption spectrum we obtained some time ago in the diamond cell (Sun Traction Fluid) (Figure 8); however, chemically it is not very different and the vibrational spectrum is very similar. It is therefore interesting to note that pressure broadened the spectrum of the traction fluid very considerably, especially in the region of the cyclohexane ring vibrations (800-1000 cm^{-1}), which are characteristic of the traction fluids. Since temperature invariably does the same, the difference between the standard spectrum of Figure 4 and the emission spectra from

the operating contact of Figures 6 and 7 are not unreasonable. Aromatic fluids and esters do not exhibit temperature/pressure broadening to anywhere near the same extent.

To obtain a quantitative idea of the broadening we replotted the absorption spectrum of Figure 4 under lower resolution (Figure 9a) and then broadened the bases of the principal bands by a factor of four, assuming simple triangular band shapes as a first approximation. Accounting for the overlaps, Figure 9b is obtained. This spectrum is very similar to the ehd spectrum of Figure 9c. The reason for the very large broadening of the ring bands is usually ascribed to changes of the mix of conformational isomers; the higher temperatures and pressures shift the equilibria in the direction of higher energy forms. The molecular movement that occurs when the cyclohexyl group changes from one conformation to another is illustrated in Figure 10. It has been associated with a secondary transition (drop of elasticity modulus as the temperature is increased) in polymers containing a cyclohexyl group. The temperature of the secondary transition is just below that of the main transition (softening) and is associated with the flip-flop. Because the behavior of a plastic in this region has some of the aspects of a viscous liquid and some of an elastic, it applies to lubricants which are viscous liquids.

The conformational changes associated with the cyclohexyl group would seem to parallel the enormous spectral band broadening with temperature and pressure. Broadening also occurs with paraffinic fluids in the C-C bond-stretching infrared region. Here the changes (Figure 11) must be attributed to rotation of CH_2 groups in a paraffin chain. The CH_2 groups in a cyclohexane ring can be considered analgous to those in a paraffin section of four carbon atoms in one line. If the

cyclohexane rings were particularly outstanding with respect to traction, polymerized olefins whose monomers have four carbon atoms in a chain, i.e. polybutenes, should have higher traction coefficients than polypropylenes or polypentens. Indeed, polyisobutylene fluid has the highest coefficient of traction of any polymerized 1-olefin. It also has a rather low viscosity index.

A sequence of four CH_2 groups in a paraffinic chain--and, as just mentioned in a cyclohexane ring--is also the minimum requirement for one or two infrared active CH_2-rocking bands near 730 cm^{-1}. There thus appear to be certain structural aspects paralleling traction properties in a fluid.

3.2 Effect of Trichloroethane Addition on the Infrared Emission Spectrum of a Traction Fluid from an EHD Contact

Contamination of bearing lubricants by chlorides is not uncommon. To study the effect on the spectra and behavior of a traction fluid, 1,1,2-trichloroethane was used because of its (i) high content of available, i.e. active,chlorine, (ii) relatively high boiling point (113°C) and (iii) readily available commercially. Its infrared spectrum is also very well understood and, initially, we planned to make use of this circumstance to determine its molecular alignment in an ehd contact. The strongest C-Cl bands occur outside the spectral range of this study and the ones that do overlap bands of the traction fluid are not intense enough, even at 30% concentration, to alter the traction fluid spectrum significantly. The molecular alignment study will have to be cone in another spectral range, but it was deferred when it became clear that the trichloroethane promoted lubricant failure. When various amounts of the trichloroethane were added to the traction fluid, some interesting changes occurred in the spectra of the 630-1230 cm^{-1} wavenumber region. Figure 12 shows in the left column the spectra as they were obtained and in the right column the differences between the corresponding

spectrum in the left column and the EHD spectrum of the pure traction fluid. The spectra in the left column were normalized (maximum amplitude made equal to unity and all the other amplitudes appropriately reduced by division by the actual value of the maximum amplitude, i.e. the greatest unnormalized amplitude or the GUA). The spectra in the right column were plotted, however, as actual differences.

The outstanding changes with trichloroethane addition are the new bands shown at the frequencies marked by the arrows in Figure 12. They are shown more clearly in the difference spectra than in the original spectra and consist of two new bands, one at 700 and one at 990 cm^{-1}. These bands hardly show at 5-percent trichloroethane concentration, but are quite prominent at 10 percent and higher. At 20 percent, the 990 cm^{-1} band is not clearly observed because the peak is folded back on itself (peak inversion). Peak emission in a hotter region of the fluid is reabsorbed in colder regions. The new bands are definitely not trichloroethane bands, but correlate well with most olefins and aromatics.

Figure 13 in a comparision of spectra obtained with the neat traction fluid and with the fluid containing 15 percent of trichloroethane by volume. The experiments were made in ascending order, i.e. b', a', b, and a. The following observations can be made when comparing the solid line (no trichloroethane and the broken line (containing trichloroethane) spectra:

(a) The GUA's (i.e. maximum band intensities) of the broken line spectra are equal to or <u>lower</u> than those of the corresponding solid-line spectra. The radiant intensity from the fluid was, therefore, generally less when trichloroethane was present. This observation also agrees with a slight lowering of the temperature measured by a thermocouple next to the diamond window. Measurements

of traction also showed a reduction for these operating conditions which, by the way, were outside the linear range of the traction -versus speed curve.

(b) The bands at 700 cm^{-1} and especially 990 cm^{-1} are more pronounced in the broken-line spectra.

(c) The spectrum with the most pronounced peak at 990 cm^{-1} is also the last spectrum of the series and has the lowest GUA.

3.3 Polarized Infrared Spectra of Traction Fluid with and without Trichloroethane

Figure 14 shows a series of traction fluid EHD emission spectra comparing different angles of the polarization plane with the conjunction plane, i.e. the plane containing the plate/ball conjunction line and the center of the ball. The principal immediate observations are that the spectra under polarization are much more structured than the one without polarization and that there are differences between the spectra at different angles of polarization. Of particular interest in the band near 990 cm^{-1}; it is barely a shoulder in the non-polarized spectrum, but is prominent as an emission or re-absorption peak in the polarized spectra. A similar situation occurs near 700 cm^{-1}. These two bands are, as pointed out in the preceding section, the new bands brought out in the unpolarized spectra by the addition of trichloroethane. Their presence here--though weak, since polarization had to be employed to bring them out--is an indication of some fluid deterioration without the addition of trichloroethane in the same way as with addition. Indeed, this sequence of spectra was run late in the series, when the fluid had been stressed for many hours. It puzzled us until we became aware later of the ubiquitous presence of chloride in our laboratory. Traces of chloride provide the same mechanism of deterioration, though it is slower. The mechanism will be discussed in Section 3.4.

The polarization of the 990 cm^{-1} band relates to an orientation of the C=C bond. It could be explained by an olefinic polymer laid down on the bounding surfaces. An infrared examination of the traces of friction polymer was, however, not carried out.

It is possible to define a dichroic ratio for an emission band as the ratio of the band intensity when the plane of polarization is parallel to the the ball/plate conjunction plane to the band intensity when the plane of polarization is perpendicular to the conjunction plane. A dichroic ratio of unity is then an indication of random molecular orientation whereas a dichroic ratio significantly greater or less then unity is an indication of preferred orientation. The reason for this deduction lies in the origin of infrared spectral bands, which is briefly explained in Appendix I.

Figure 15 shows plots of the dichroic ratio of four reasonably well characterized infrared bands of the traction fluid with and without trichloroethane (15%) against sliding speed for low and medium loads. Unfortunately the spectral region above 1250 cm^{-1} was not run with the trichloroethane so that comparisons cannot be made. Even though only two points are shown for every line on these graphs, the results are consistent with data on other bands so that comparisons can be made. Note that

(i) in general, the dichroic ratio deviates from unity more for the low load than for the intermediate load,

(ii) the dichroic ratio is near unity for all bands at the higher speed except for 917 cm^{-1} and 1380 cm^{-1} bands at low load,

(iii) the slopes at 690 cm^{-1} and at 917 cm^{-1} for the higher load, trichloroethane-containing runs are opposite

(iv) the dichroic ratios at 690 cm^{-1} and at 917 cm^{-1} are unusually high (the band is very strongly polarized, indicating a high degree of molecular orientation) at low speed and low load for the fluid containing trichloroethane, and

(v) the dichroic ratios for the fluid containing the trichloroethane are generally more different from unity--indicating a higher degree of fluid orientation--than those for the fluid not containing the trichloroethane, all under comparable operating conditions.

3.4 Effect of Trichloroethane Addition on the Traction of Two Traction Fluids

The measurements of Figures 16 and 17 represent traction versus sliding speed at different loads for both Santotrac P-50 and the new Sun Co. traction fluid both with and without trichloroethane addition. The ordinate is the strain gauge reading with the ball/plate apparatus described in Section 2.1. Since the apparatus was built to duplicate the conditions of the ball/plate contact interfaced with the infrared spectrometer, very low sliding speeds could not be used (some minor design changes are underway to allow measurements at smaller speeds) so that the ascending portion of the curves could not be measured. The very low sliding speeds are interesting for traction measurements--they determine the linear portion of the traction -versus- speed curves--but very unlikely to produce enough infrared radiation for our spectral measurements. The theoretical shape of these curves is shown schematically in Figure 18, which has been taken from Tevaarwerk [5].

Inspection of both Figures 16 and 17 shows that trichloroethane addition (2%) does not affect the traction curves significantly except in the case of high loads and high speed for the Santotrac fluid, where it reduces traction. It does not influence the traction of the Sun Fluid significantly at all,

although it would seem, if anything, to raise it. However, it should be pointed out that the traction of the Sun fluid is considerably lower than that of the Santotrac fluid in any case. The two fluids are therefore quite different with respect both to traction and to trichloroethane susceptibility of traction.

The lower traction of the Santotrac fluid containing the trichloroethane at high speed and load is consistent with the lower infrared emission and film temperature under these conditions.

3.5 Scanning Electron Microscope (SEM) Analysis and Surface X-ray Analysis of of Steel Ball

The stainless steel ball used extensively with the traction fluid/trichloroethane mixtures was later used to obtain EHD infrared emission spectra with 5P4E polyphenyl ether lubricant at room temperature in the reservoir cup. The first spectrum (Figure 19) obtained was very distorted compared to a normal spectrum under these conditions. The system failed when a second spectral run was attempted. The ball was seriously scored (it had shown a barely perceptible track before it was used with 5P4E) and the fluid was black and contained many carbon particles.

SEM X-ray analysis of the ball showed chlorine covering all the surface. However, the covering was particularly thick on the track, because it was not possible to obtain any metal peaks there. Clearly the fresh metal surface of the track reacted more vigorously than the remainingly ball surface.

3.6 Infrared Emission Spectra of 5P4E (Polyphenyl Ether) at Low Temperature from an EHD Contact. Effect of Trichloroethane at Low Concentration (2-3%).

Since the Santotrac P-40 bands from the EHD contact were rather broad and difficult to assign, it was decided to go back to polyphenyl ether (5P4E) for a detailed spectal study of polarization and the effect of trichloroethane addition

on it (in very small concentration, 2-3%) as a function of the operating parameters of our ball/plate sliding contact. The work reported here used both a stainless steel and a bronze ball of the same diameter. Gold-coated steel and ceramic balls will be studied in the future. In all cases the fluid in the reservoir was cooled by circulating ice water through the cooling coil surrounding the ball/plate (diamond) contact. The emphasis was on the 630-1230 cm^{-1} spectral region, but many spectral runs were repeated in the 1275-1850 cm^{-1} spectral region. For these spectral runs the apparatus was completely re-aligned and maximum attention was given to detail; as a result, successive spectra under equal operating conditions could be reproduced quantitatively to better than 5% in spectral response and to better than 2 cm^{-1} in resolution.

With the help of results communicated in a recent report by Hamrock and Dowson [6] it was possible to establish the EHD regime that prevailed when our spectra were taken. Our ball/plate contact is circular and characterized by Figure 20, which has been adapted from this report, mainly by extension of the coordinate ranges. Since diamond's elastic modulus is very high ($\sim 10^{12}$ pascal), the reduced elastic modulus for the steel ball/diamond window combination is also high, ~ 0.30 to 0.35×10^{12}, depending on the nature of the particular diamond, compared to $\sim 0.22 \times 10^{12}$ for a steel ball on a steel plate. The elastic modulus does not influence the viscosity parameter (ordinate) at all, but does enter the elasticity parameter (Abscissa), which it could reduce by a factor of at most $(1/2)^{2/3} = 0.63$ compared to a steel/steel combination. This factor is appreciable but is not enough ever to force our system into the isoviscous-rigid regime. For example, we operated our apparatus with 5P4E polyphenyl ether cooled to an inlet temperature of $33^{o}C$ ($\eta_o = 0.881$ Pa.s) and at a ball speed of 200 RPM or 0.6 m/sec.

At this temperature the pressure-viscosity coefficient of 5P4E is 39.3 x 10^{-9} Pa^{-1}. We used minimum load (3 kg), i.e. the weight of the ball and platform alone. Even for these conditions, which are conducive to very thick film, we operated at the point marked "very low load" in Figure 20. It lies near the viscous-rigid and viscous-elastic boundary, but probably in the former regime (average Hertzian pressure 400 MPa). The corresponding infrared emission spectrum was Figure 21a. Note the relatively strong band at 780 cm^{-1}, almost as strong as the 690 cm^{-1} band to the left. When the load was doubled, the spectrum of Figure 21b was obtained, for conditions corresponding to the "low load" operating point just within the viscous-elastic regime. Doubling the ball's rotational velocity produced the operating conditions characterized by the operating point just within the viscous-rigid regime and the infrared absorption spectrum of Figure 21c. The most interesting result is the almost complete absence of the 780 cm^{-1} emission band in the middle spectrum and a bare indication of it in the bottom spectrum. Since all the other spectral features remained nearly constant and since the 780 cm^{-1} band is well-known to be caused by the "umbrella" mode of vibration of the aromatic ring, in which the change of dipole moment vector is perpendicular to the plane of the ring, it would seem logical to conclude that the ring is indeed oriented with its plane parallel to the window when the load exceeds a certain critical value. With this molecular orientation the optic axis of the interferometer system is coincident with--or at least parallel to--the change of dipole moment associated with this vibration so that an electromagnetic wave cannot be propagated toward the detector. However, because of different substituents on the phenyl ring of 5P4E, the dipole moment vector of the umbrella vibration is not exactly perpendicular to the plane of the ring. Rotation of the plane of polarization about the

optic axis by a polarizing disc will therefore change the intensity of this band somewhat if the molecules are preferentially oriented with respect to the flow direction. Other bands, whose dipole transition vectors have large components in a plane parallel to the faces of the diamond window, are also expected to change substantially, again if the molecule is preferentially oriented with respect to the flow direction.

A more detailed discussion of the relationship between infrared polarization, dichroism, and molecular alignment is given in Appendix II.

Series of EHD contact spectra of 5P4E polyphenyl ether with and without 3% trichlorethane were then obtained with the steel ball/diamond setup and ice-water cooling. Under these conditions the temperature measured by the thermocouple next to the diamond window was still in the neighborhood of $39^{o}C$, but the spectra were more structured and reproducible than ever before. The excellent quality of these spectra is the result of many factors, but the lack of vibrations transmitted through the shaft, the isolated optical table, and the new location of the chopper below the lens were the principal causes of the good results.

For understanding the following spectra it is important to explain the coding. The first two digits stand for speed and load, N,V, or H stand for not polarized, polarized in the conjunction plane, i.e. the plane containing the ball center and the Hertzian contact, and polarized perpendicularly to the conjunction plane. In most cases both the 630 - 1230 cm^{-1} and the 1275-1850 cm^{-1} spectral region were scanned. The presence of (3%) trichloroethane is indicated by the letter A.

3.6.1 EHD Spectra in the 1275 - 1850 cm^{-1} Region. Figures 22 and 23 contain emission spectra under equal high load/high speed conditions,* with and without trichloroethane, in the 1275 - 1850 cm^{-1} spectral region. These

* 700 MPa average Hertzian pressure, 1.8 m/s linear speed

spectra are essentially identical as far as the major bands are concerned; neither polarization nor trichloroethane addition seem to have a significant effect. The strongest bands are at about 1480 cm^{-1} and at 1600 cm^{-1}, both non-degenerate C-C in-plane stretching fundamentals involving ring carbon atoms. Since these vibrational modes involve dipole moment vector changes in the plane of the ring plane parallel to the diamond window (in contrast to the 780 cm^{-1} band mentioned earlier, which is caused by an out-of-plane dipole moment vector change) or along the flow direction should not and does not affect the band intensity. The constancy of the 1480/1600 cm^{-1} band intensity ratio to $\pm$ 5% is an excellent measure, therefore, of our spectral reproducibility. The spectra of the trichloroethane containing fluid were obtained about two months later than the spectra of the neat fluid. During this time the instrument was completely realigned and yet all the spectra are still about equal! The situation of the other spectra in this region is similar so that no further discussion is necessary.

3.6.2 EHD Spectra in the 630-1230 cm^{-1} Spectral Region. Figures 24 and 25 contain the EHD emission spectra of the neat and additive-containing fluid in the lower frequency region (630-1230 cm^{-1}) under the same high speed/high load conditions as those used for the preceding two figures. Now it is quite obvious that the intensity ratio of the strongest two bands at 990 cm^{-1} and at 1150 cm^{-1} is changed with polarization; under H-polarization the 990 cm^{-1} is stronger than the 1150 cm^{-1} band, while the opposite is true, though to a much smaller extent, under V-polarization. The intensities of these bands change somewhat in the presence of trichloroethane, but the most evident spectral changes brought about by 3% of trichloroethane are the improved resolution of minor bands on the slope of the low frequency side of the 990 cm^{-1} band peak and the deteriorated resolution of minor bands on the high frequency

side of the same peak. The 990 and 1150 cm^{-1} bands originate from different vibrational modes, the former from ring expansion (a kind of C-C stretch) and latter from C-H in-plane deformation. Orientation of the molecule in the flow direction should be reflected by an intensity change of the 1150 cm^{-1} band with respect to the 990 cm^{-1} band, which should not be affected.

Reduction of the load at the same speed inverts the 990/1150 cm^{-1} band intensity ratio under V-polarization and reduces it under H-polarization under neat conditions (Figure 26), but has essentially no effect when 3% of trichloroethane is present (Figure 27). Thus the trichloroethane maintained the lubricant in the same orientation as before when the load was doubled at the same flow velocity. This effect of the chlorine additive seems to be significant.

Reduction of the speed at the highest load did not change the 990/1150 cm^{-1} band intensity ratio appreciably under N or H polarization (perhaps it did cause a slight change under V-polarization) without the additive and produced even less change with the additive, consistent with the previous observation (Figures 28, 29).

Reduction of speed and load from the maximum to the intermediate reduced the 990/1150 cm^{-1} band intensity ratio for H-polarization in the absence of trichloroethane, but, as before, left the polarization ratio essentially the same when trichloroethane was present (Figure 30, 31).

When the speed was minimized and the load kept at maximum and the chloride was present, the 990/1150 cm^{-1} band intensity ratio was increased for both V and H polarization over that at maximum speed/maximum load conditions (Figure 32).

From the foregoing it would thus appear that an effect on EHD emission spectra of trichoroethane addition to 5P4E polyphenyl ether is to increase the 990/1150 cm^{-1} band intensity ratio. Since both of these bands are produced by in-plane dipole moment vector changes at a constant angle with respect

to each other, the addition of trichloroethane causes 5P4E-polyphenyl ether molecules to be oriented more readily with respect to the flow direction.

3.6.3 Dichroism of Infrared Emission Spectral Bands of 5P4E Polyphenyl Ether with or without 3% Trichloroethane from a Steel Ball/Diamond Contact under Different sliding Speeds and Loads. In order to recognize possible effects of speed and load on the polarization of the infrared spectrum emitted from the EHD sliding contact, a detailed analysis of the dichroic ratio was made. For the purpose of this report it will be recalled that it is sufficient to define ratio as the ratio of the band intensities for radiation transmitted through mutally perpendicular planes of polarization (V and H polarization). Accordingly, band intensities were obtained by graphical integration of the band traces and correction of the result by multiplication with the appropriate normalization factors. The plots in the following figures represent the V/H polarization ratio for the indicated bands. The 990 cm^{-1} band and the 1150 cm^{-1} band were described in the preceding section.

Figure 33 is a plot of dichroic ratio against load for the 1000 cm^{-1} band for different speeds. Neat or (3%) trichloroethane-containing polyphenyl ether fluids are differentiated by corresponding hollow and solid points. Note that the black marked points are generally more distant from the unit ordinate (unpolarized) line than the clear points and that the slopes are opposite for black marked and clear points. This observation could mean that the additive causes the cirection of orientation of the bulk fluid to be different. Such a polarization reversal does not occur for the 1150 cm^{-1} band (figure 34); however, the additive generally increases the dichroic ratio. These results are consistent with the molecular structure of the polyphenyl ether and could be used to estimate it orientation with respect to the contact plane.

Similar observations can be made from the plots of Figures 35 and 36; here ball speed is the abscissa and different plots represent different loads. Comparison of Figures 34 and 36 would seem to indicate that at 1150 cm^{-1} increased load at constant speed can increase the degree of polarization while increased speed at constant load may change it but little. The dichroic ratios for the 1150 cm^{-1} band are generally highest for the highest speed and load, i.e. the highest shear rates, but for the 1000 cm^{-1} band they are generally close to unity (low degree of orientation) for the highest shear rates; the presence of trichloroetnane may invalidate this generalization.

Film thickness data should become available soon. At that time these data will be replotted against shear rates.

The dichroic ratios for the 690 and 760 cm^{-1} bands representing different out-of-plane C-H deformation vibrations are plotted against speed in Figures 37 and 38. The 760 cm^{-1} band is caused by a dipole moment vector change perpendicular to the phenyl ring and is of low intensity because the ring appears to be aligned parallel to the diamond window in the conjunction plane (see Section 3.6). If the ring were substituted completely symmetrically, orientation of the emitted radiation by the axially turning polarizer would be ineffective. As it is not, the band can be further polarized and theoretically in a direction opposite to that of the 690 cm^{-1} band. Casual inspection of Figures 37 and 38 shows that this is the case e.g. for the highest load/trichloroethane situation. For these bands as well, the trichloroethane additive has enhanced polarization and thus molecular orientation. The corresponding plots of dichroic ratio against load are shown in Figures 39 and 40. Note that the slopes of the lines connecting equivalent points are mostly of opposite sign for the two bands.

3.6.4 Traction Measurements of 5P4E Polyphenyl Ether with and without 3% Trichloroethane Added. With our new ball/plate apparatus, strain gauge measurements were made to compare the traction of 5P4E polyphenyl ether with and without 3% trichloroethane at several loads and at two temperatures, ambient and at 50°C (reservior temperatures). The measurements could not be carried out reliably at very low ball speeds because of the design of our apparatus; however, the maximum readings were obtained for every set of conditions (Figures 41, 42, 43, and 44).

It was gratifying for us to note that our traction/sliding speed plots checked the literature, especially at the higher loads and at the higher temperature; for example, Figure 45 taken from Tevaarwerk's article [5] resembles our Figure 42. At room reservoir temperature the presence of trichloroethane reduced the traction everywhere very considerably (Figures 41 and 42), but at 50°C reservoir temperature it increased the traction at the low speeds, but decreased it slightly or left it unchanged at the higher speeds. Standard viscosity determination (capillary viscometer)did not show a difference between trichloroethane-containing and neat polyphenyl ether (5P4E); hence the film thickness very likely remained the same. Therefore, it would appear that trichloroethane, by absorbing on the bounding surfaces, changes the tractions. The deduction in contradictory to the present view of traction as a bulk fluid property unless an influence of the surface on the bulk fluid is assumed. In addition to the dichroic ratio determinations discussed in the proceding section, the bronze ball spectra and traction measurements described in the following sections seem pertinent.

3.6.5 Dichroism of Infrared Emission Spectral Bands from a Bronze Ball/Diamond Plate Contact for Polyphenyl Ether (5P4E) with and without 3% Trichloroethane under Different Sliding Speeds and Loads. When the dichroic

ratio was obtained fro the 690 cm^{-1} aromatic band with a bronze ball under the same conditions as for the steel ball of same dimensions, the plot of Figure 45 against ball speed could be drawn. Comparison of this figure with the corresponding one for steel (Figure 37) shows some interesting points. Again the empty markers are drawn for the neat case and the double point markers for the case of 3% trichloroethane added. Note that (i) for both the steel and the bronze ball the dichroic ratio approches unity (unpolarized state) at high speed, but with a positive slope for the steel ball and a negative slope for the bronze ball and that (ii) the dichroic ratio is not significantly changed by trichloroethane in the case of the bronze ball, but is significantly changed in the case of the steel ball.

4. DISCUSSION

4.1 Mechanism of Traction Fluid Deterioration by 1,1,2-Trichloroethane

Originaaly we proposed a free radical mechanism because the traction fluid (Santotrac P-40), even without the presence of the trichloroethane, deteriorated to give olefins and aromatics in the same way as the fluid containing substantial amounts of the trichloroethane, although at a considerably slower rate. After a while, it became clear to us, however, that some chlorine contamination existed all the time. X-ray analysis of the bearing ball surface in the scanning electron microscope invariably showed the presence of chlorine. We therefore changes our thinking and now believe that an ionic mechanism is much more likely.

A review of the literature showed that Kovacic and co-workers [2] had proposed a very pertinent mechanism for the reaction between methylcyclohexane and ferric chloride some time ago. Since our traction fluid has a structure not dissimilar from methylcyclohexane and since the Kovacic mechanism accounts for both olefines and aromatics very beautifully it should be applicable. The following steps are involved:

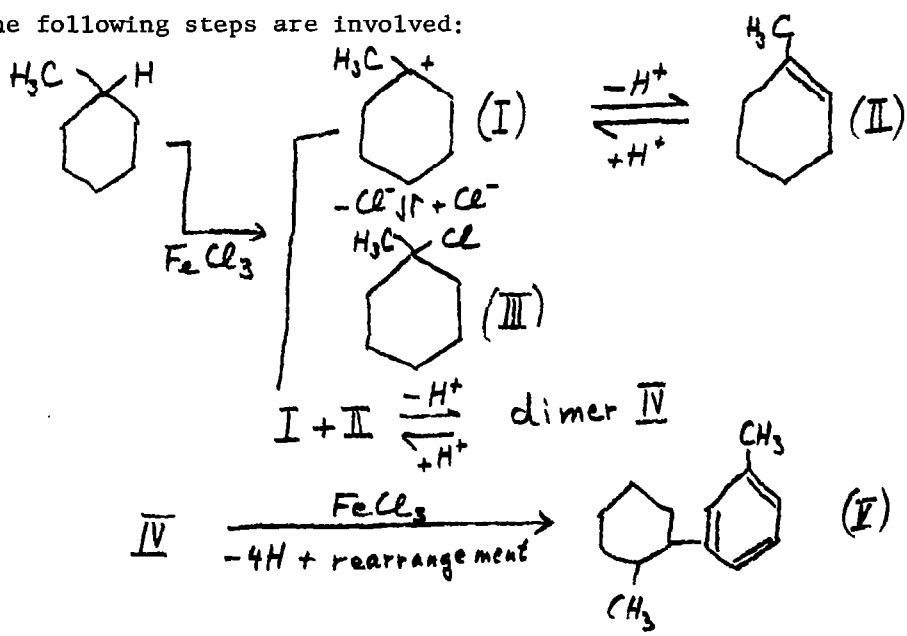

Note that intermediate II is a cyclohexene, an olefin, which can form a polymer, and indeed "carbon" and friction polymer were found.

While the above mechanism is very plausible, it has not been proved. Kovacic's experiments started with 2:1 mole ratios of methycyclohexane and ferric chloride, while the situation in a bearing is quite different. Obviously the study of some related chemistry would be very much to the point.

4.2 Mechanism of Polyphenyl Ether (5P4E) Deterioration by 1,1,2-Trichloroethane

Ethers are basic because of the unpaired electron on the oxygen. Polyphenyl ether would therefore react readily with an alkyl halide to form alkyl derivatives in the presence of ferric chloride formed on the steel ball and at the same time break the ether linkage, e.g.

These materials would then react further on the metallic surface to form radical ions, acids, and resins by a Goldblatt [3] mechanism as shown below.

Metallic surface $\xrightarrow{\text{sliding}}$ virgin metal surface (VM)

VM + aromatic (ARO) $\longrightarrow$ M; Aro (absorbed aromatic on metal)

M; Aro $\longrightarrow$ M^+; $Aro^{\bullet -}$ (adsorbed radical anion)

M ; $Aro^{\bullet -}$ $\longrightarrow$ $M^+ + Aro^{\bullet -}$ (desorbed radical anion)

$Aro^{\bullet -}$ + metal or metal oxide $\longrightarrow$ reduced metal oxide or abrasives + metal $\longrightarrow$ abrasive wear

$Aro^{\bullet -} + H_2O \longrightarrow Aro{-}H^{\bullet} + OH^- \longrightarrow$ dihydronaphthal

$Aro^{\bullet -} + O_2 \longrightarrow Aro + O_2^{\bullet -} \longrightarrow$ peroxides $\longrightarrow$ acids or resins

$Aro^{\bullet -}$ + aliphatic $\xrightarrow{\Delta}$ adduct + higher mol. wt. products

$Aro^{\bullet -}$ + aliphatic + $O_2 \longrightarrow$ peroxides (of aliphatics) $\xrightarrow{\Delta}$ acids (of aliphatics) or resins.

In presence of moisture a somewhat different mechanism will account for the acids and resins eventually formed. The main point to be raised here is that polyphenyl ethers, for all their thermal stability are really very active chemically, especially in the presence of virgin metal surfaces. Study of the chemistry involved should lead to better protection and avoidance of lubricant and metal surface breakdowns.

4.3 Influence of Bounding Surfaces on Lubricating Film Alignment

Our EHD dichroic ratios for 5P4E polyphenyl ether have shown significant changes, even inversions for some infrared bonds when trichloroethane was present in small concentration in the case of the steel ball/diamond contact. In the case of the bronze ball/diamond contact, the changes produced by trichloroethane were much smaller or even insignificant. In the case of the Santotrac P-40 traction fluid, the dichroic ratios were also affected by a small concentraction of trichloroethane, primarily at low speeds and loads and generally in such a way as to alter the direction of dichroic ratio change with increasing speed and load. These changes can best be interpreted in terms of adsorbed boundary layers influencing the orientation of the bulk fulid, since it is only the bulk fluid that our spectrometer is seeing.

Such a conclusion is not as far-fetched as it seemed to me at first, for a literature review revealed that X-ray diffraction studies carried out by Clark, Sterrett, and Lincoln [7] in 1936 showed such effects. They say: ". . . . the addition of this chlorinated compound (viz. methyl dichlorostearate,) greatly improves the orientation of the hydrocarbon molecules of paraffin and paraffin-oil films. Thus, besides orienting in films of the pure polar compounds, even in small amounts they show a marked tendency to regiment surrounding molecules which are only weakly polar".

I believe our dichroic ratios not only confirm the results of these X-ray studies--which, by the way, had to be performed with simulated materials, viz. solid wax instead of oil, in order to see the X-ray diffraction pattern--but provide us with molecular orientation data likely to lead us to superior fluid formulations.

Clark, Sterrett, and Lincoln also rated different metal surfaces in terms of their ordering tendency for "addition agents" on a scale from 1 to 4, in order of increasing orientation, the orientation being determined by the X-ray diffraction pattern. The most oriented addition agent was trichlorophenol, which was rated 4 on copper, but only 1 on iron. Stearic acid was rated 1 on copper and 0 on iron. These authors' X-ray data are in remarkable agreement with our dichroic ratio data for steel and bronze.

Furthermore, the same authors presented evidence from X-ray diffraction data that chlorinated addition compounds alone and in oil blends when heated in the presence of metals, form a resistant surface layer on the metal and themselves undergo a chemical change, considered a chemical condensation. Some of the chlorine atoms are pulled out from the organic compounds presumably forming metal chlorides.

4.4. Traction Fluids

Traction is considered to be a fluid property in the EHD contact region, for which the conditions are set in the EHD inlet sone. There is now abundant evidence for the correctness of this view. Consistent with this view a small concentration of trichloroethane does not change the traction behavior of the Sun traction fluid, as we have shown. On the other hand, this same material did change (lower) the traction of the Monsanto fluid (Santotrac P-40) at high ball speed and load. The traction of 5P4E, polyphenyl ether, (reservoir temperature

50°) which is not considered a traction fluid, was increased by trichloroethane (2%) at low speed, but decreased at high speed and low load, as we have seen. Of course, prolonged use of high concentrations of the chloride caused failure.

Rounds [8] reported in 1972 that the addition of a chlorinated wax to hydrocarbon base oils changed the measured coefficients of static and kinetic friction. The addition of 2.5% of chlorinated wax to an oil containing less than 2% of aromatic carbon decreased the friction only slightly at low speeds, but very much at high speeds, while the same addition to an oil containing more than 15% of aromatic carbon increased the traction at low speeds and slightly decreased it at high speeds. These findings are in exact agreement with our results for the Monsanto traction fluid Santotrac P-40 and polyphenyl ether (5P4E) at the 50°C reservoir temperature. Rounds related these results to the surface concentration of chlorine in the boundary surfaces and spoke of an "aromatic effect" in terms of competition between an organic chloride and aromatic materials for surface adsorption sites. Oxidation products of the aromatics in particular may also affect surface coating formation.

Polycyclohexyls were included among Rounds' fluids and he states: "... Although the improvement in tractive effort available from such fluids is generally attributed to bulk-oil physical property changes occurring in the contact region, the data of Figure 2 (showing the effect of chlorinated wax addition) point out that surface chemistry cannot be ignored". Indeed, data we obtained with the scanning electron microscope and corresponding surface X-rays show chlorine reacted on with our bearing ball, and much more so on the track containing the EHD contact than on the rest of the ball. On the other hand, preliminary data with this ball used in measuring traction of neat Santotrac P-40 fluid did not show reduced traction when compared to a clean ball. If substantiated, it would mean that the trichloroethane reduces

traction by a bulk fluid effect and that the chloride coating is coincidental. In this connection it is worth noting that the addition of chlorine to many polymers changes the mechanical properties, notably an elastic/plastic transition. The presence of the cyclohexyl group in some of the polymers brings in a secondary transition corresponding to the same movement that occurs in low molecular weight cyclohexyl derivatives when the cyclohexyl group changes from one conformation to another (Figure 40). This flip, called Hejboer flip, after its discover, [9] could be of importance to traction.

5. WORK PLANNED

5.1 Failure of EHD Lubrication

The effect of surface composition on traction and failure will be explored with gold-plated and platinum-plated stainless steel balls, alumina balls, silicon nitride balls and balls plated with titanium and vanadium carbides. For this purpose various additives and contaminants will be studied. We have some of these balls on hand already, donated to us through the courtesy of SKF Corporation (Sweden); others will be provided to us at nominal cost by Laboratoire Suisse de Recherches Horlogeres (Dr. Hans Hintermann, Director). Some of these surfaces are used without lubricants, notably the non-metallic ones. The non-metallic surfaces also possess characteristic infrared spectra which are indicative of their crystalline structure. For example, silicon nitride has different bands depending on whether it is cubic or hexagonal; near 200°C, it was reported [9], the transition from one form to the other occurs. If lubricant deterioration is catalyzed by a metal surface, as is likely to be the case for Santotrac containing trichloroethane, then an inert metal (gold) or a non-metallic surface should provide longer bearing life.

The problem of scuffing failure is intimately related to lubricant failure. Dyson postulates two types of failure, hydrodynamic film failure and boundary film failure. The latter must clearly be chemically influenced.

Additives to be looked at are tricresylphosphate, zinc dithiophosphate, stearic acid and 12-hydroxystearic acid, and halogenated stearic acid. Among the fluids under study will be wet and dry polyphenyl and C-ethers, esters, and mixed polyphenyl ethers to provide constant film thickness for different operating conditions. Our new interferometer with the rotating polarizers should help reduce times considerably.

5.2 Improved Traction Fluids

We intend to pursue the clue infrared polarization changes (dichroic ratios) seem to provide by their apparent correlation with the viscoelastic/plastic transition (high dichroic ratio--low slip). Heijboer's transition for cyclohexyl rings is related to free volume changes in fluid. A theoretical analysis will be made, to be followed by a synthesis and tests of proposed materials.

REFERENCES

1. Lauer, James L., "Determination of Physical and Chemical States of Lubricants in Concentrated Contacts--Part 1". NASA CR-3204 (Grant NSG-3170), November 1979.

2. Kovacic, P., Morneweck, S.T., and Volz, H.C., "The Nature of the Methylcyclohexane--Ferric Chloride Reaction," J. Am. Chem. Soc. 28, 2551-4 (1963).

3. Goldblatt, I.L., "Model for Lubrication Behavior of Polynuclear Aromatics, "Ind. Eng. Chem. Prod. Res. Develop. 10, 270-278 (1971).

4. Winer, W.O., and Sanborn, D.W., "Surface Temperatures and Glassy State Investigations in Triboloby," NASA CR-3031, June 1978.

5. Tevaarwerk, J.L., "Spin Traction Prediction" in Suh, N.T., "Fundamentals of Triboloby," MIT Press, 1980, ISBN: 0-262-19183-0, pp 1129-47.

6. Hamrock, B.J., and Dowson, D., "Minimum Film Thickness in Elliptical Contacts for Different Regimes in Fluid Film Lubrication", NASA Technical Paper 1342, Oct. 1978.

7. Clark, G.L., Sterrett, R.R., and Lincoln, "X-ray Diffraction Studies of Lubricants", Ind. and Engng Chem. 28, 1318-1328 (1936).

8. Rounds, F.G., "Effect of Aromatic Hydrocarbons on Frictions and Surface Coating Formation with Three Additives." ASLE Transactions, 16, 2, 141-149 (1972).

9. Heijboer, J., Kolloid, Z., 148, 36 (1956).

APPENDIX I

POLARIZED INFRARED RADIATION

Like any other electromagnetic radiation infrared radiation is produced by oscillating dipoles. As the electric charges move back and forth, the dipole moment vector changes and electromagnatic waves are generated whose electric vector is parallel to the direction of the dipole moment. In Figure 47, where the dipole moment change is along the z-axis, electromagnetic waves are propagated in the x and y direction but not in the z-direction. No polarizing filter is needed for this result which, conversely, is evidence for the orientation of the change of dipole moment.

Polarizing filters (discs) are so constructed that they transmit radiation plane-polarized for only one direction of the electric vector. Their rotation about an axis perpendicular to their plane allows a different component of the incident radiation to pass. Figure 48 shows two dipoles radiating along the z-direction but differently oriented in the x/y plane. Intensity maxima occur whenever the electric vector of the transmitted plane-polarized radiation is parallel to one of the radiating dipoles.

APPENDIX II

ORIGIN OF INFRARED DICHROISM

Figures 48 and 49 show a model of diphenyl vibrating in the ring-puckering mode. Alternate carbon atoms are above the plane of the ring and below the plane of the ring at a given instant. The resultant dipole moment vector vibrates in a direction perpendicular to the plane of the ring. Hence if the ring is oriented horizontally, i.e. in the x/y plane, this mode of vibration cannot be observed along the z-axis (Figure 48), but if vertically (Figure 49), it can.

If the ring is vibrating in a mode in which all the ring atoms move in the plane of the ring and parallel to the x-axis, the transition moment will change along the x-axis and radiation will be transmitted along the z-axis. Rotation of the polarizer about the z-axis will transmit a maximum of radiation whenever the electric vector is parallel to the x-axis. Conversely, this situation will be consistent with the axis of the diphenyl oriented parallel to the x-axis. If most of the molecules are so oriented, but some are randomly oriented in the x/y plane, then the corresponding dichroic ratio, defined as the radiation transmitted along the x-axis divided by the radiation transmitted along the y-axis, will be high.

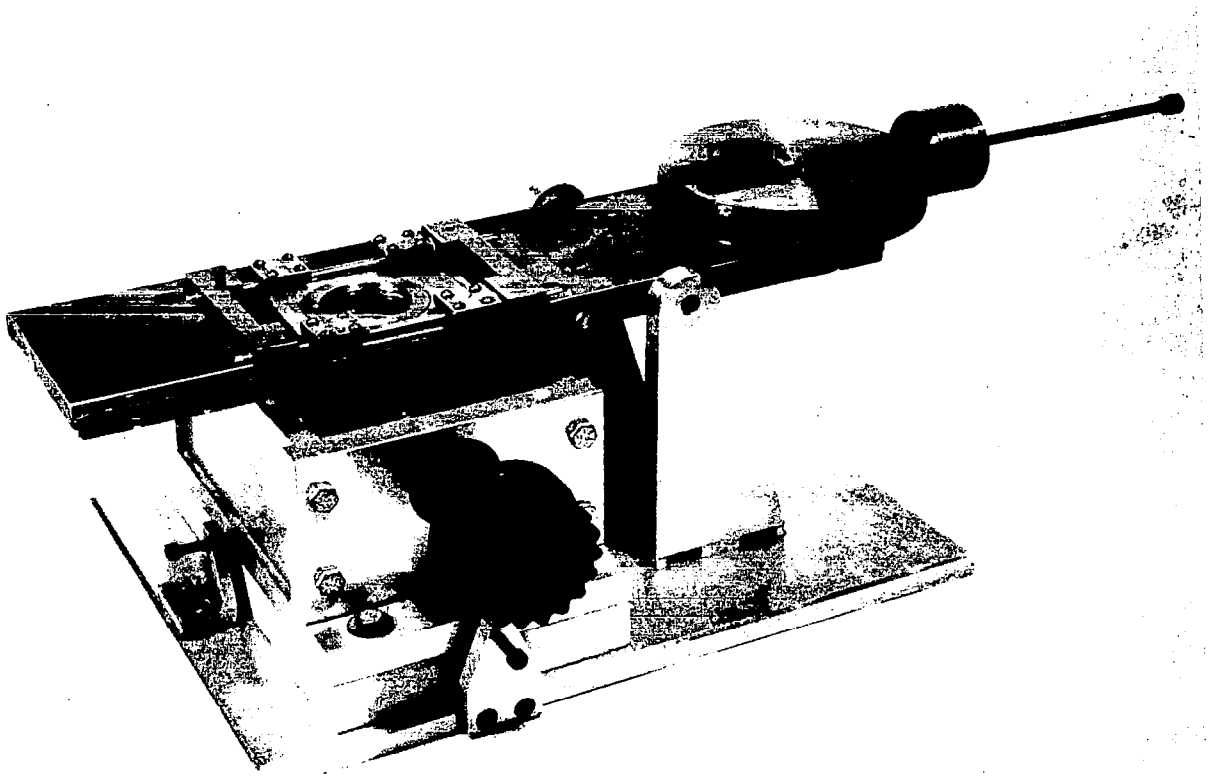

Figure 1 Apparatus for measuring lubricant film thickness, traction, and fluorescence of lubricants in operating bearing contacts

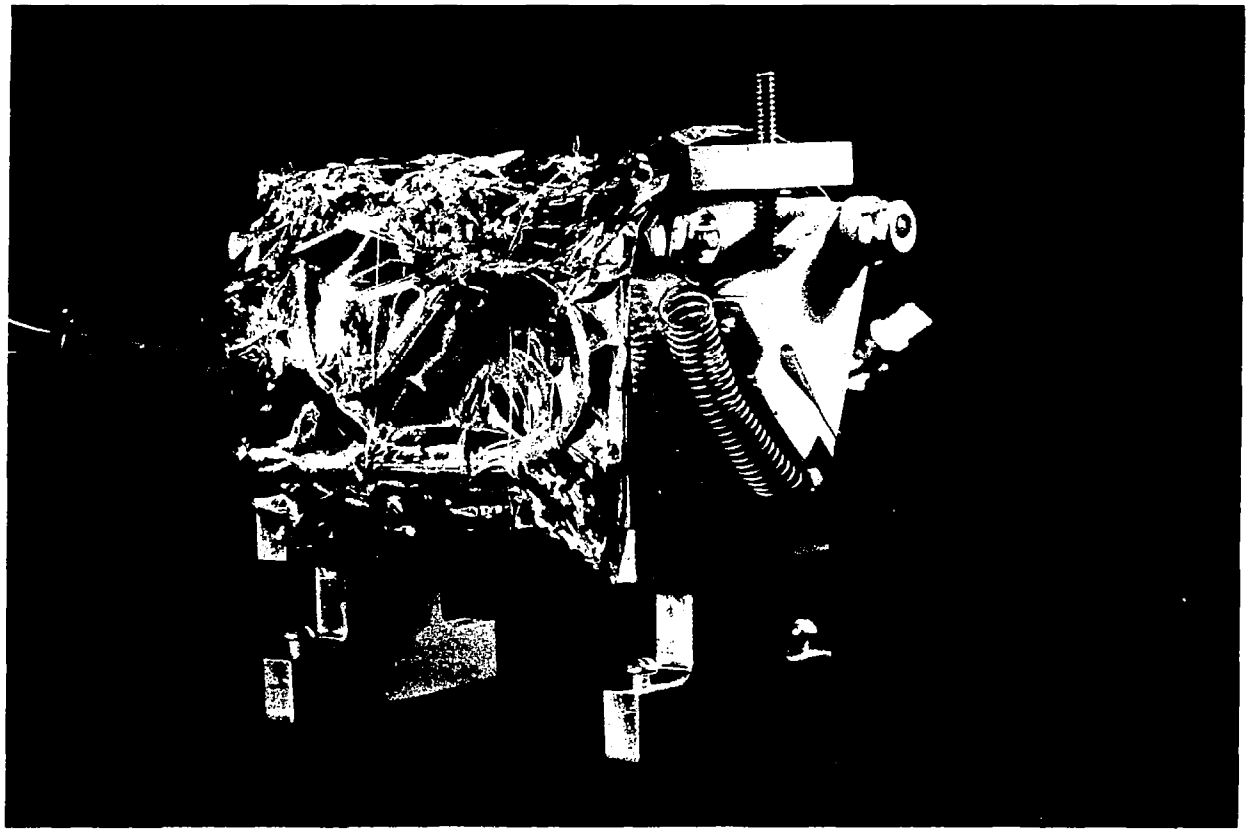

Figure 2 Standard Blackbody Source

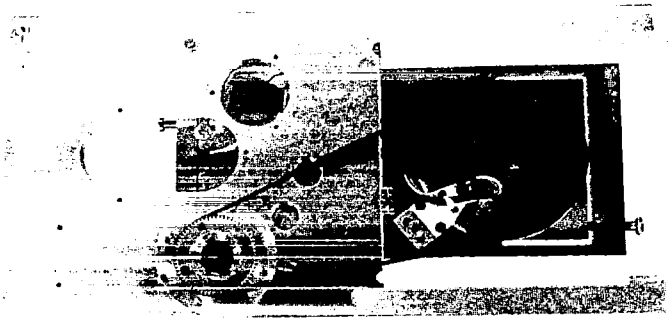

rotating polarizer

photocell reference pickup

Figure 3 Polarizing Chopper Wheel

Figure 4 Grating Infrared Spectrum of Santotrac P-40

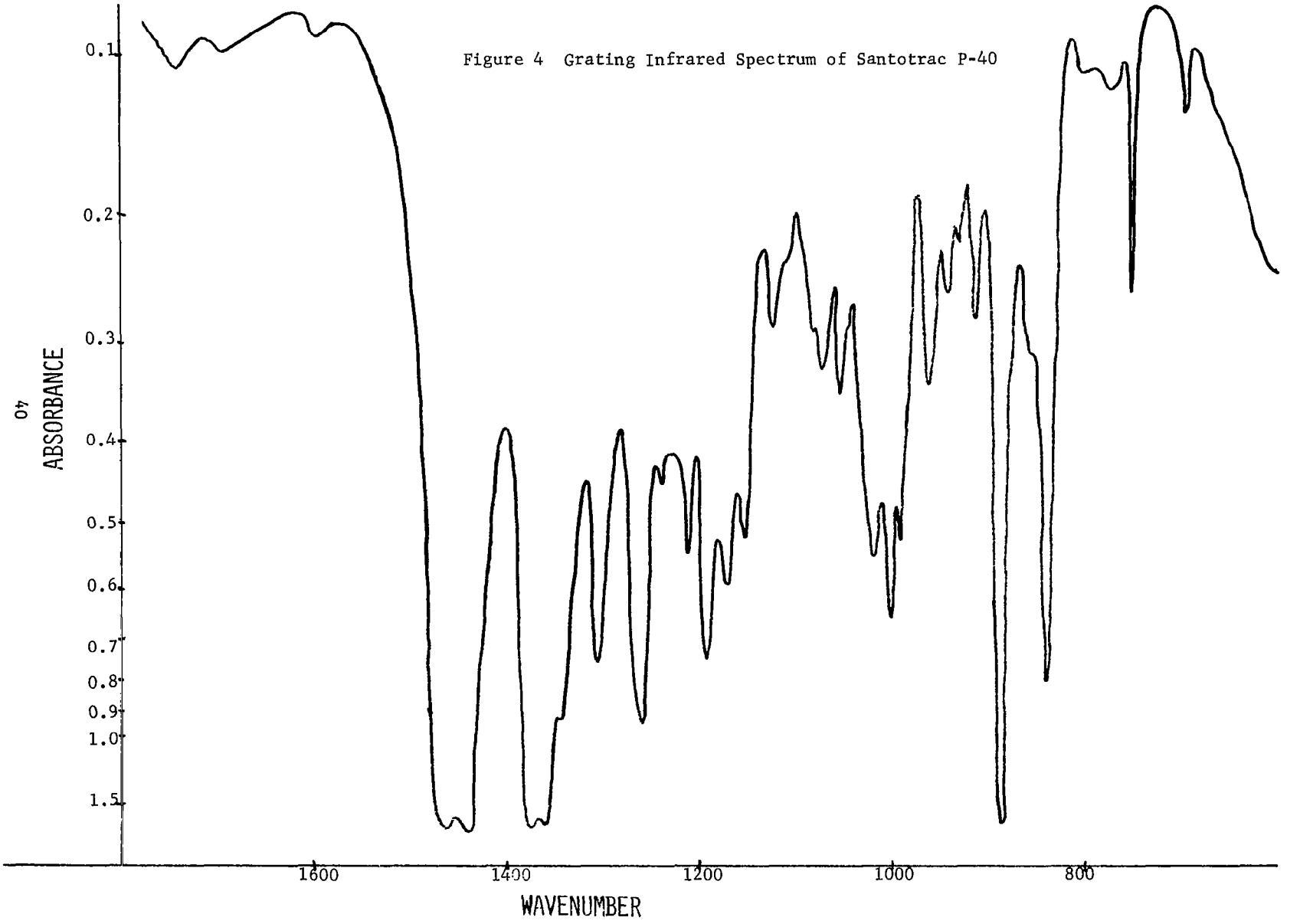

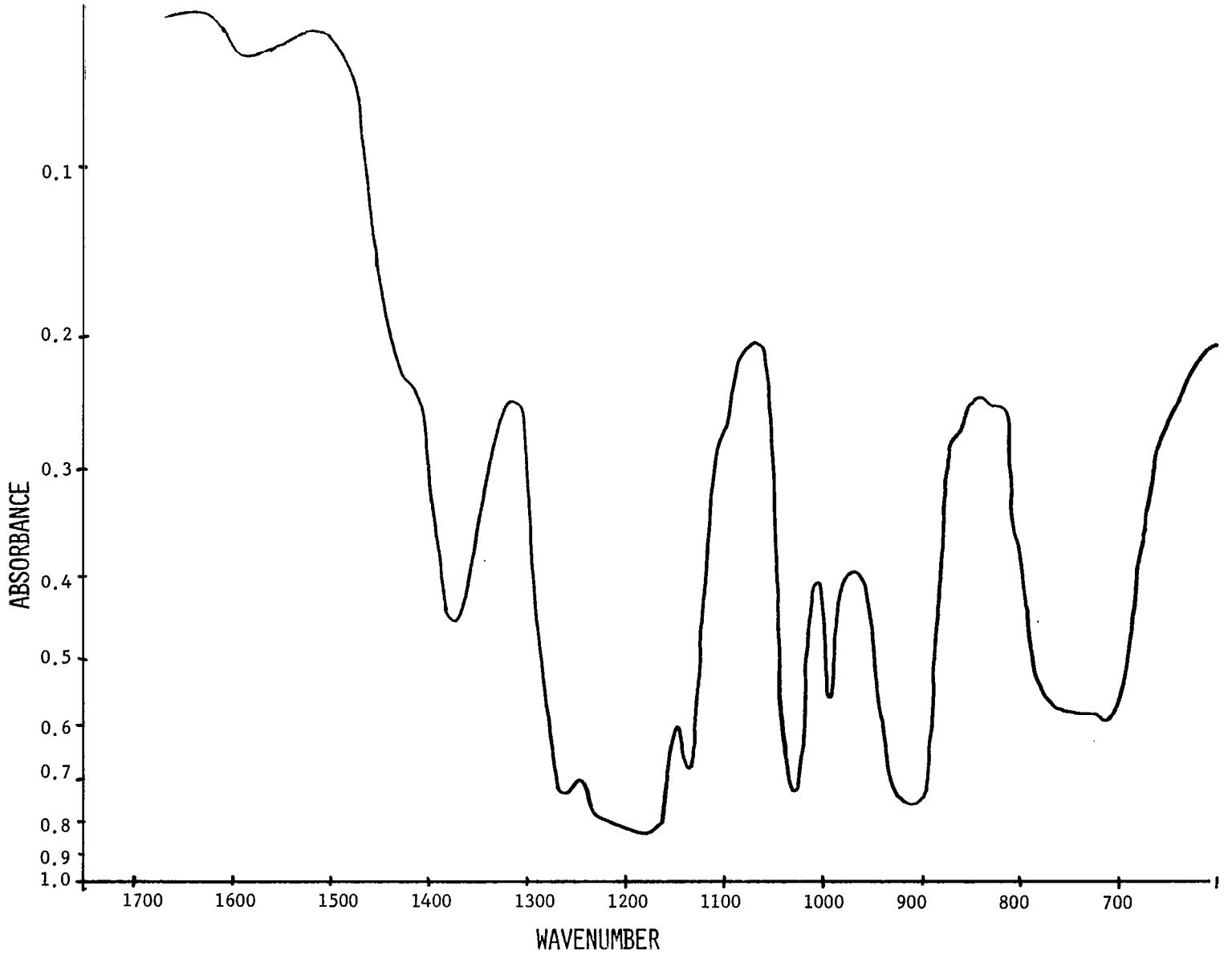

Figure 5 Grating Infrared Adsorption Spectrum of 1,1,2-Trichloroethane

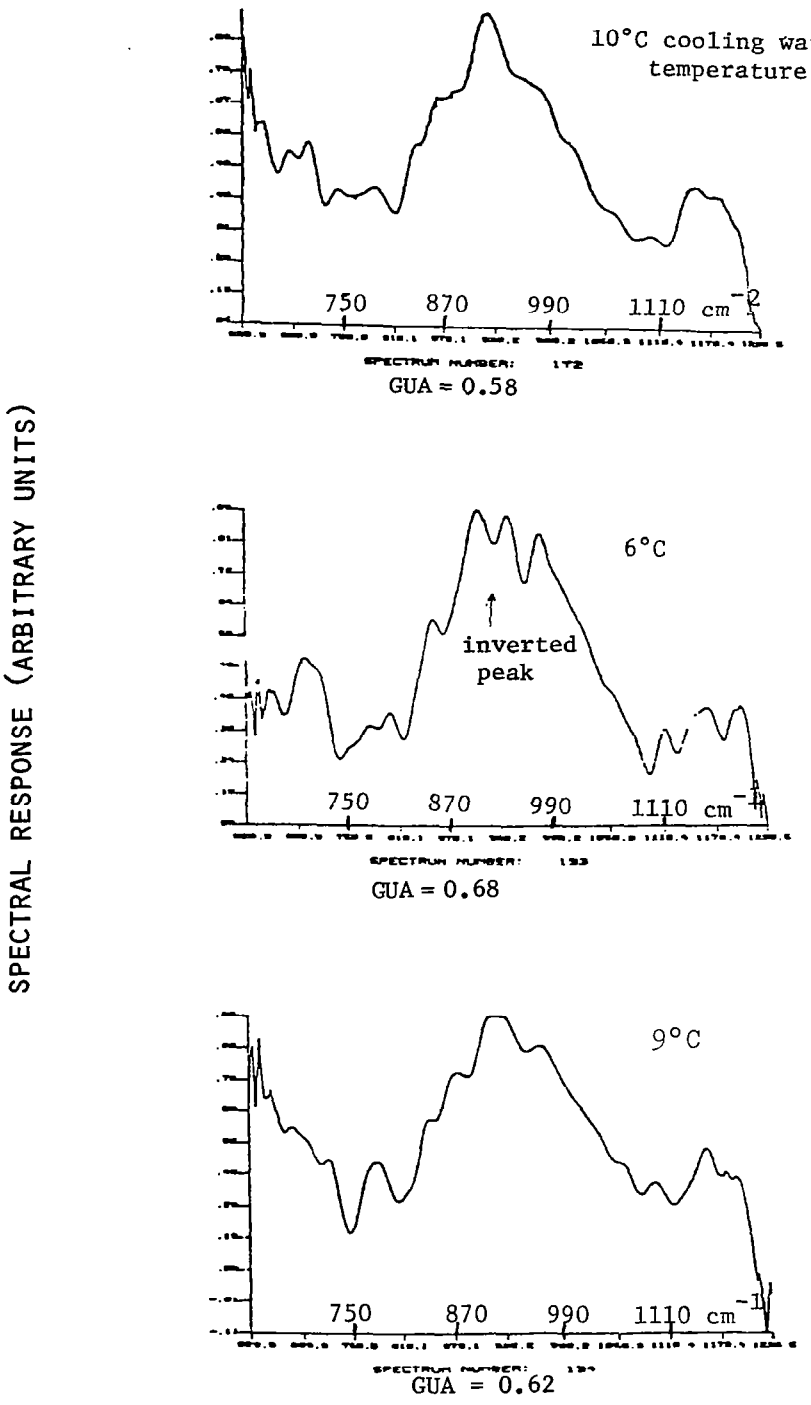

Figure 6 Comparison of Santotrac P-40 Spectra with Different Lubricant Temperatures 1/m/sec Linear Speed, ave. Hertzian Pressure 600 MPa, Not Polarized

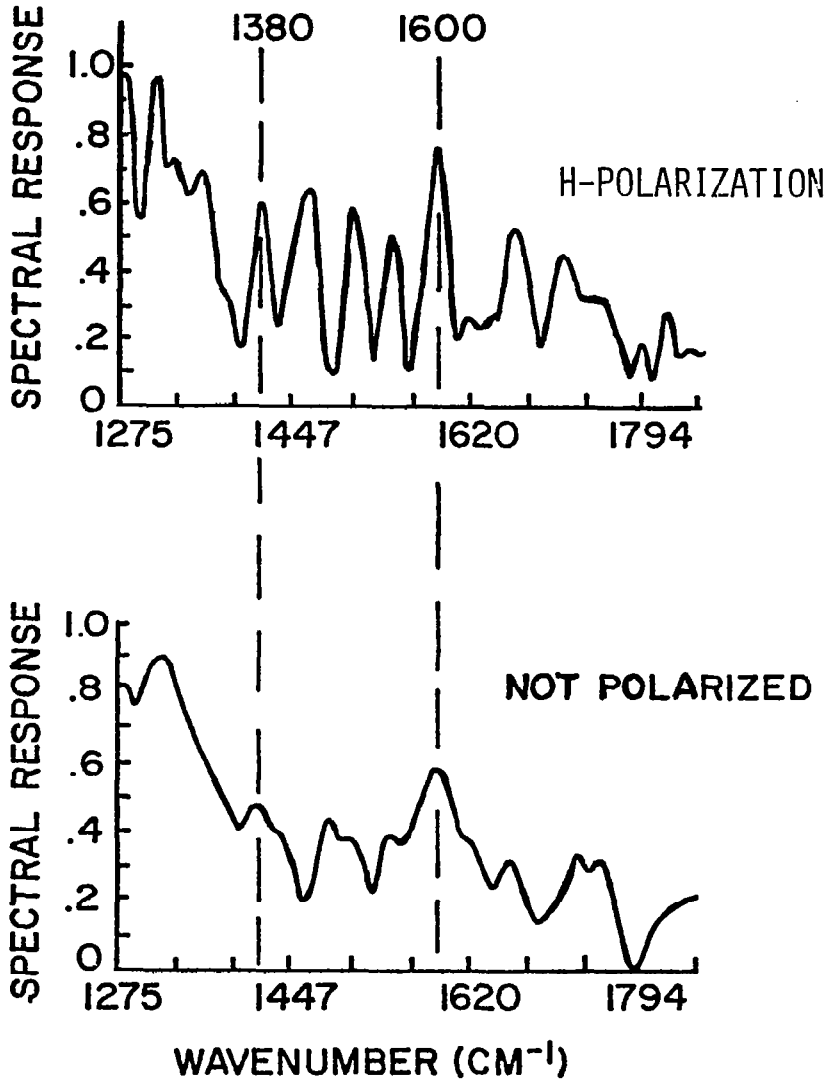

Figure 7 EHD spectra of Santotrac P-40 under high speed and load and with a ball that had much previous use. The upper spectrum was polarized in a plane perpendicular to the conjunction plane.

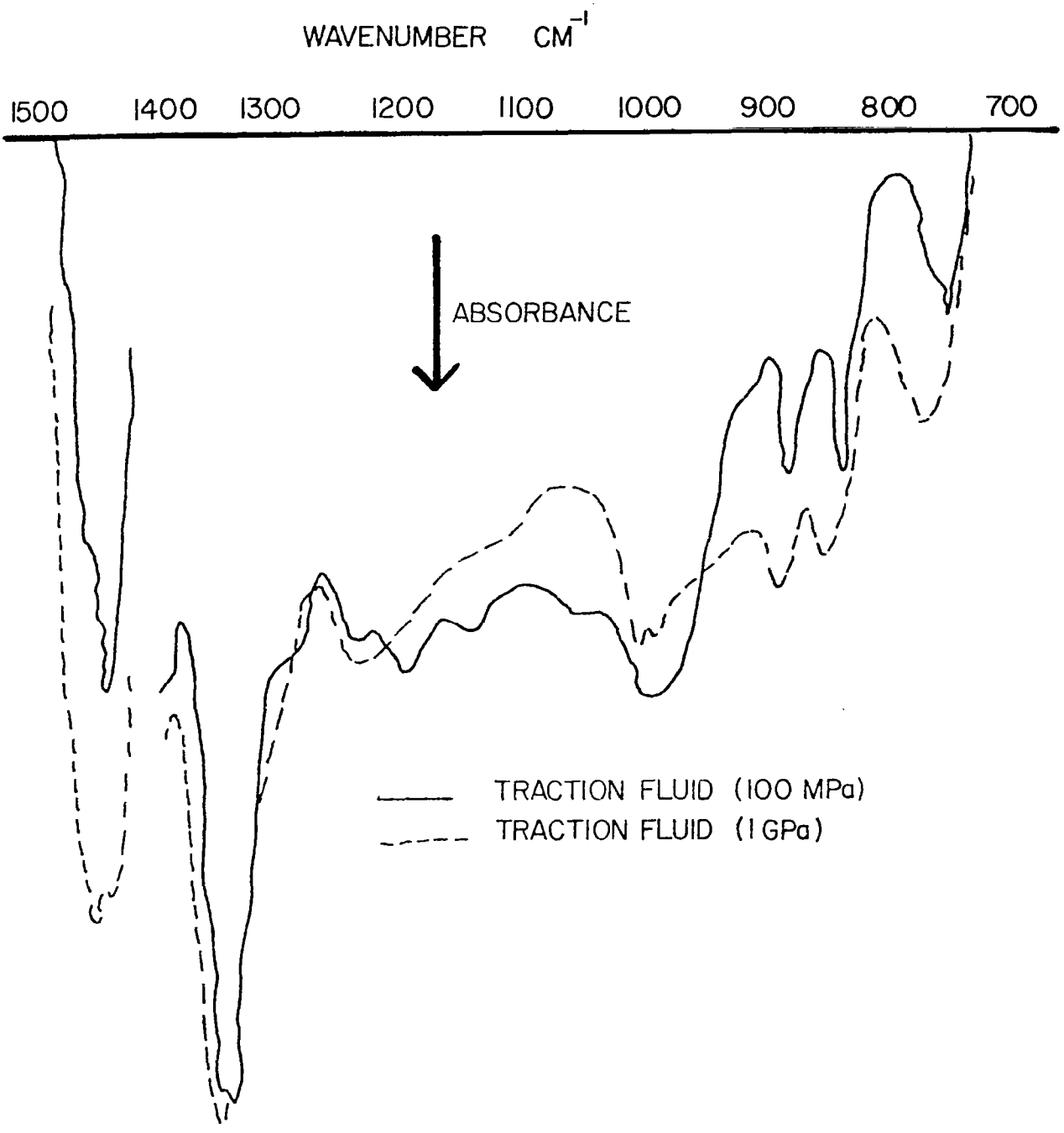

Figure 8 Diamond Cell Infrared Adsorption Spectra of Sun Company Traction Fluid under Pressure

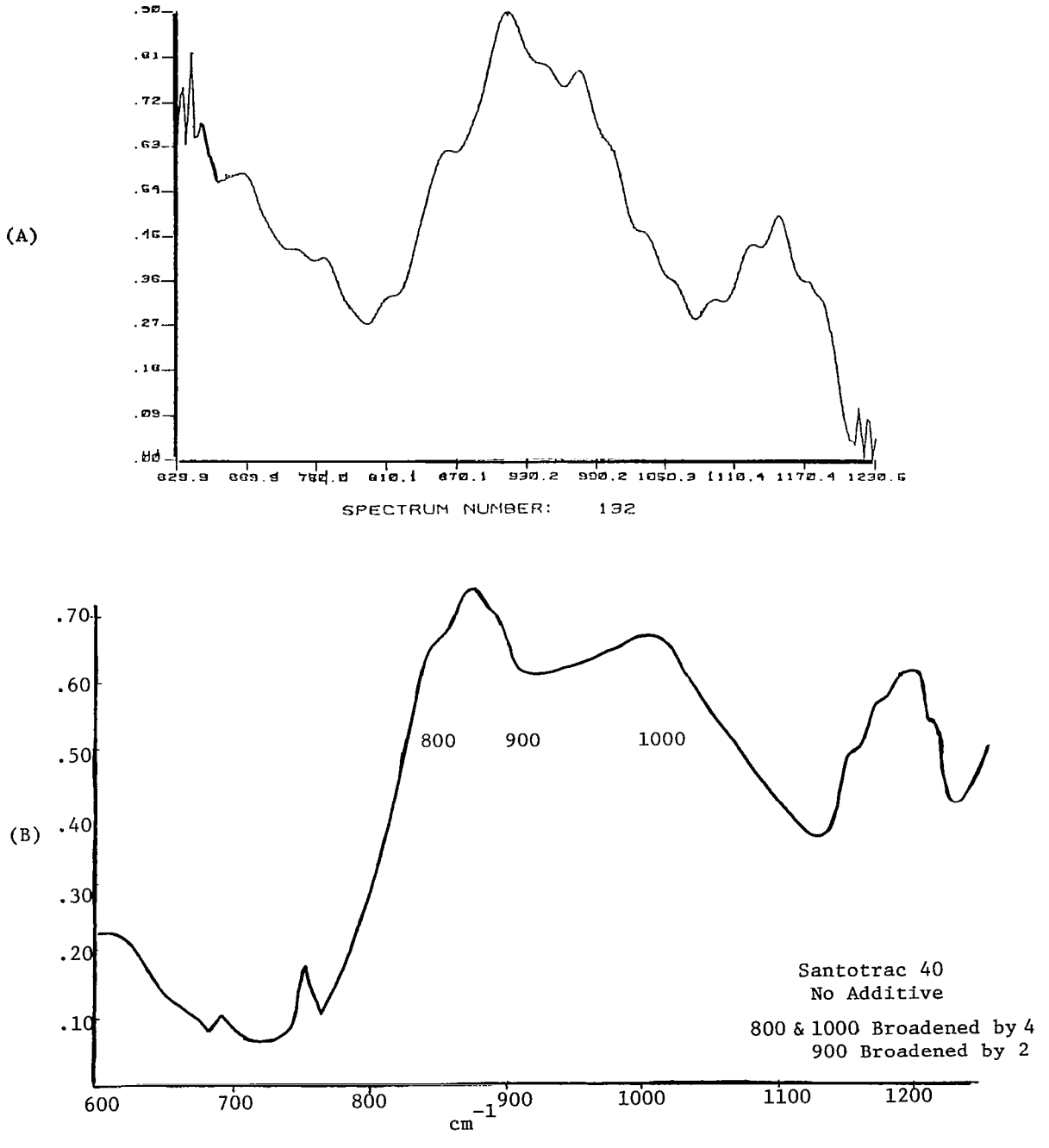

Figure 9 Infrared Emission Spectrum of Santotrac P-40 compared with broadened Absorption Spectrum

A) Emission Spectrum
B) Absorption Spectrum plotted as Absorbance against wave number

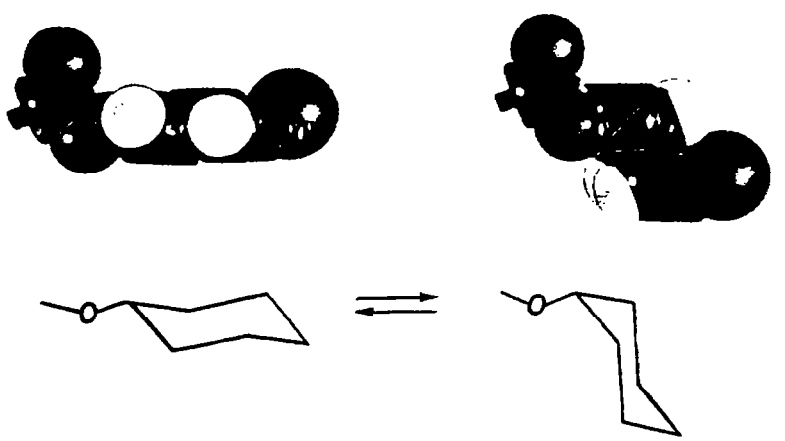

Figure 10 The Molecular Movement in the Cyclohexyl Group which Corresponds to the Secondary Transition (The oxygen atom shown schematically as a connecting link).

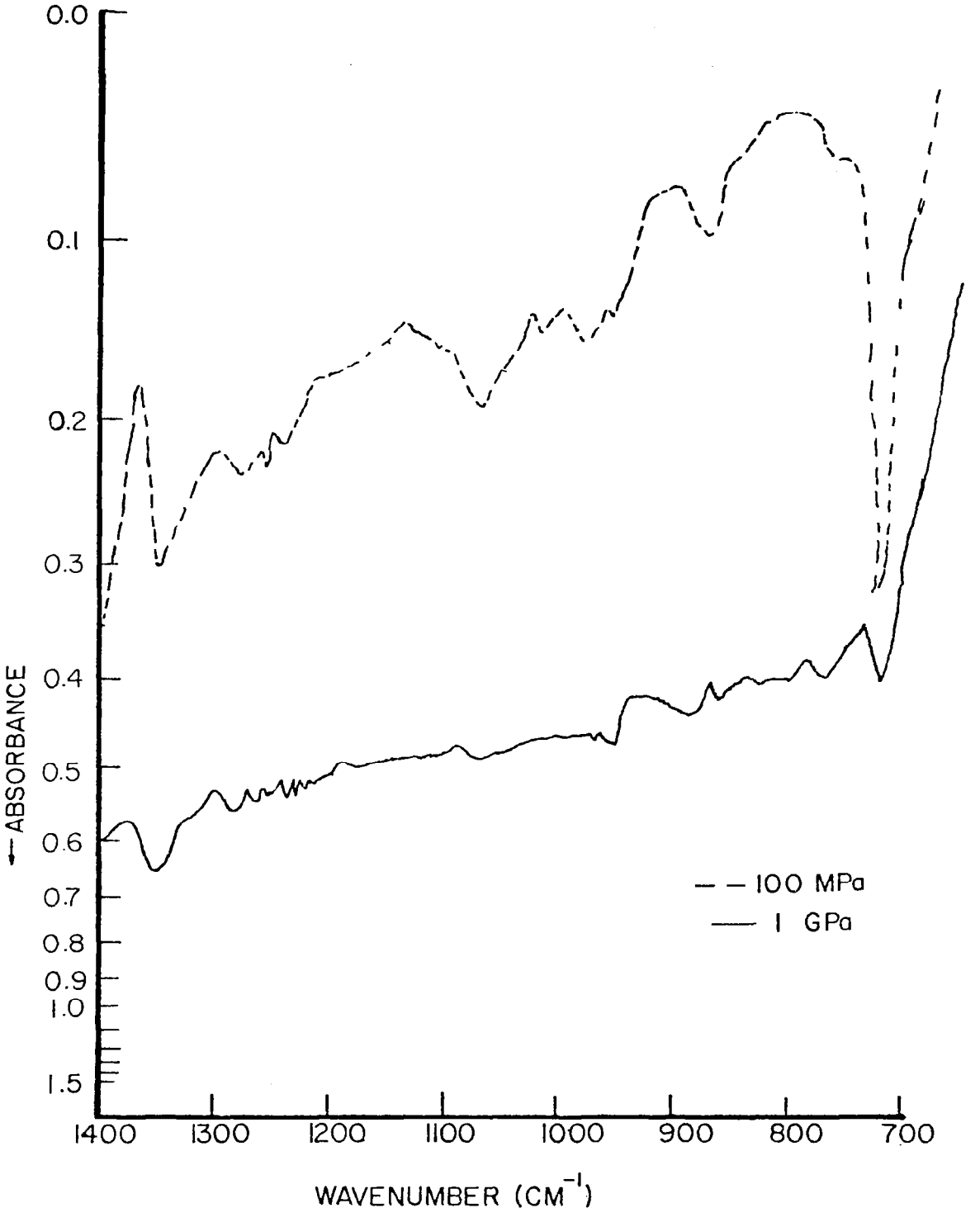

Figure 11 Diamond Cell Infrared Adsorption Spectra of Synthetic Paraffinic Oil

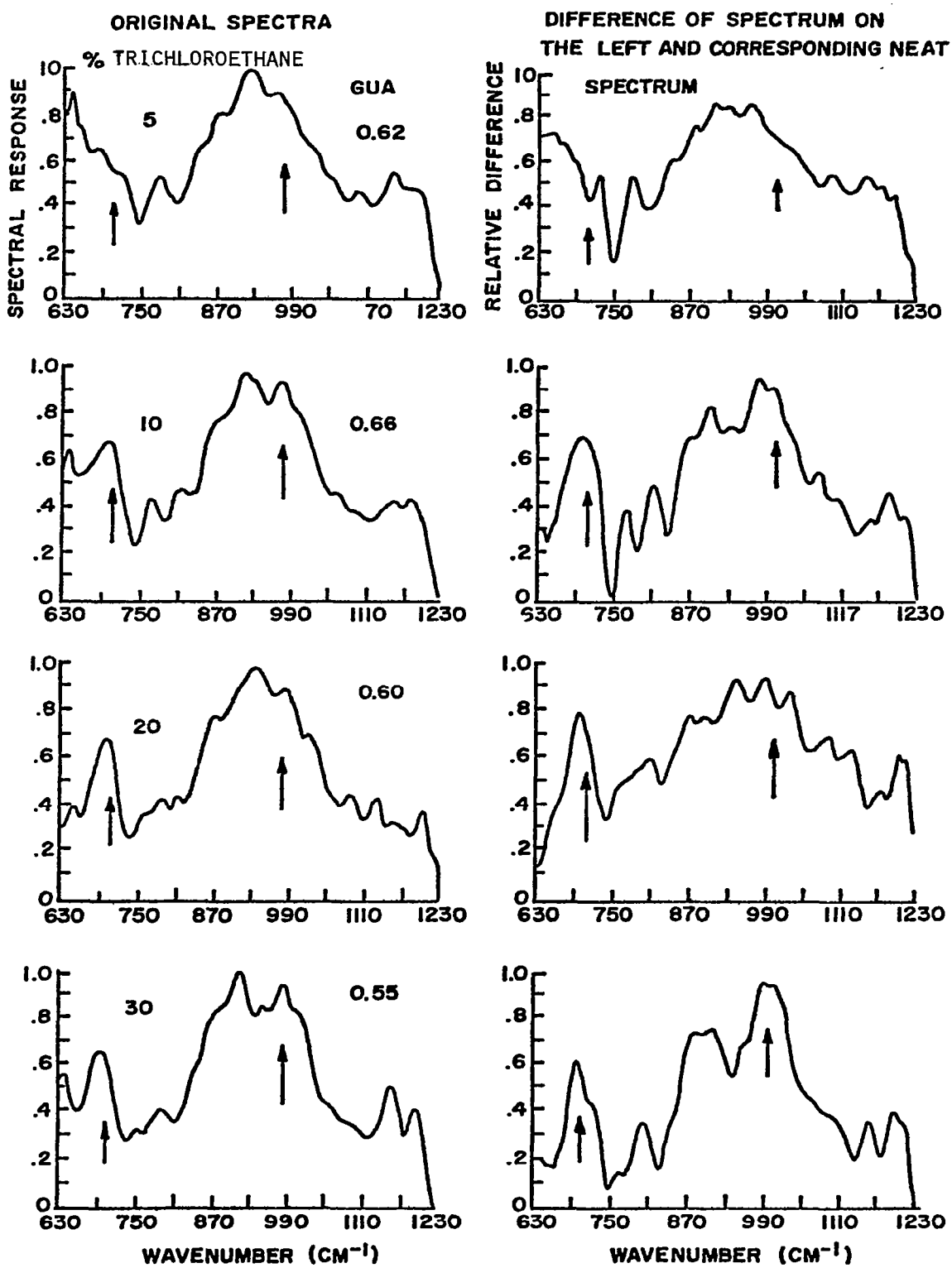

Figure 12 EHD Infrared Spectra of Traction Fluid Containing Various amounts of Trichloroethane

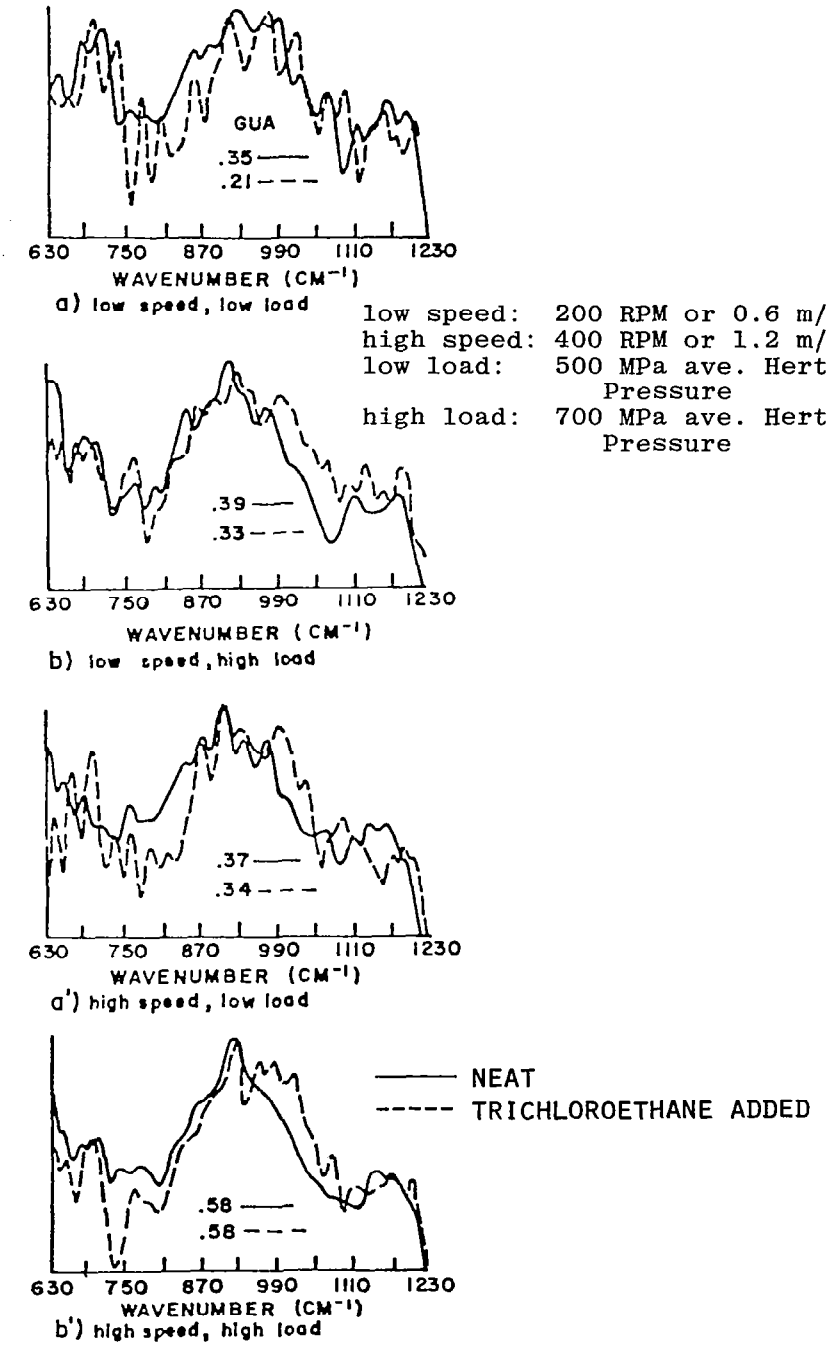

Figure 13 EHD Infrared Spectra of traction fluid, both neat (solid line) and containing 15% trichloroethane by volume (broken line). All spectra are normalized to an ordinate (spectral response) scale of unity; however, the greatest unnormalized spectral response (GUA) is given for comparison

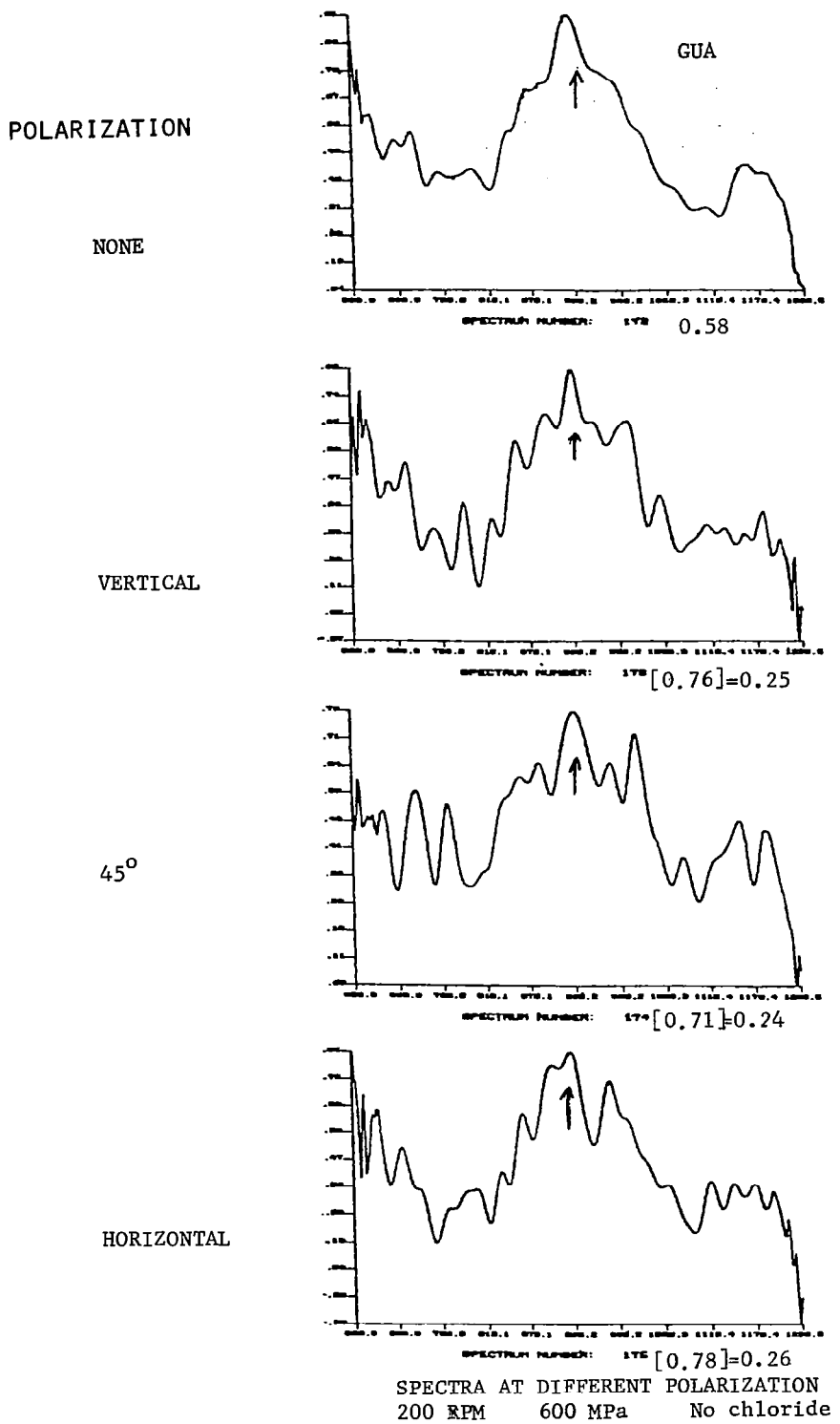

Figure 14 Effect of polarization plane angle variation on a Santotrac P-40 fluid EHD contact emission spectrum (the bracketed GUA's were obtained at different gain).

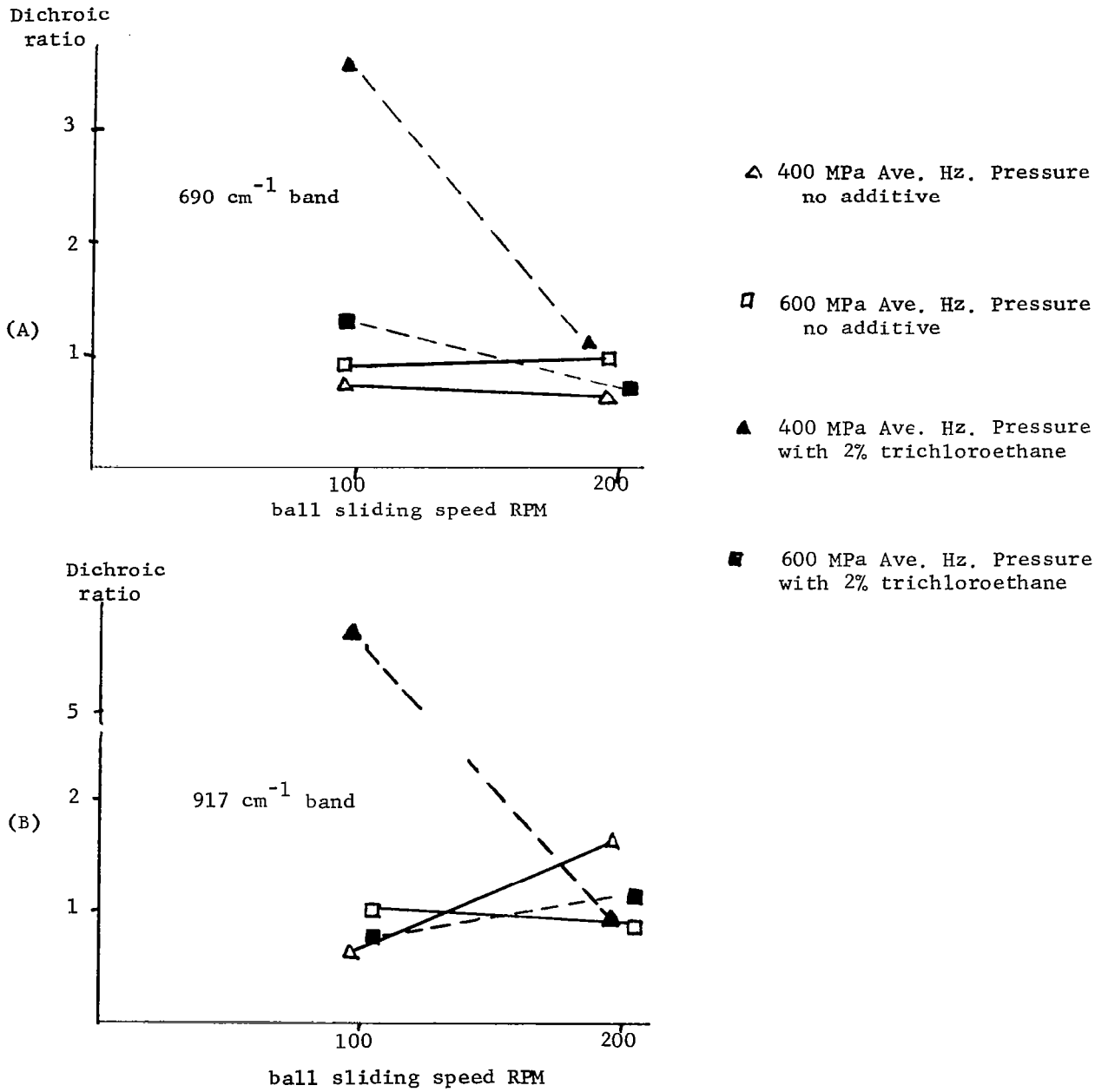

Figure 15 Relation between Dichroic ratio and Ball Speed for Different Loads with Santotrac P-40 and Trichloroethane Additive

(A)(B) 690 and 917 cm^{-1} bands resp.

(C)

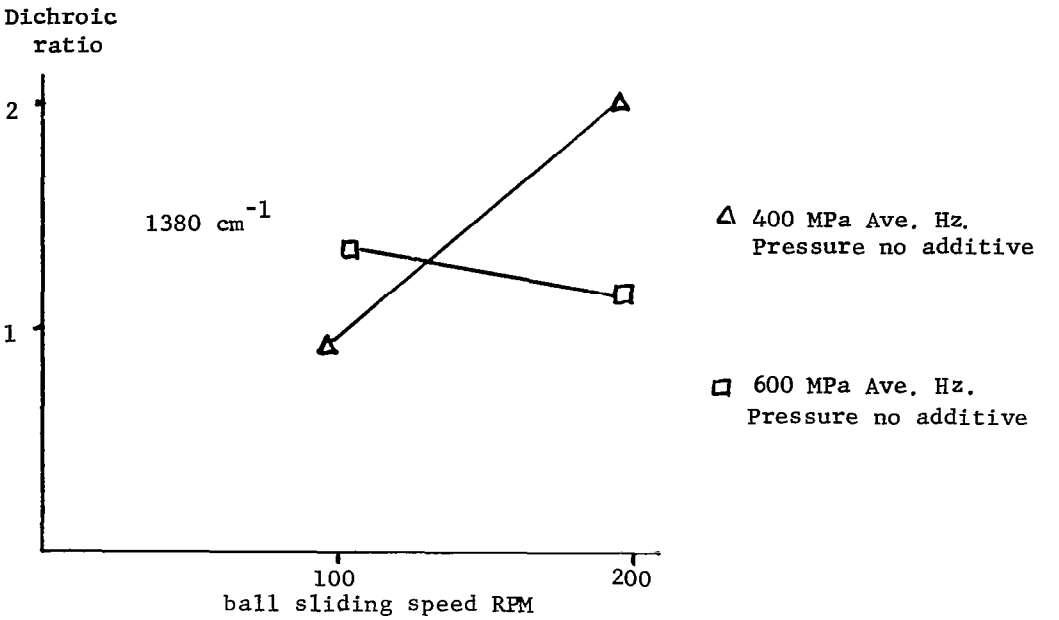

(D)

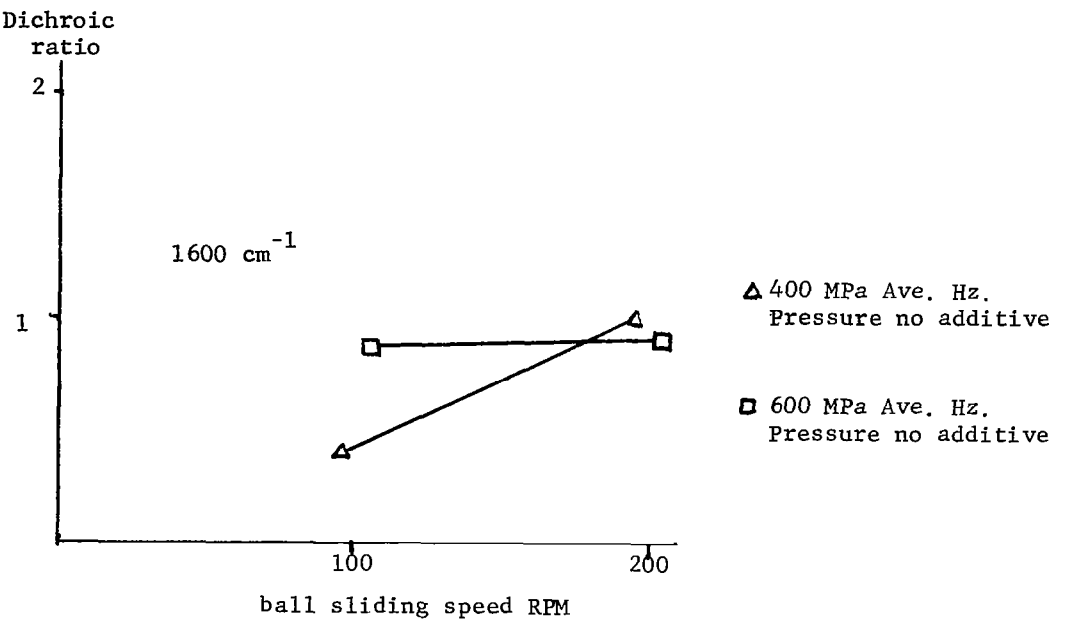

Figure 15b Relation between Dichroic ratio and Ball Speed for Different Loads with Santotrac P-40 and Trichloroethane Additive

(C)(D) 1380 and 1600 cm^{-1} bands resp.

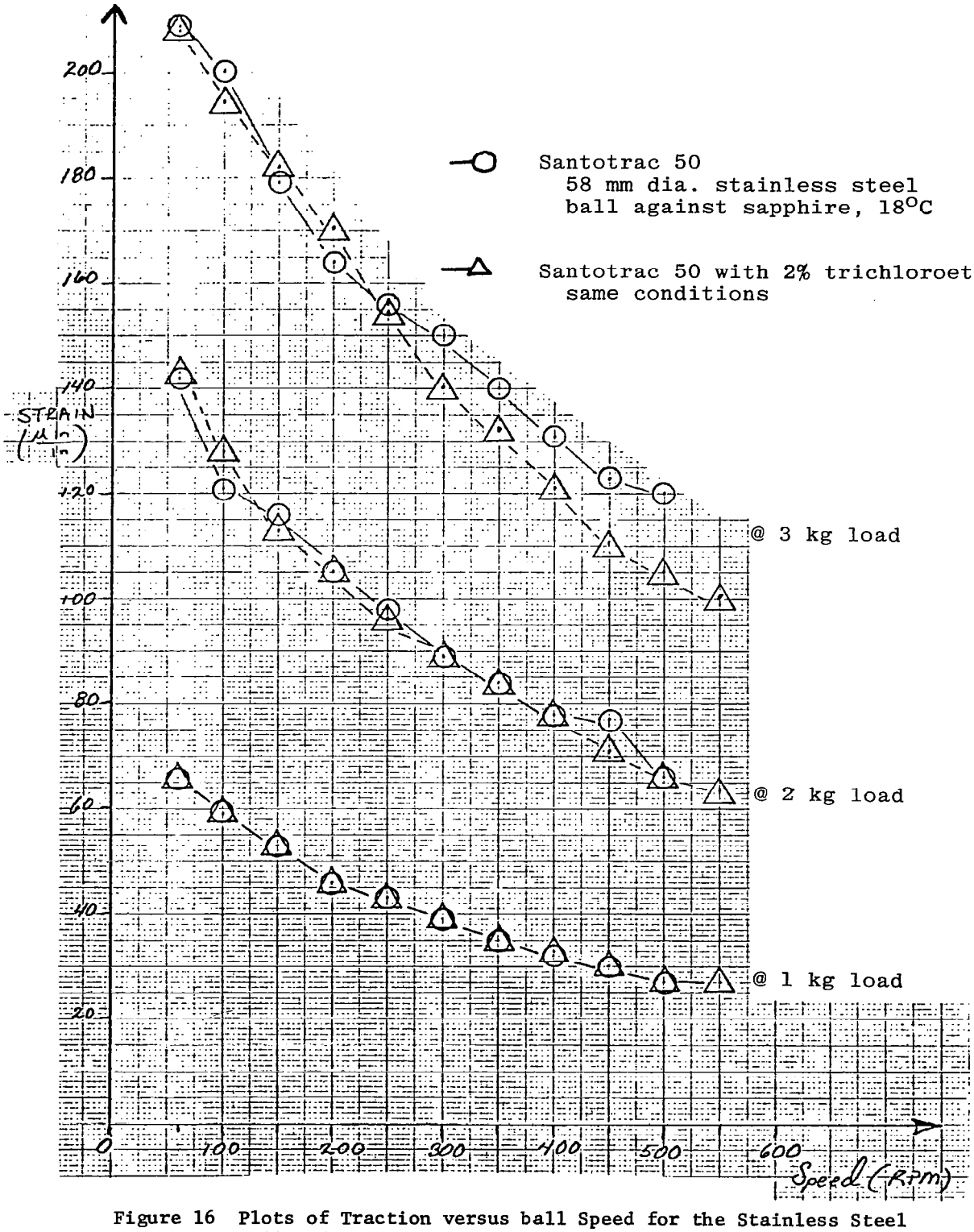

Figure 16 Plots of Traction versus ball Speed for the Stainless Steel Ball and Santotrac-50 Fluid with and without 2% of Trichloroethane at 18°C.

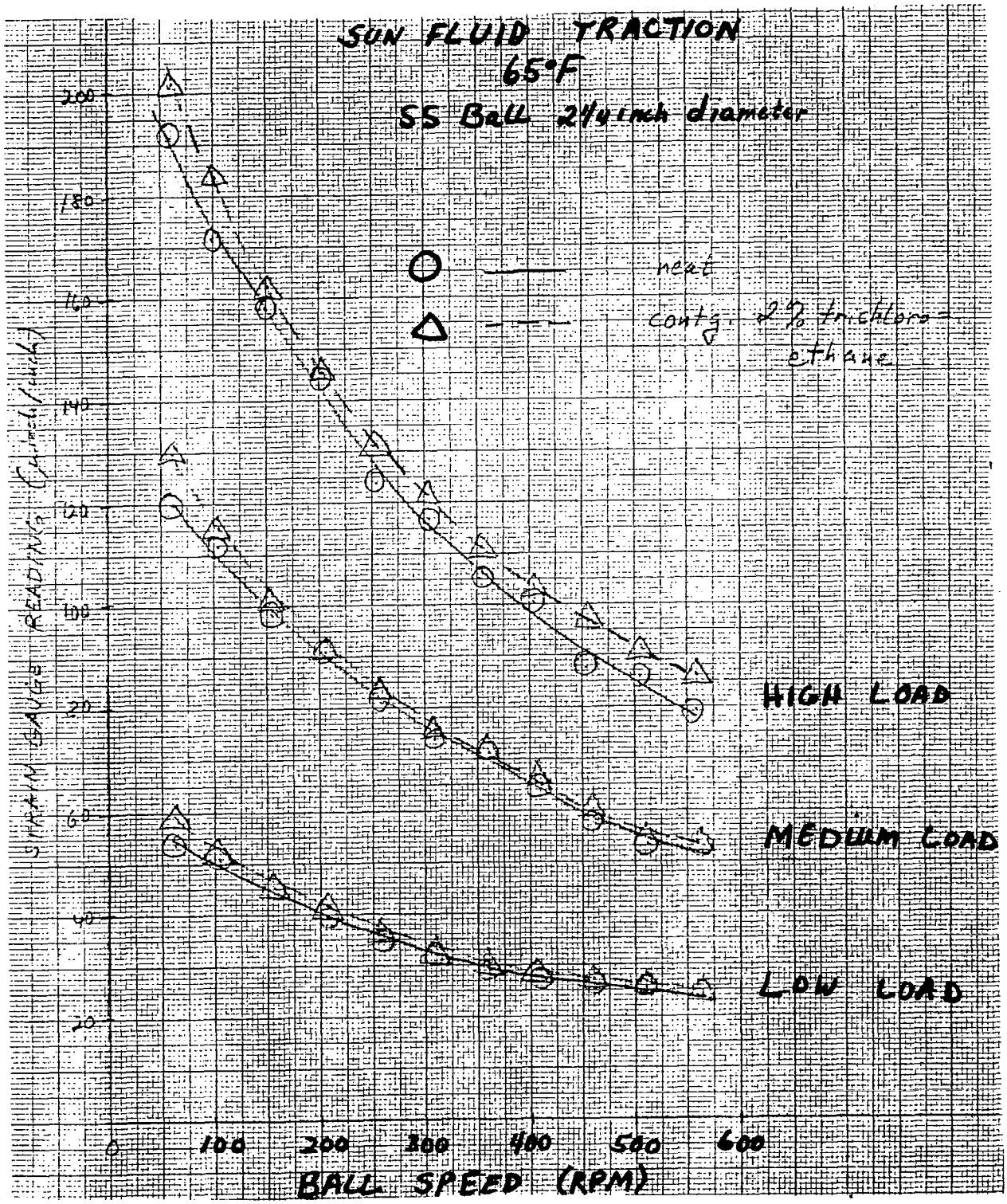

Figure 17 Plots of Traction versus Ball Speed for the Stainless Steel Ball and Sun Company Traction Fluid with and without 2% of Trichloroethane at 18°C.

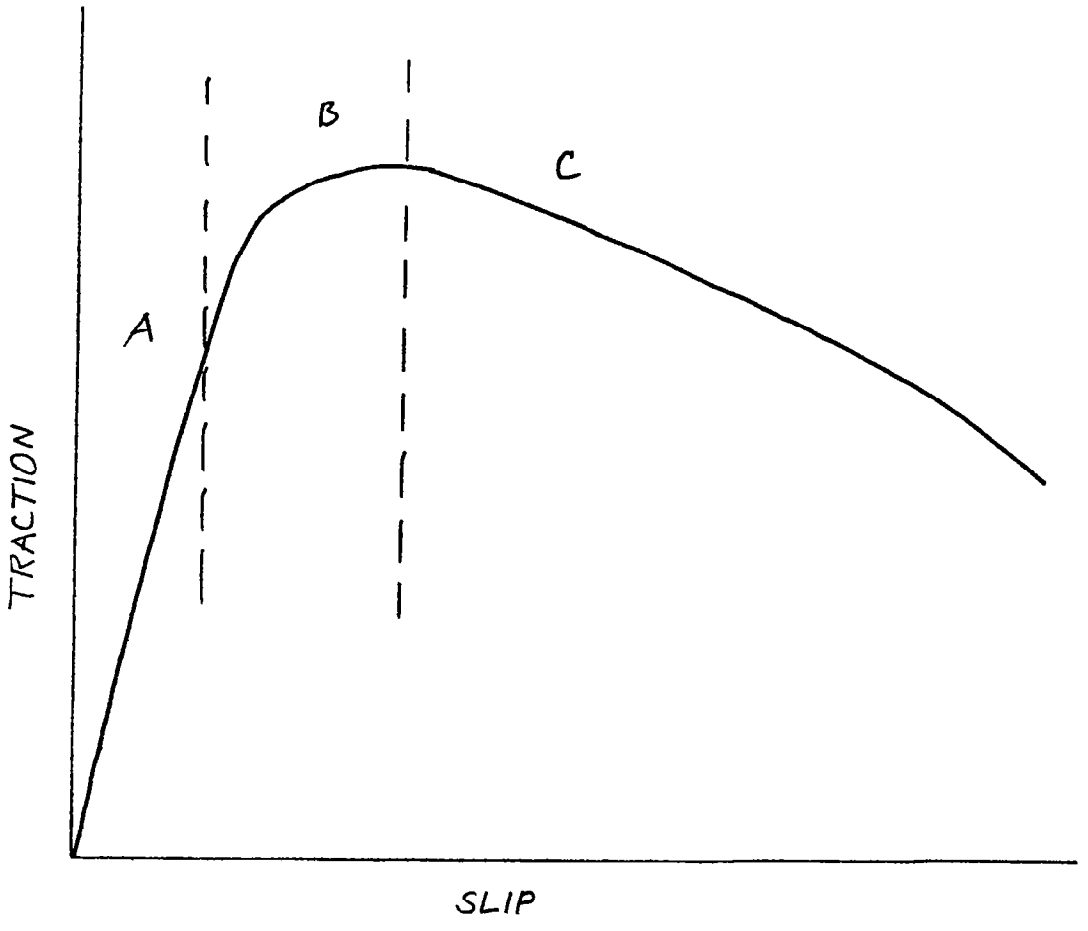

Figure 18 Typical Traction curve with three commonly designated regions. Region A, small strain linear region; Region B, isothermal non-linear region; Region C, thermally influenced region (after Tevaarwerk [5].)

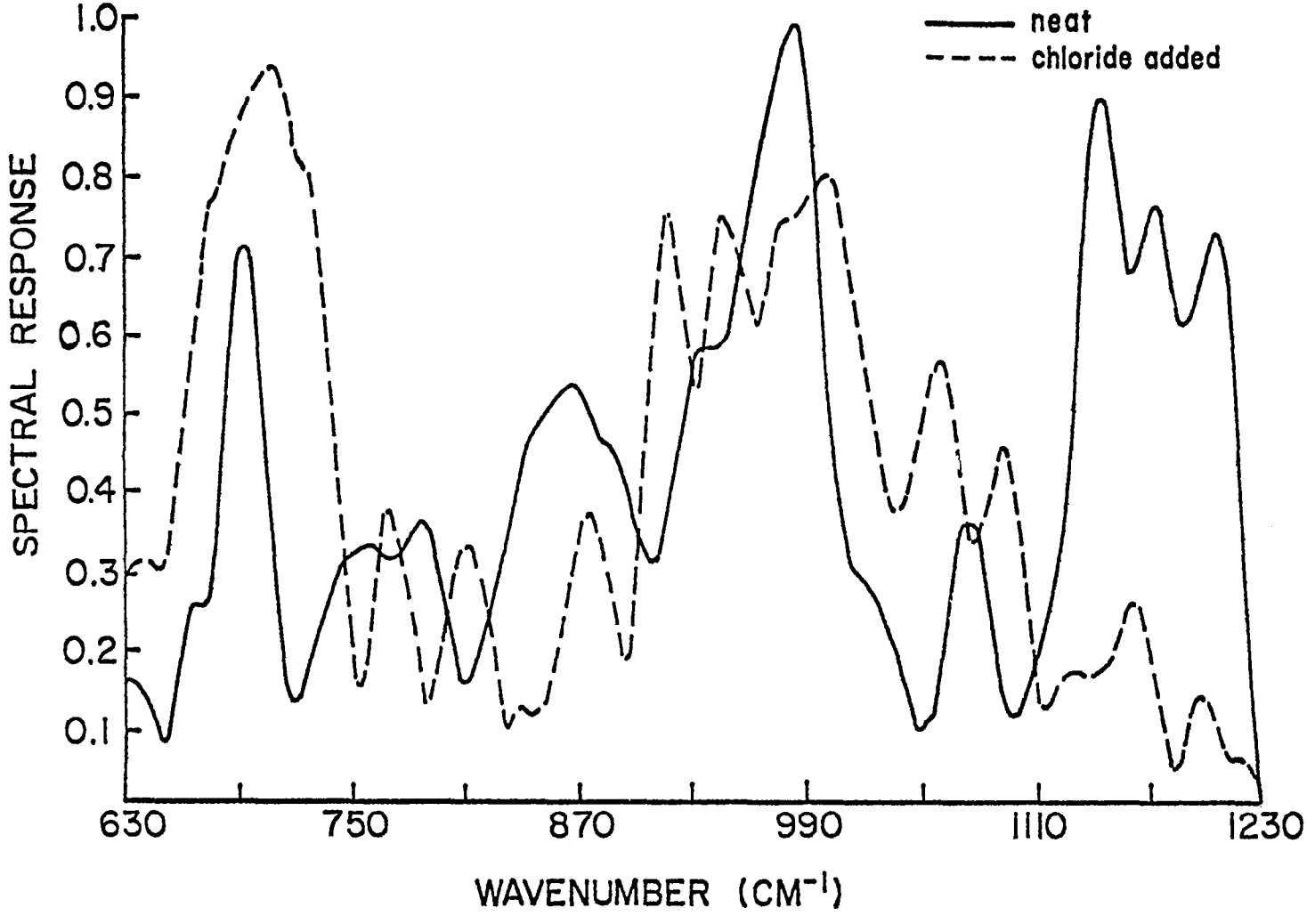

Figure 19 EHD spectra of 5P4E polyphenyl ether with a clean ball and with a ball containing absorbed chlorine on it surface

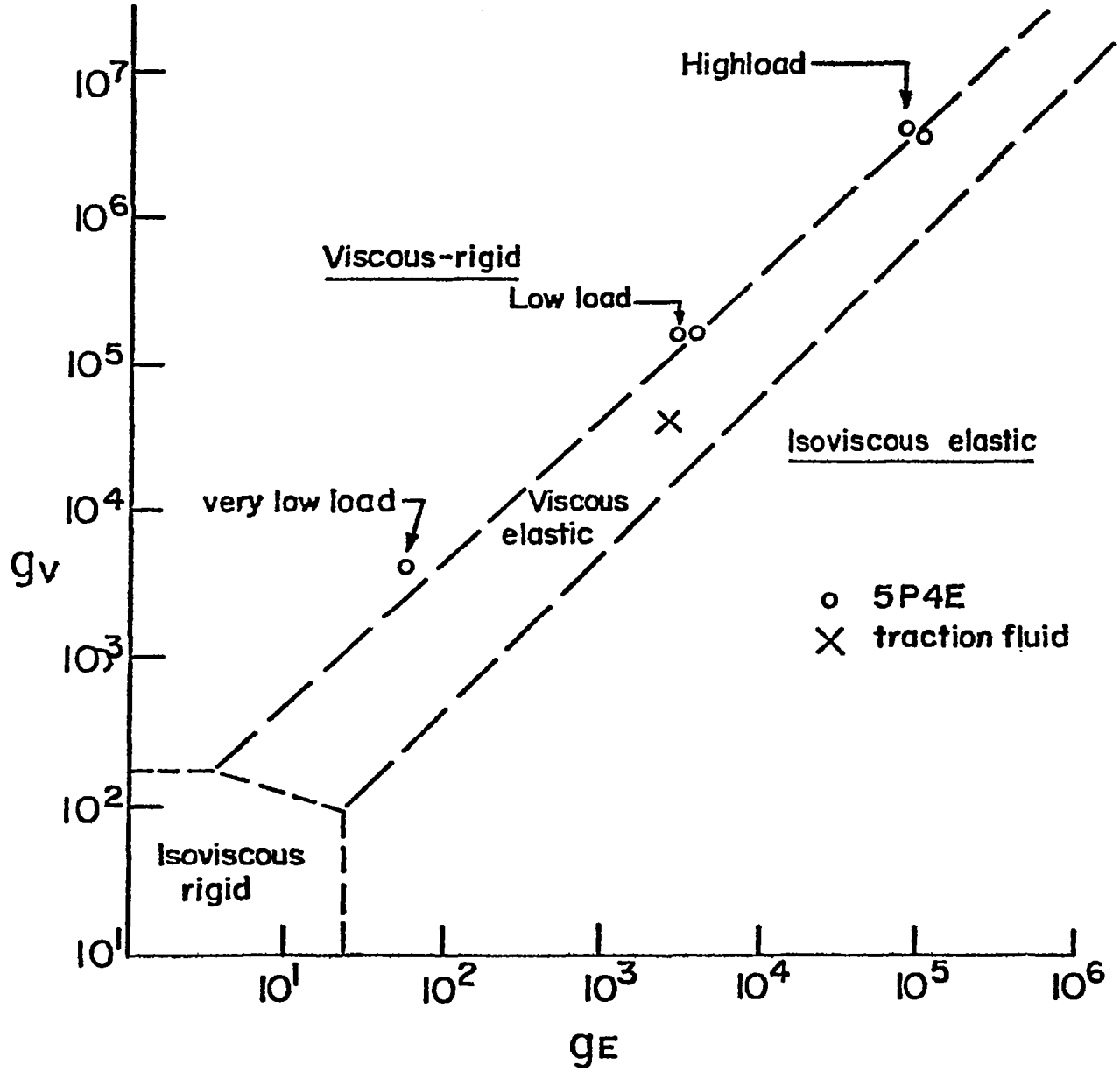

Figure 20 Lubrication regimes on log-log grid of dimensionless viscosity and elasticity parameters for a circular contact (after Hamrock and Dowson[6])

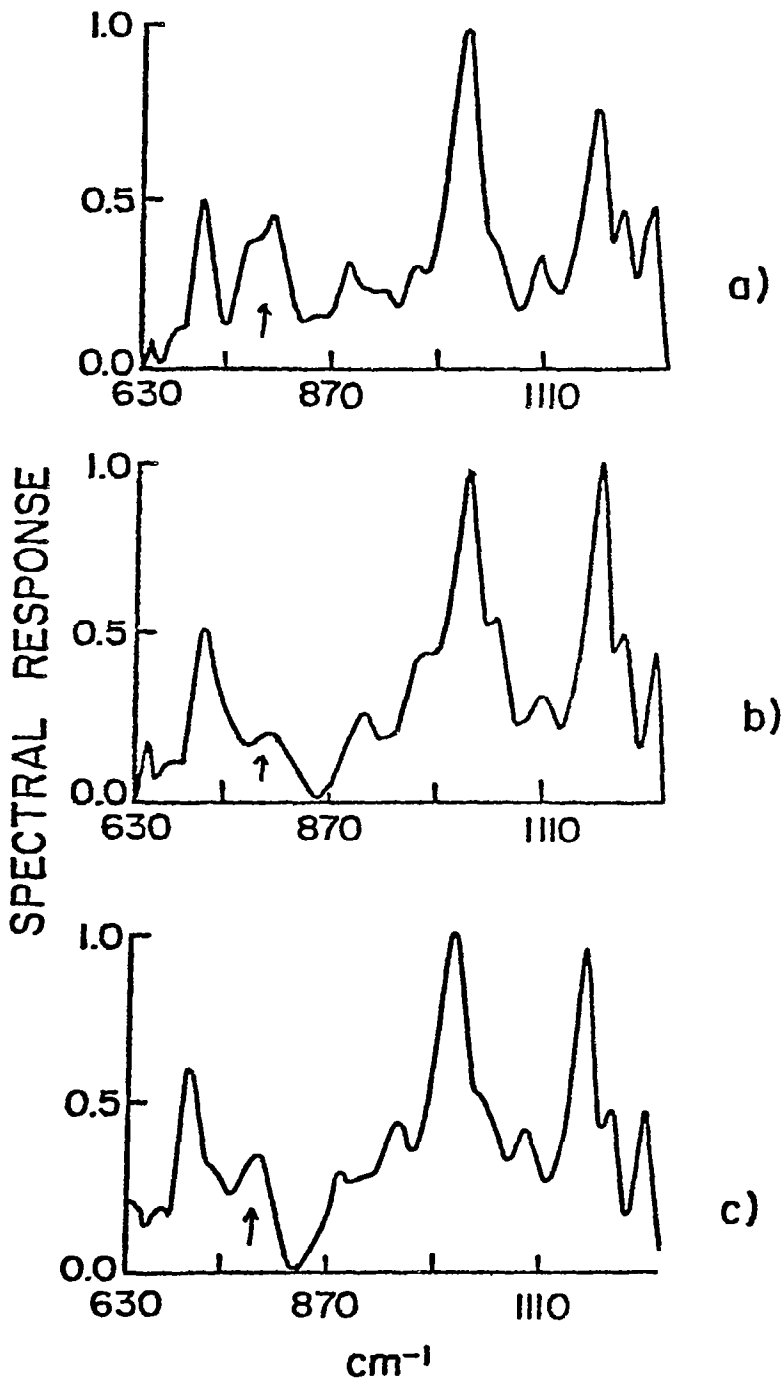

Figure 21 Infrared emission spectra of 5P4E from the ball/plate conjunction
(a) low speed (200 RPM) and low load (400 MPa Ave. Hz. pressure)
(b) low speed (200 RPM) and high load (600 MPa Ave. Hz. pressure)
(c) high speed (400 RPM) and high load (600 MPa Ave. Hz. pressure)

Note the arrow pointing to the 780 cm^{-1} band

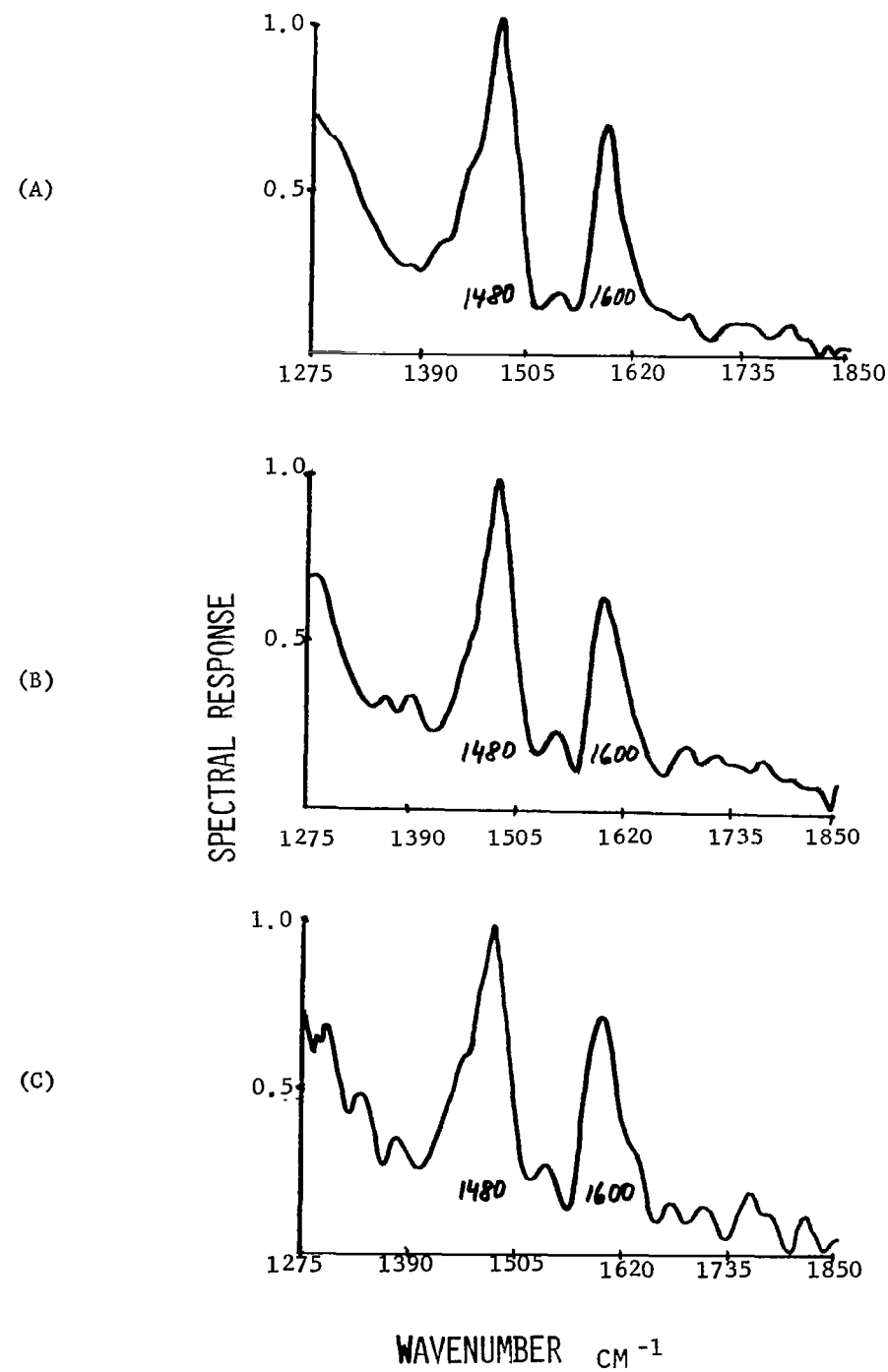

Figure 22 Infrared emission spectra (1250 - 1850 cm^{-1}) of 5P4E polyphenyl ether (stainless steel ball, 1.2 m/s, 700 MPa)

(A) not polarized
(B) polarized along the conjunction line
(C) polarized normal to the conjunction line

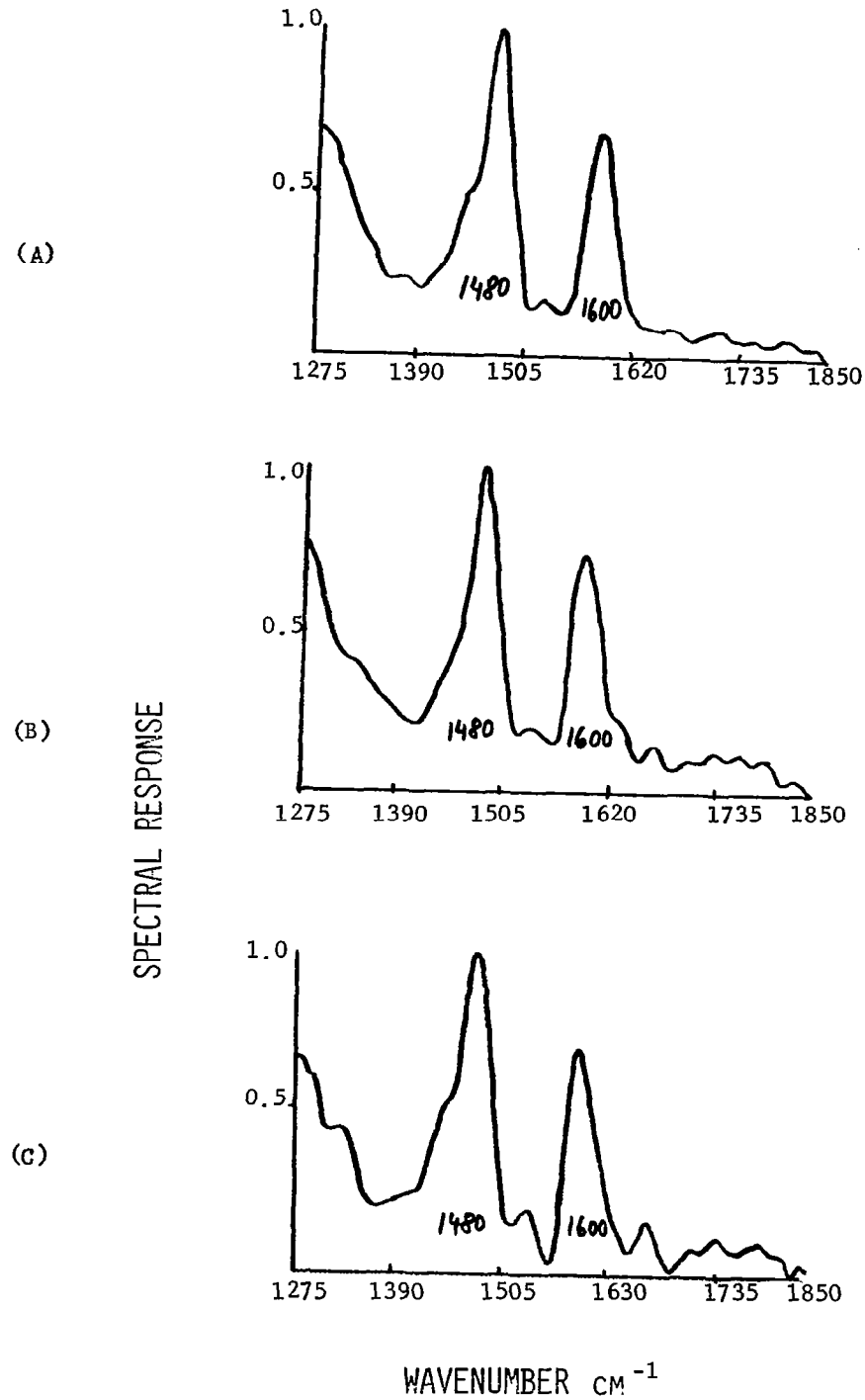

Figure 23 Infrared emission spectra (1250 - 1850 cm^{-1}) of 5P4E polyphenyl ether containing 3% of trichloroethane (stainless steel ball, 1.2 m/s, 700 MPa)

(A) not polarized
(B) polarized along the conjunction line
(C) polarized normal to the conjunction line

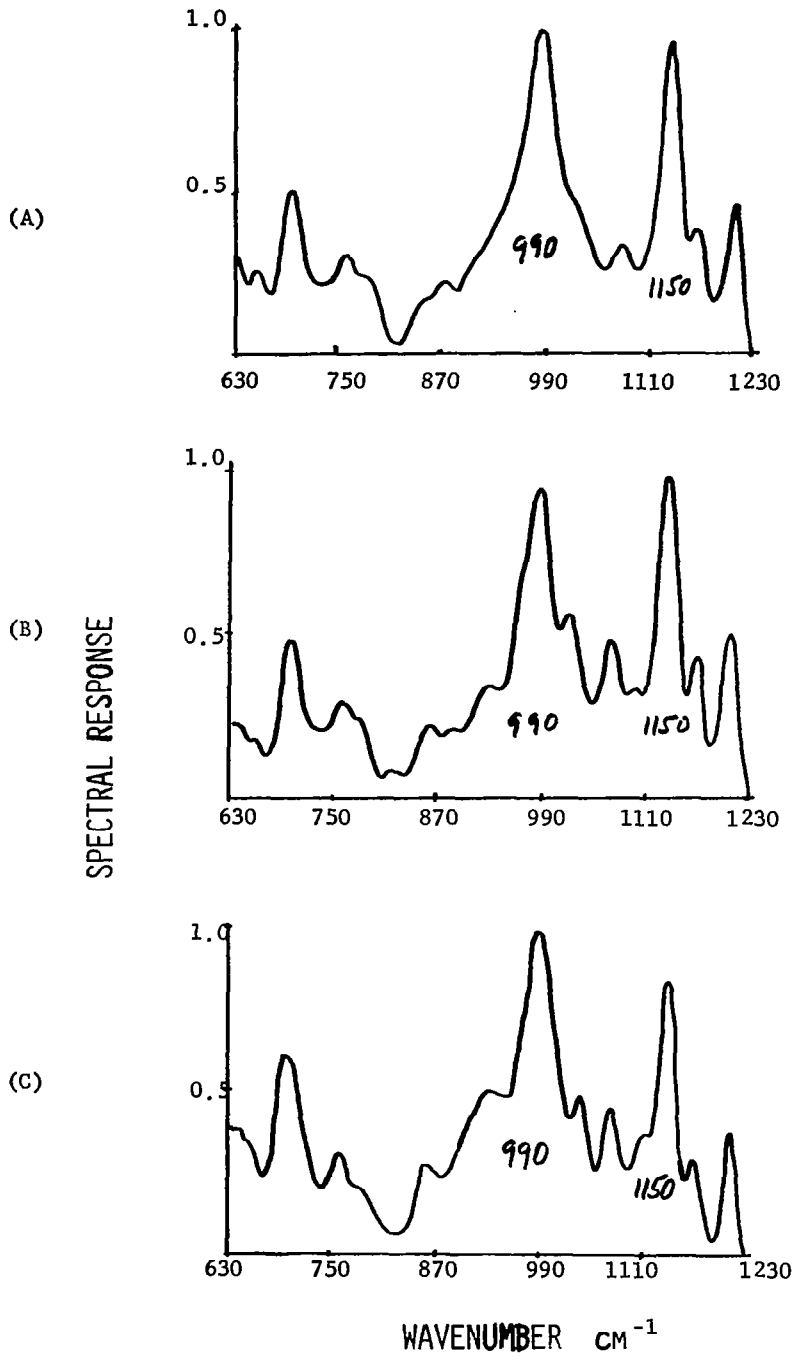

Figure 24 Infrared emission spectra (630 - 1230 cm^{-1}) of 5P4E polyphenyl ether (stainless steel ball, 1.2 m/s, 700 MPa)

(A) not polarized
(B) polarized along the conjunction line
(C) polarized normal to the conjunction line

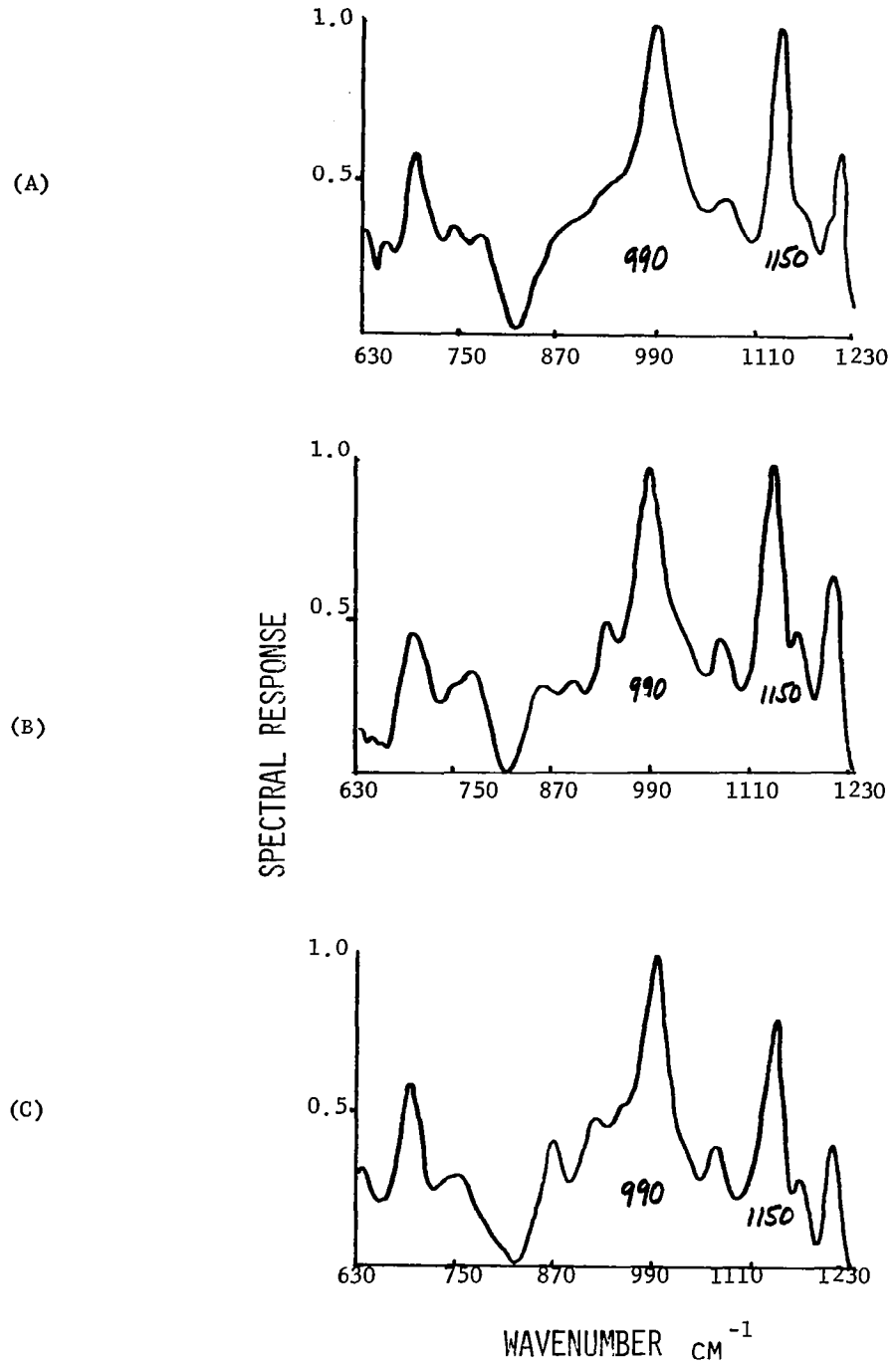

Figure 25 Infrared emission spectra (630 - 1230 cm^{-1}) of 5P4E polyphenyl ether containing 3% of trichloroethane (stainless steel ball, 1.2 m/s, 700 MPa)

(A) not polarized
(B) polarized along the conjunction line
(C) polarized normal to the conjunction line

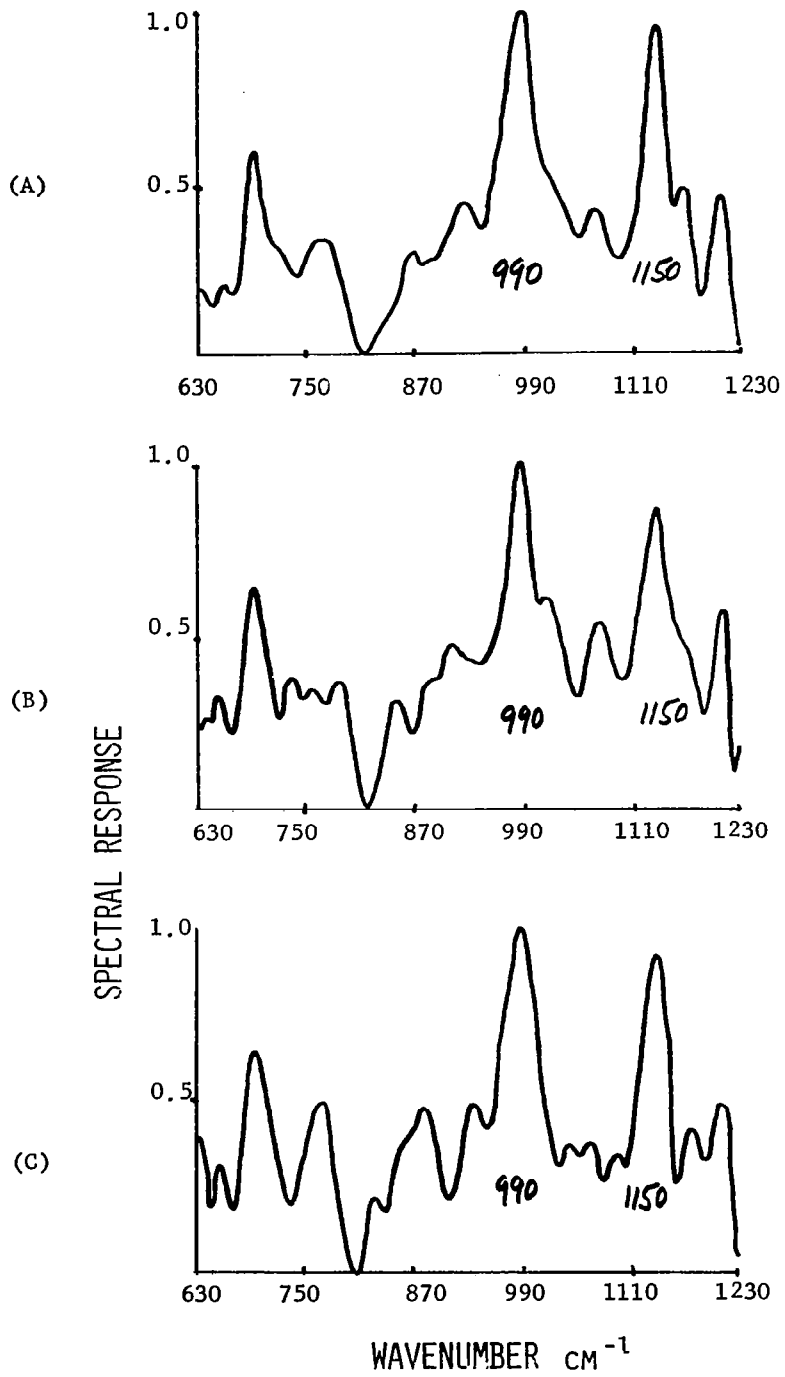

Figure 26 Infrared emission spectra (630-1230 cm^{-1}) of 5P4E polyphenyl ether (stainless steel ball, 1.2 m/s, 500 MPa)

(A) not polarized
(B) polarized along the conjunction line
(C) polarized normal to the conjunction line

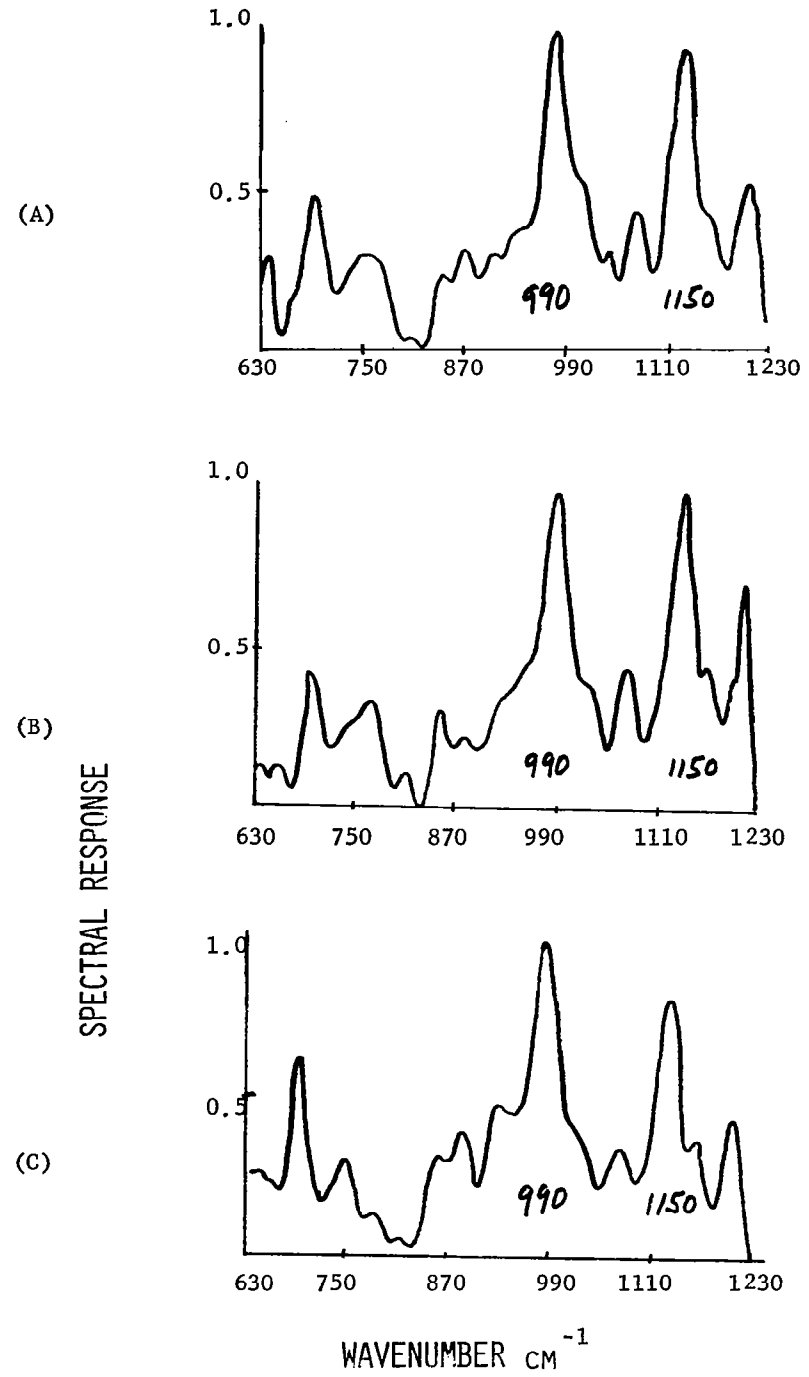

Figure 27 Infrared emission spectra (630 - 1230 cm^{-1}) of 5P4E polyphenyl ether containing 3% of trichloroethane (stainless steel ball, 1.2 m/s, 500 MPa)

(A) not polarized
(B) polarized along the conjunction line
(C) polarized normal to the conjunction line

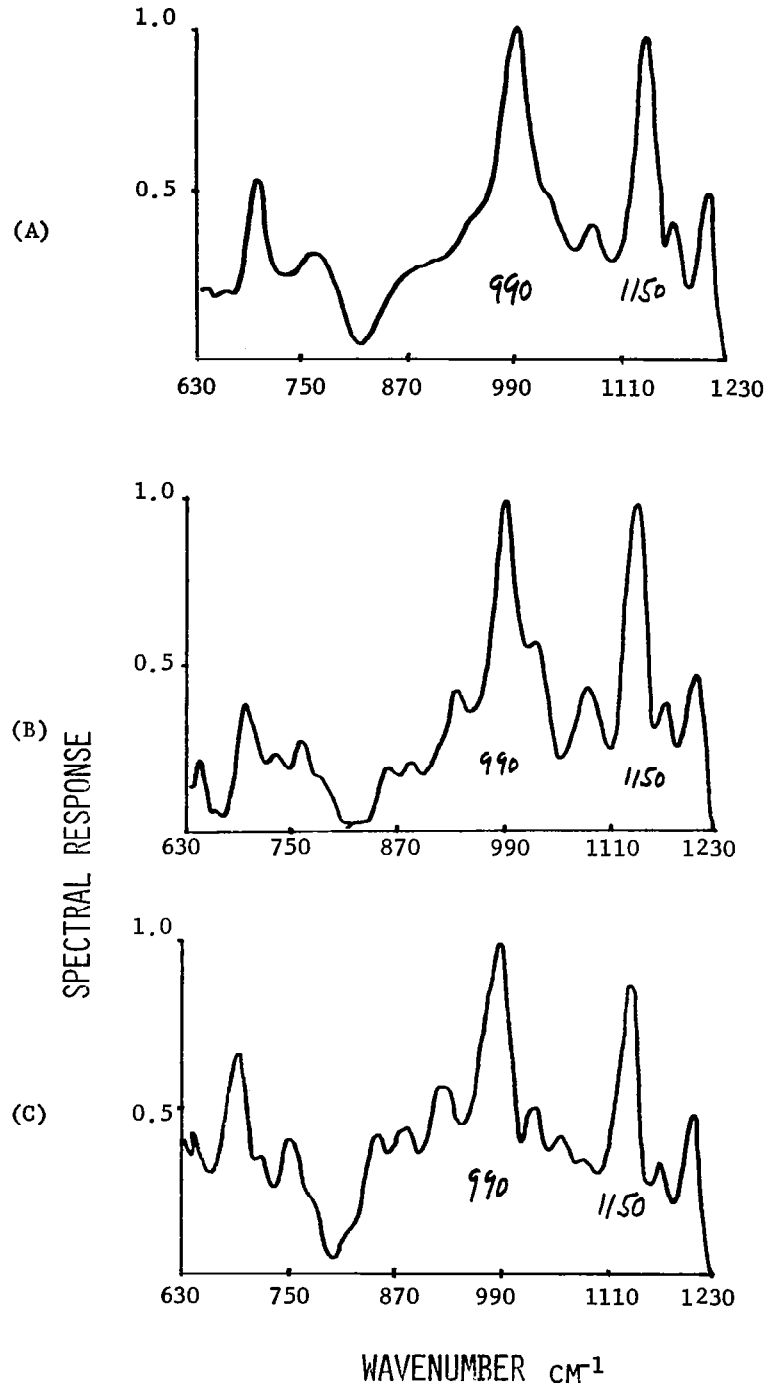

Figure 28 Infrared emission spectra (630 - 1230 cm^{-1}) of 5P4E polyphenyl ether (stainless steel ball, 0.6 m/s, 700 MPa)

(A) not polarized
(B) polarized along the conjunction line
(C) polarized normal to the conjunction line

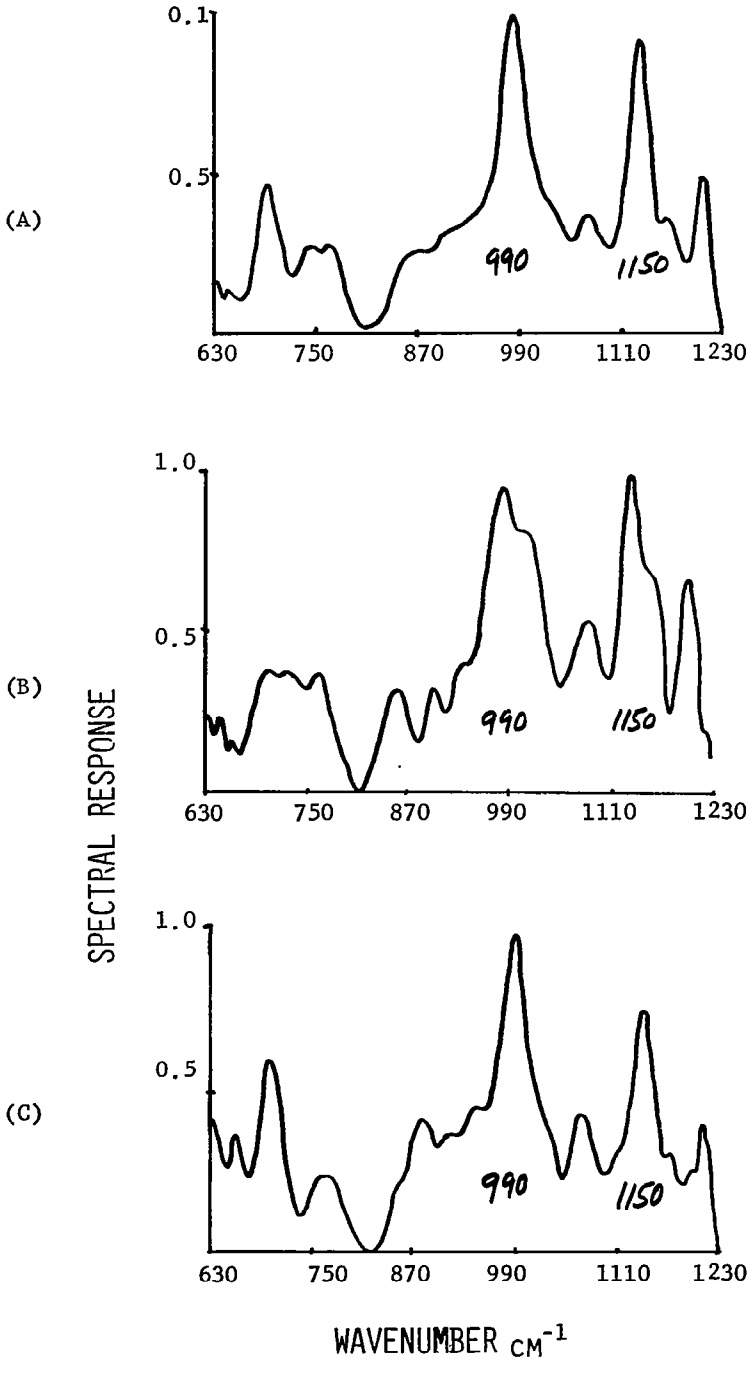

Figure 29 Infrared emission spectra (630 - 1230 cm^{-1}) of 5P4E polyphenyl ether containing 3% of trichloroethane (stainless steel ball, 0.6 m/s, 700 MPa)

(A) not polarized
(B) polarized along the conjunction line
(C) polarized normal to the conjunction line

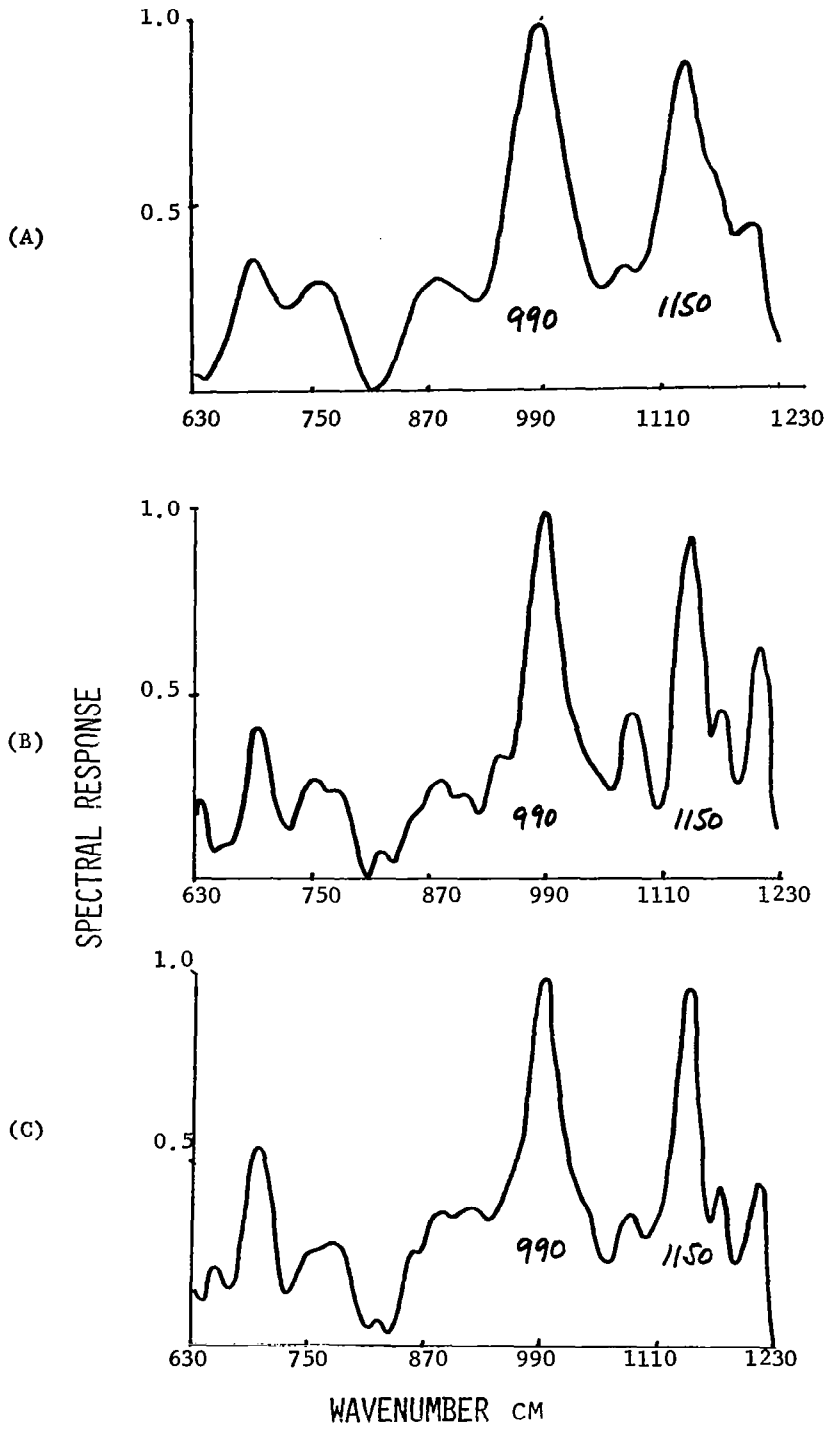

Figure 30 Infrared emission spectra (630 - 1230 cm^{-1}) of 5P4E polyphenyl ether (stainless steel ball, 0.6 m/s, 500 MPa)

(A) not polarized
(B) polarized along the conjunction line
(C) polarized normal to the conjunction line

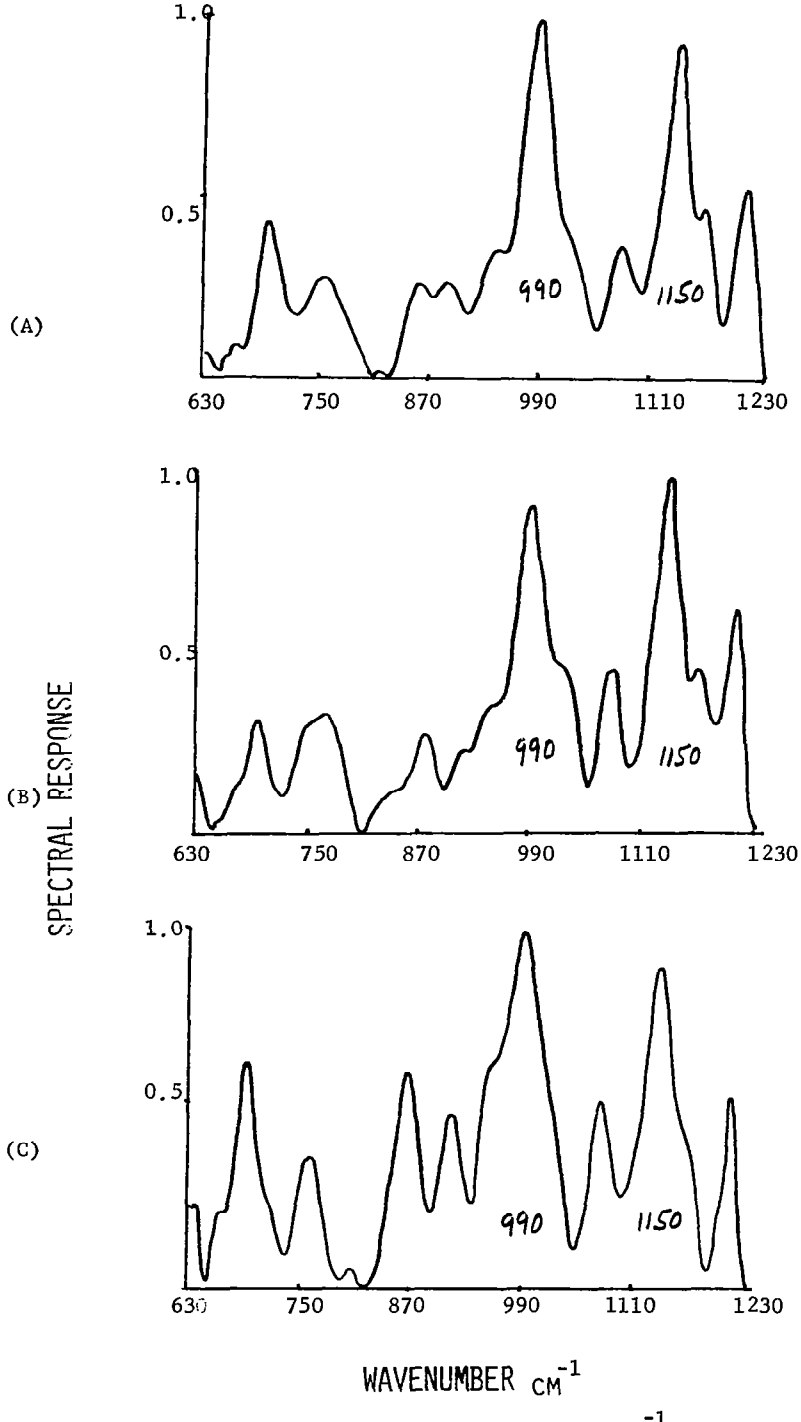

Figure 31 Infrared emission spectra (630 - 1230 cm^{-1}) of 5P4E polyphenyl ether containing 3% of trichloroethane (stainless steel ball, 0.6 m/s, 500 MPa)

(A) not polarized
(B) polarized along the conjunction line
(C) polarized normal to the conjunction line

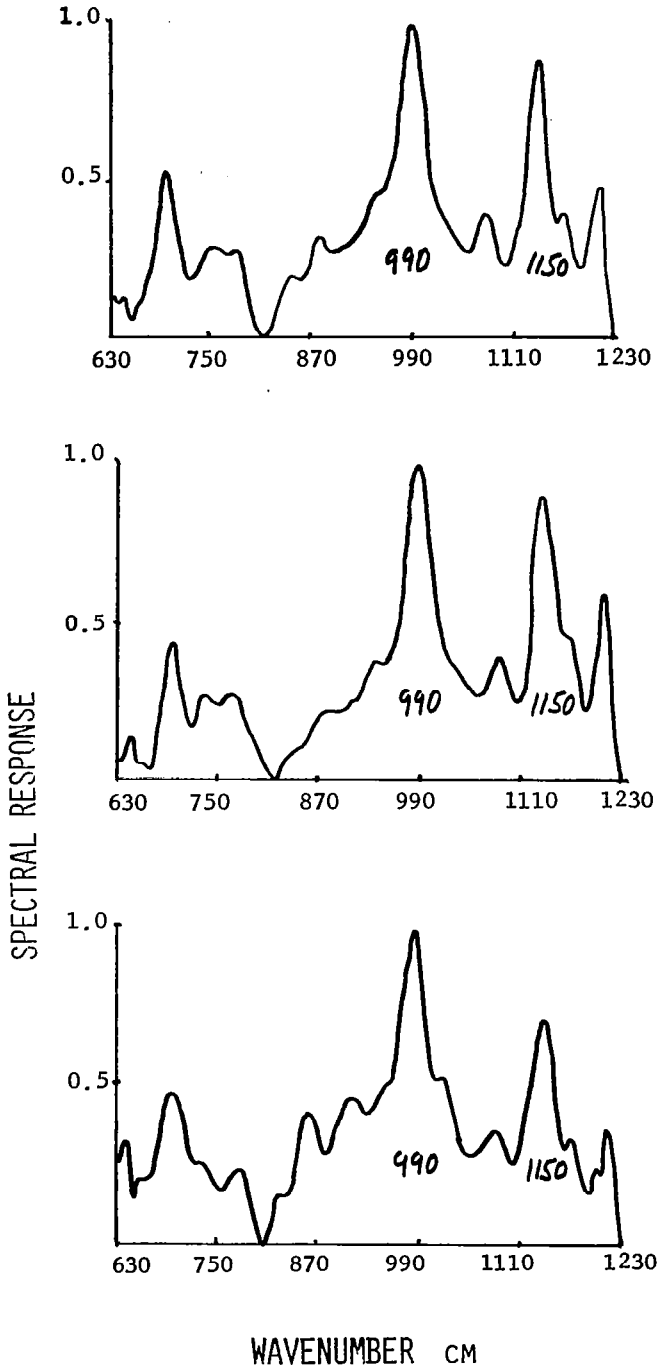

Figure 32 Infrared emission spectra (630 - 1230 cm^{-1}) of 5P4E polyphenyl ether containing 3% of trichloroethane (stainless steel ball, 0.2 m/s, 700 MPa)

(A) not polarized
(B) polarized along the conjunction line
(C) polarized normal to the conjunction line

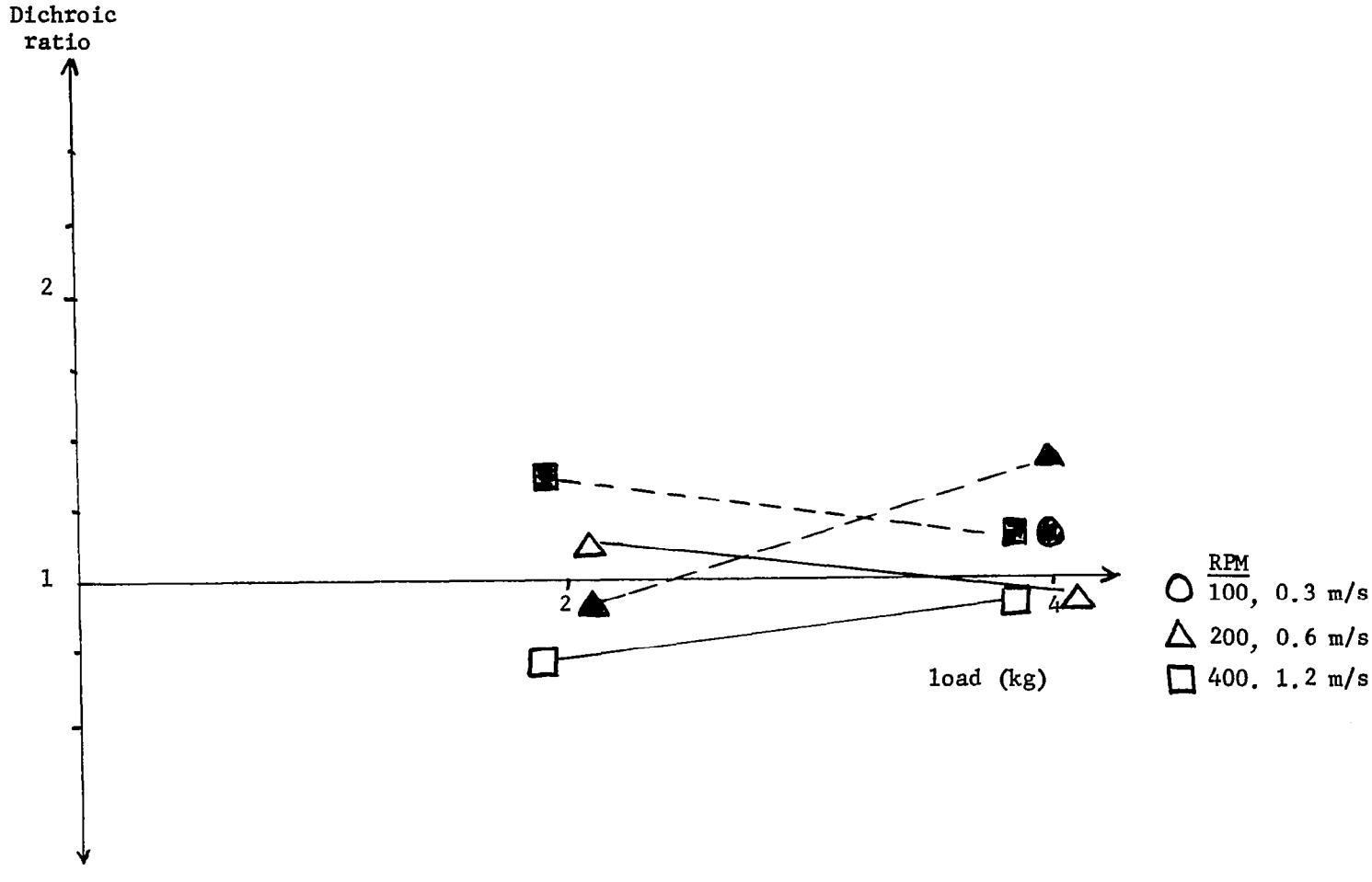

Figure 33 Dichroic ratio of the 990 cm^{-1} emission band in the EHD spectrum of 5P4E polyphenyl ether as a function of load, when a stainless steel ball was used.

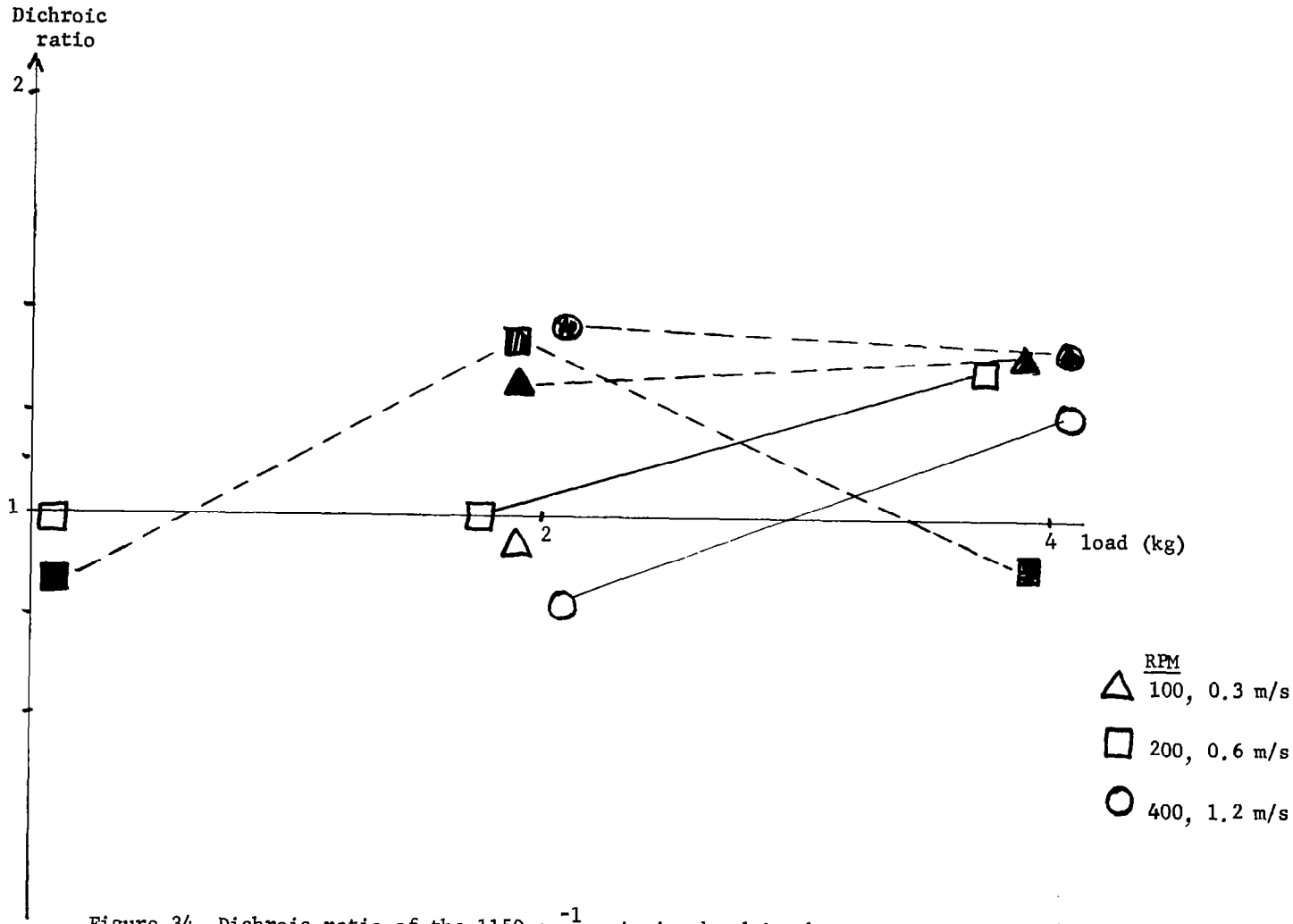

Figure 34 Dichroic ratio of the 1150 cm^{-1} emission band in the EHD spectrum of 5P4E polyphenyl ether as a function of load, when a stainless steel ball was used.

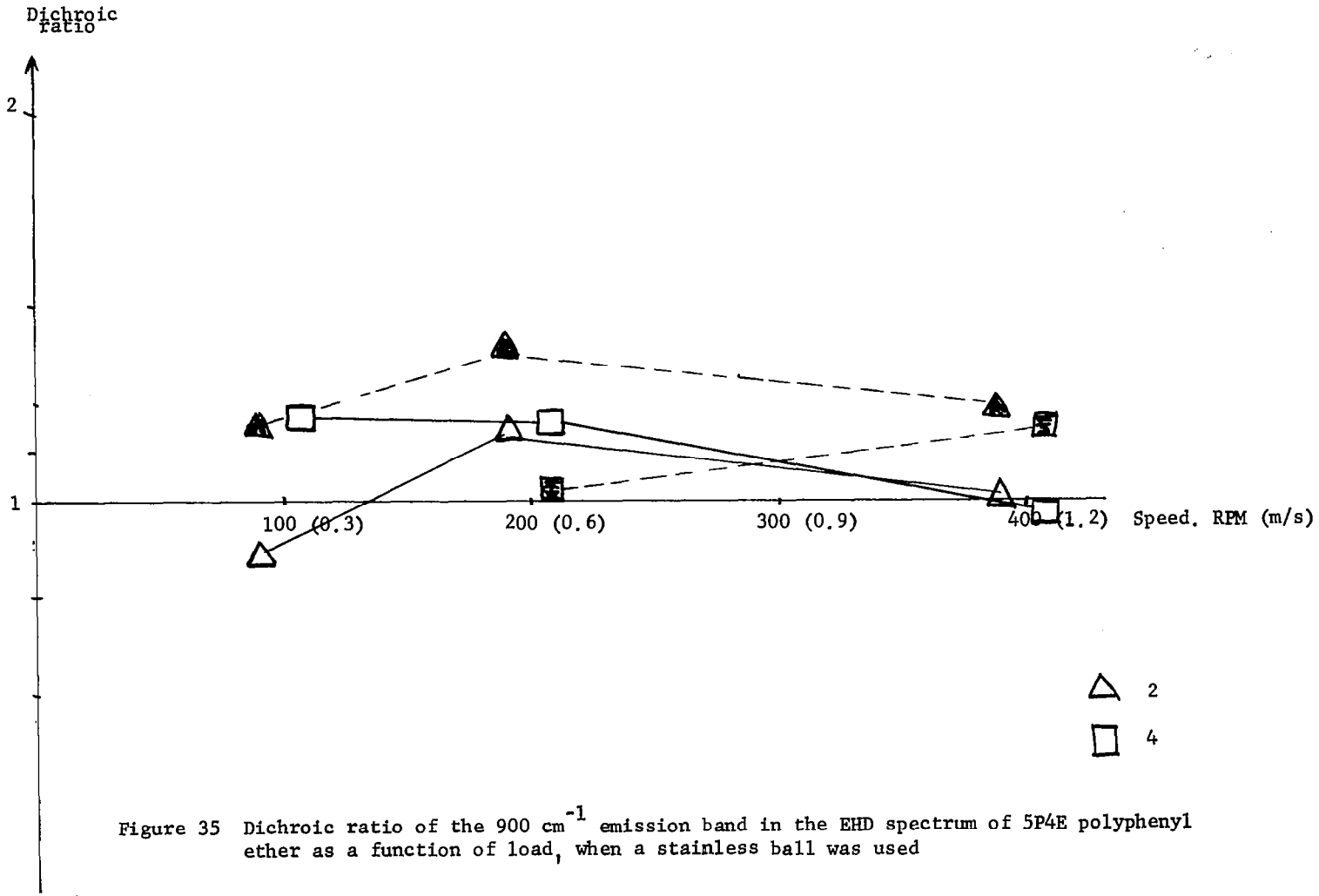

Figure 35 Dichroic ratio of the 900 cm^{-1} emission band in the EHD spectrum of 5P4E polyphenyl ether as a function of load, when a stainless ball was used

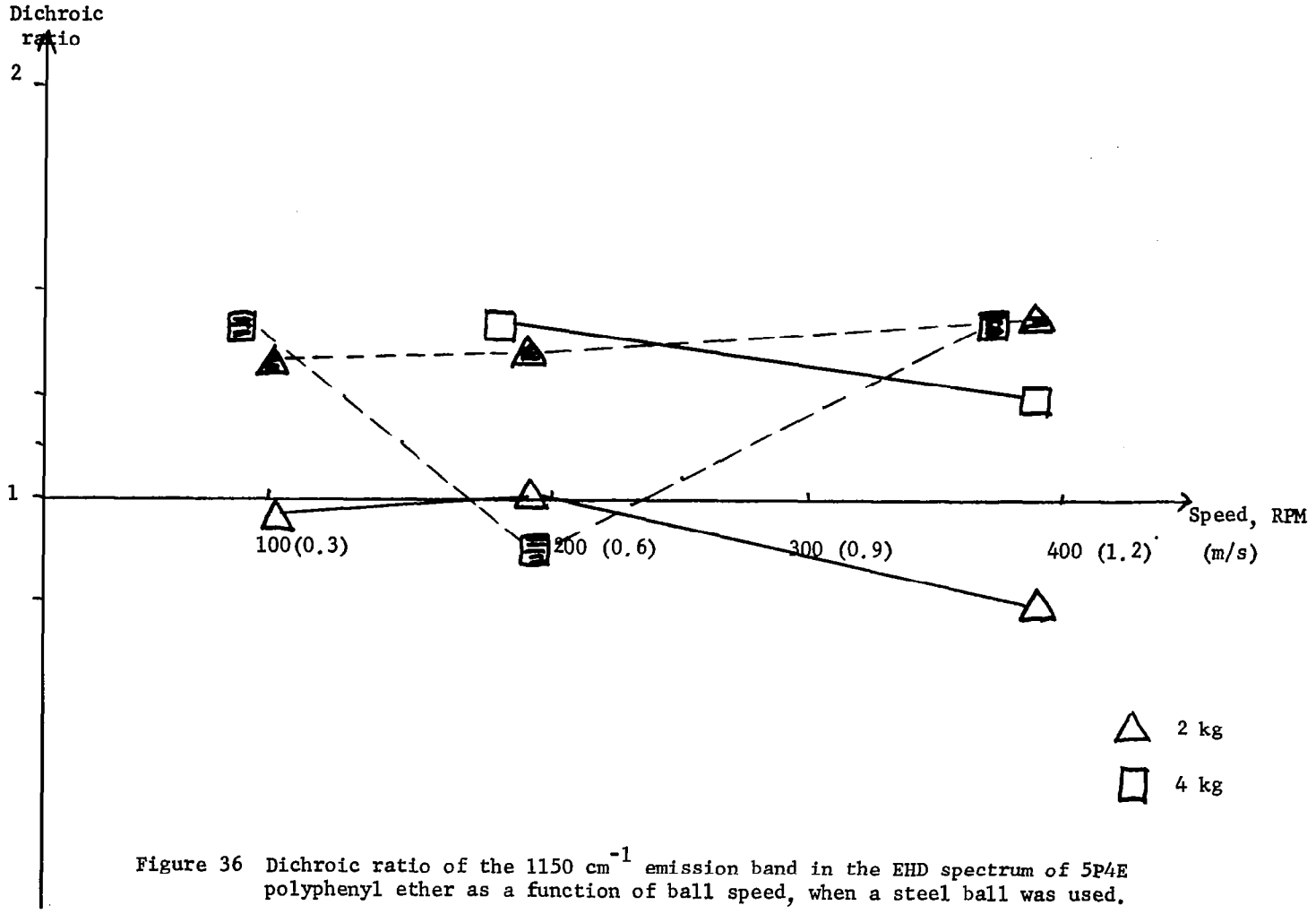

Figure 36 Dichroic ratio of the 1150 cm^{-1} emission band in the EHD spectrum of 5P4E polyphenyl ether as a function of ball speed, when a steel ball was used.

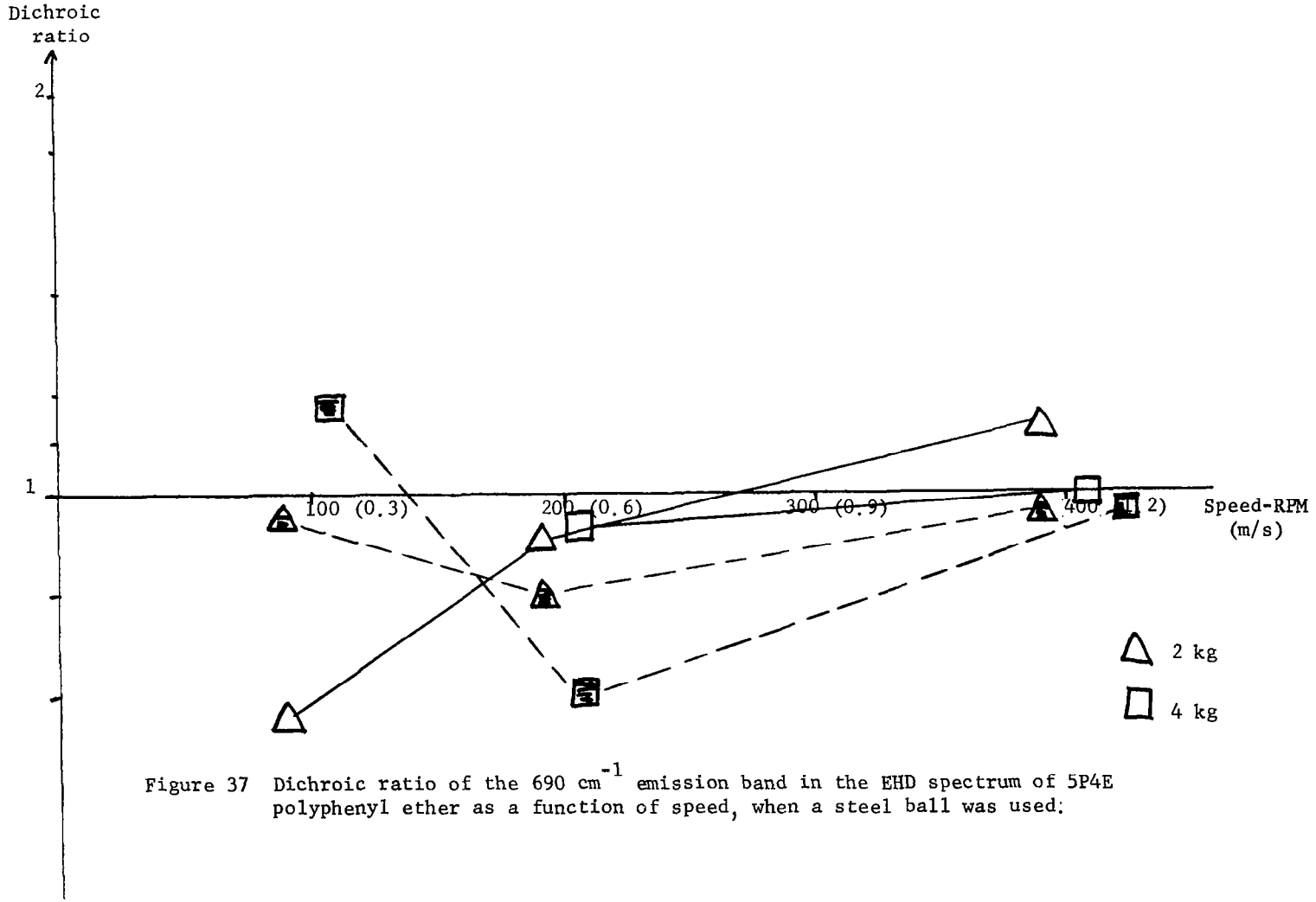

Figure 37 Dichroic ratio of the 690 cm^{-1} emission band in the EHD spectrum of 5P4E polyphenyl ether as a function of speed, when a steel ball was used.

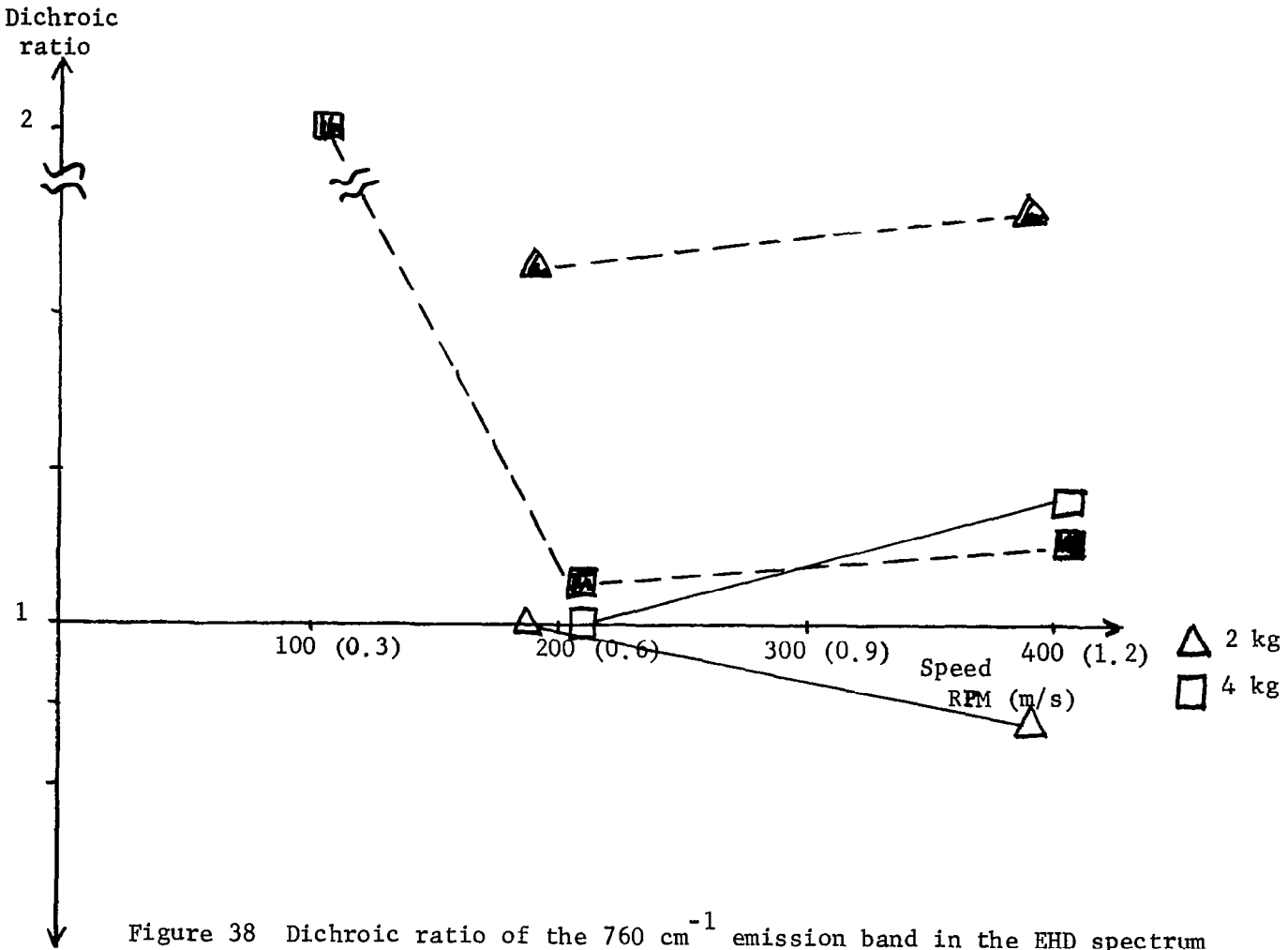

Figure 38 Dichroic ratio of the 760 cm^{-1} emission band in the EHD spectrum of 5P4E polyphenyl ether as a function of ball speed, when a steel ball was used.

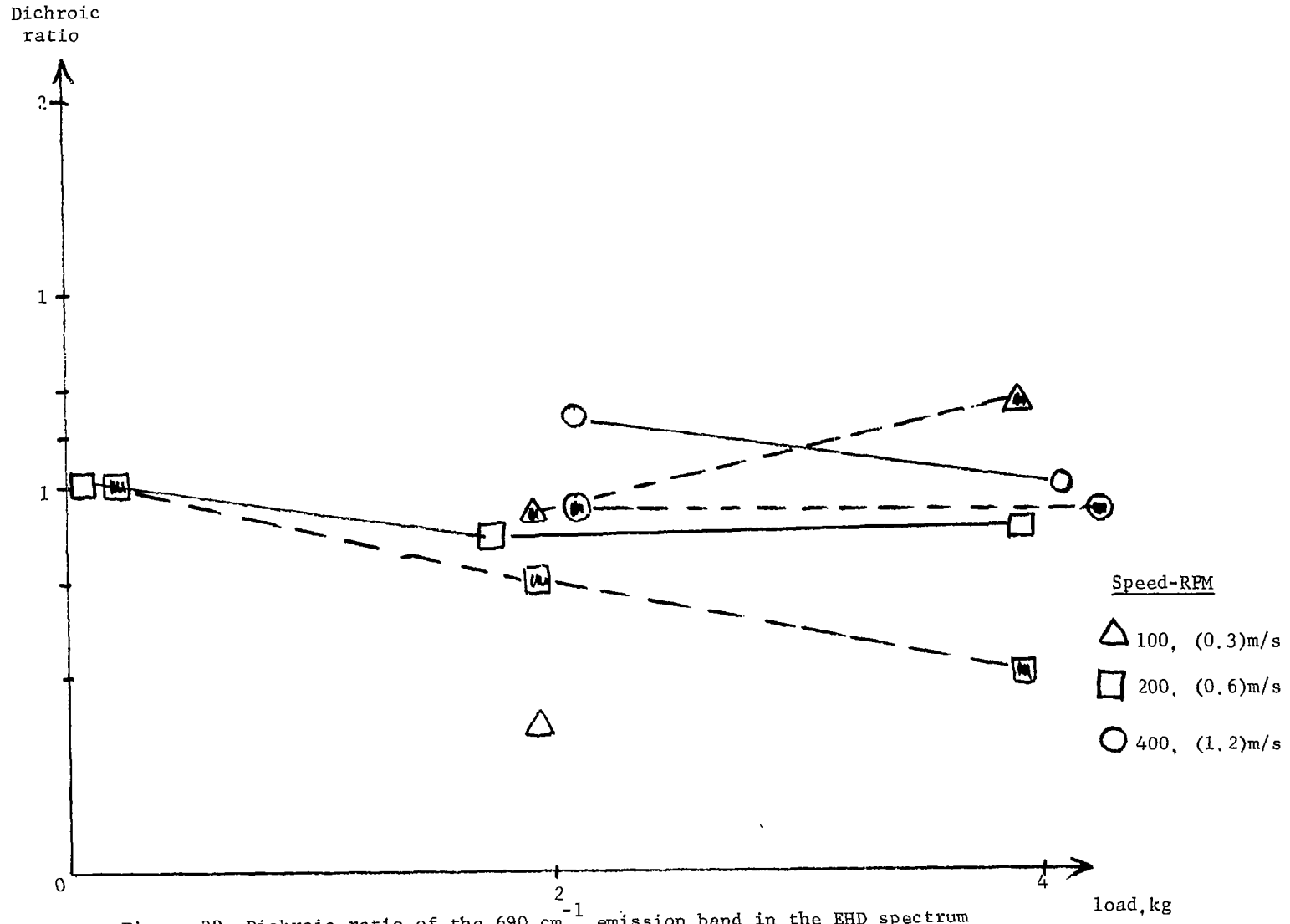

Figure 39 Dichroic ratio of the 690 cm^{-1} emission band in the EHD spectrum of 5P4E polyphenyl ether as function of load, when a steel ball was used.

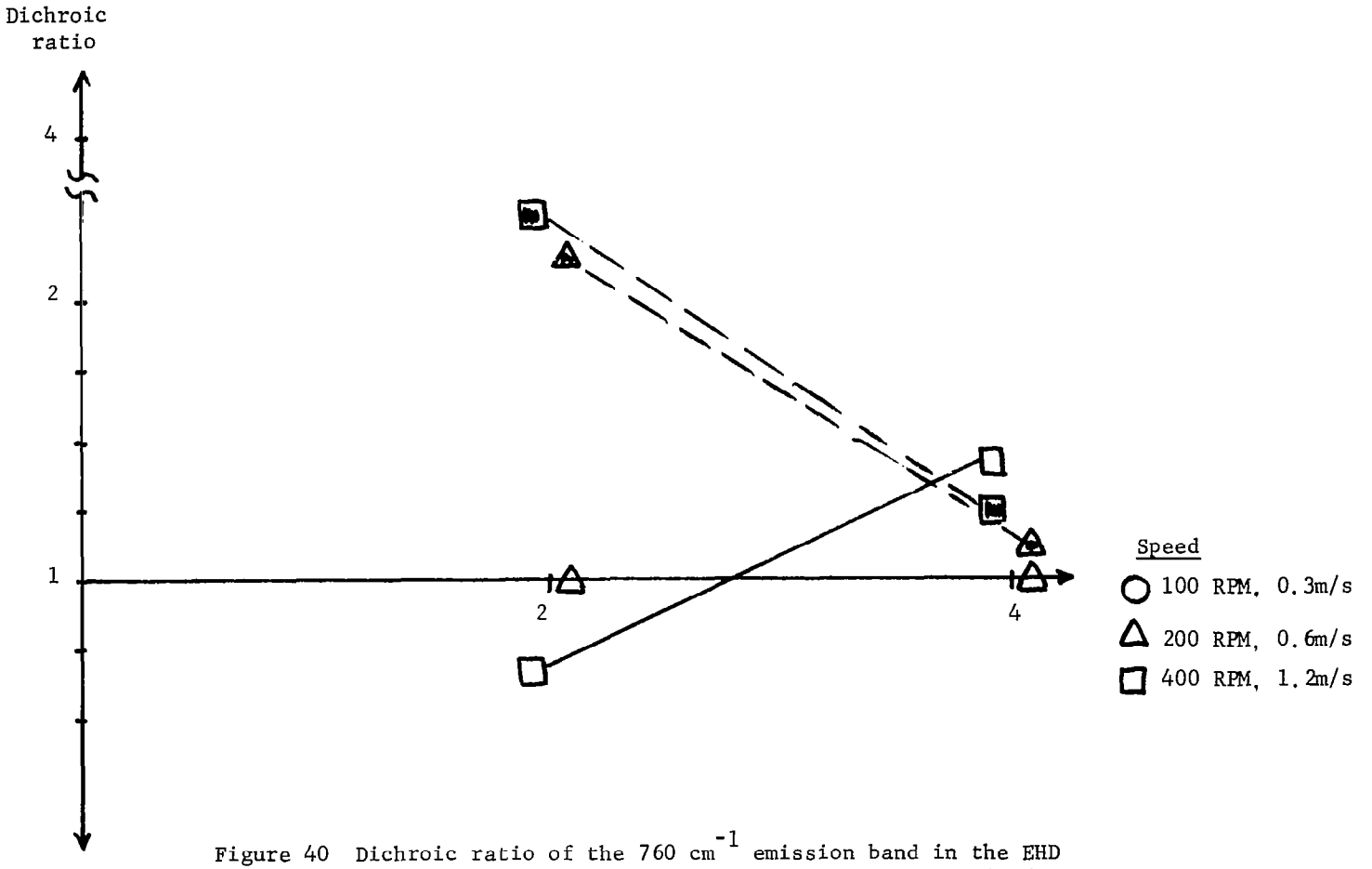

Figure 40 Dichroic ratio of the 760 cm^{-1} emission band in the EHD spectrum of 5P4E polyphenyl ether as function of load, when a steel ball was used.

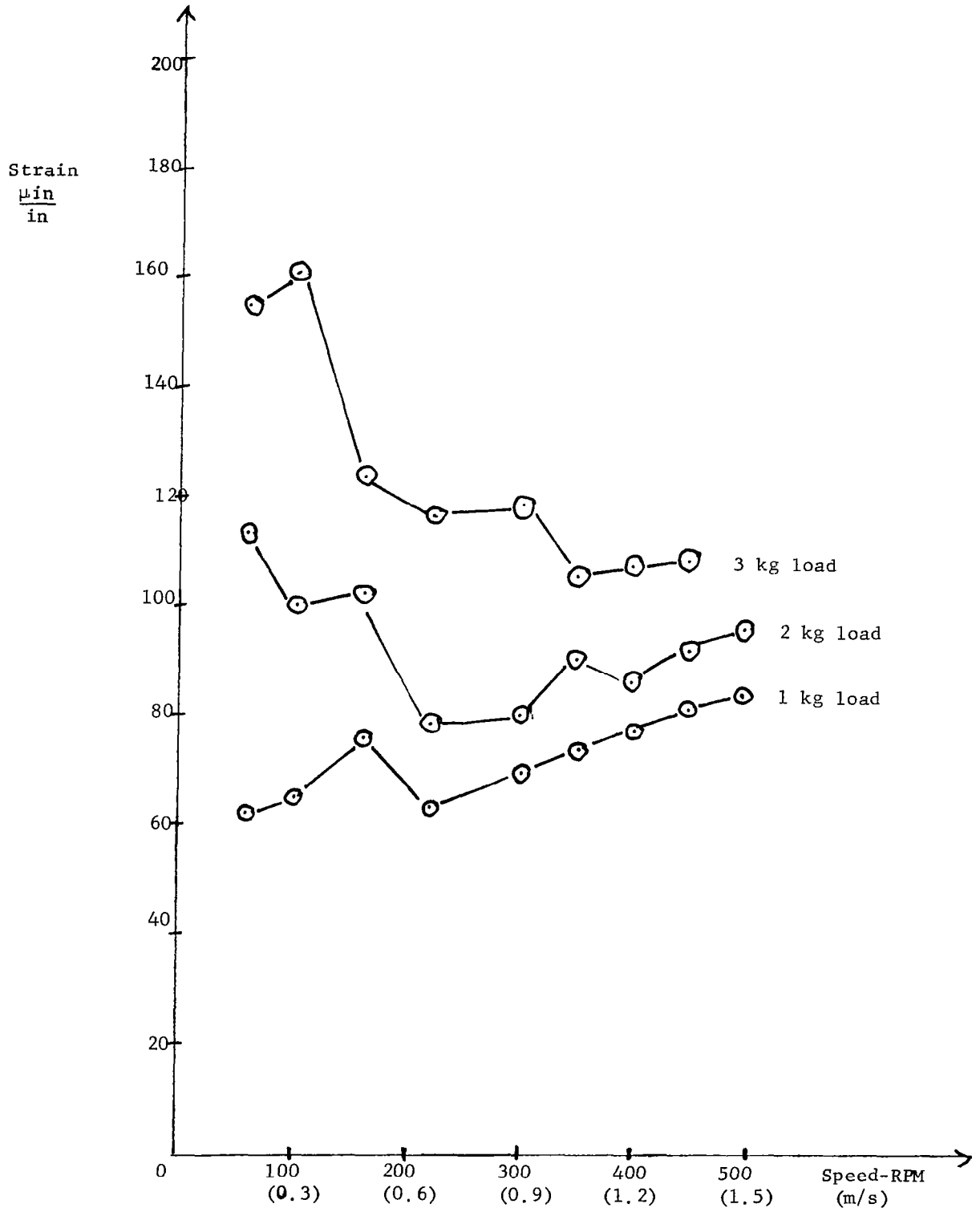

Figure 41 Traction of 5P4E polyphenyl ether at 18°C

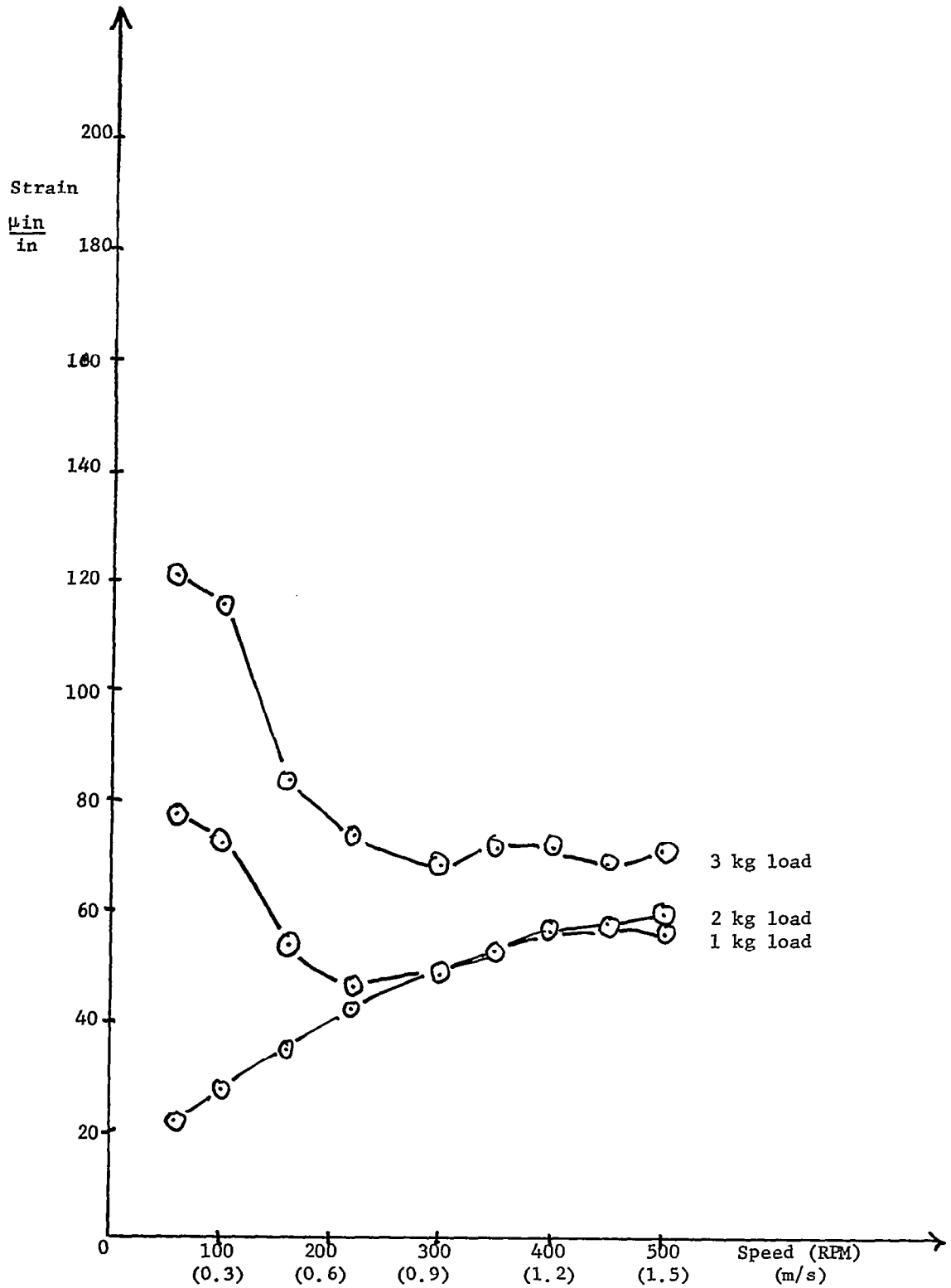

Figure 42 Traction of 5P4E polyphenyl ether containing 3% of trichloroethane at 18°C

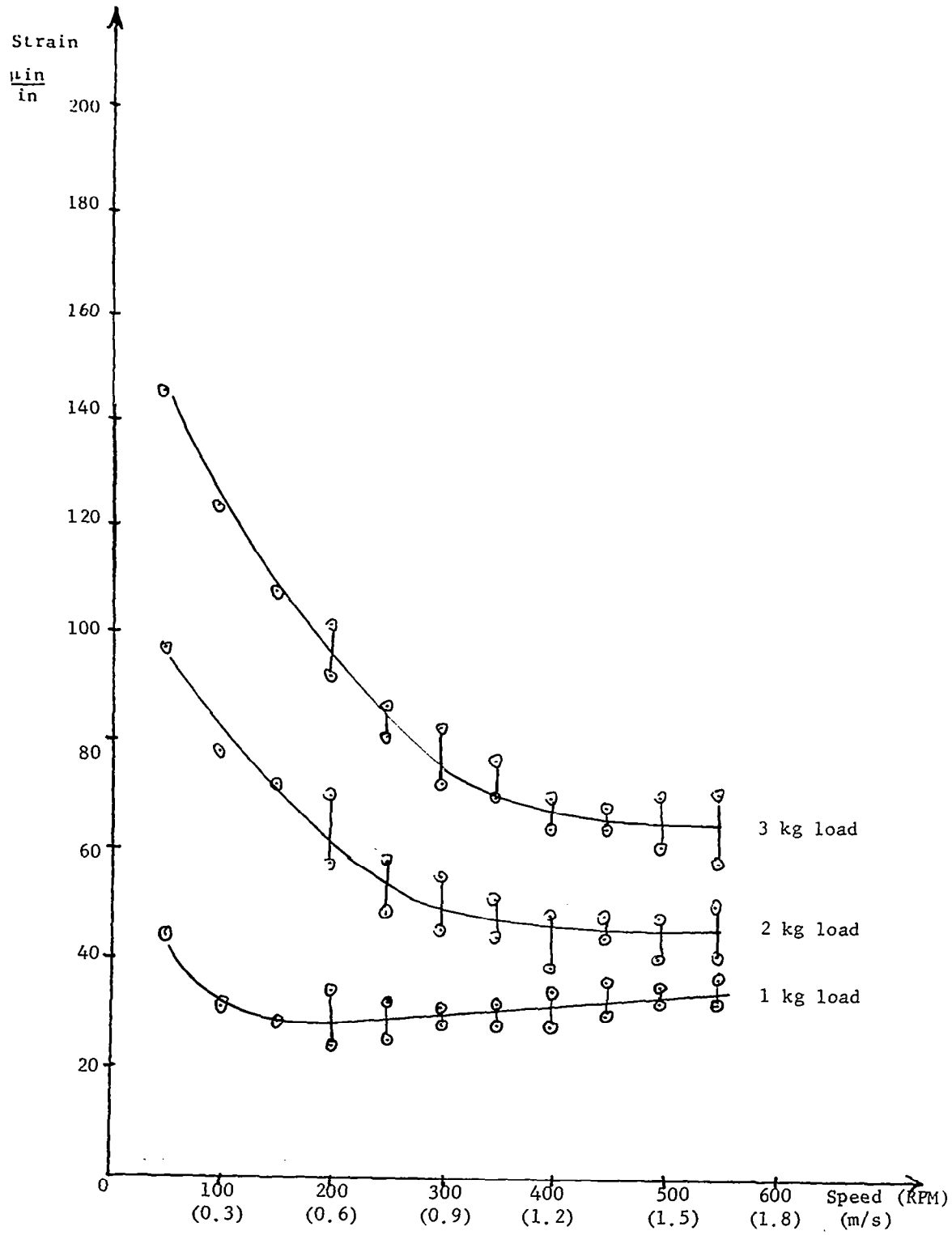

Figure 43 Traction of 5P4E polyphenyl ether at 50°C

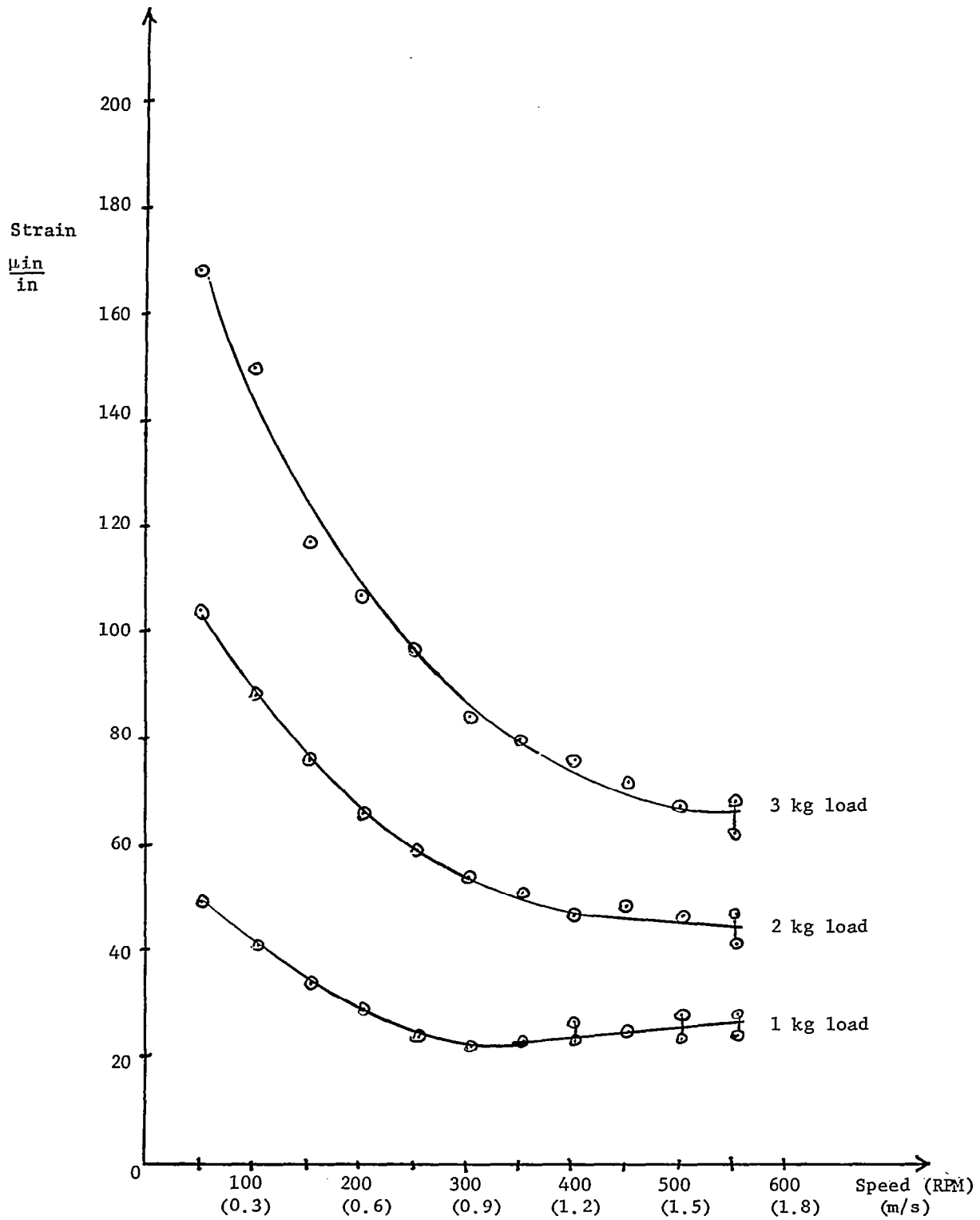

Figure 44 Traction of 5P4E polyphenyl ether containing 3% of trichloroethane at 50°C

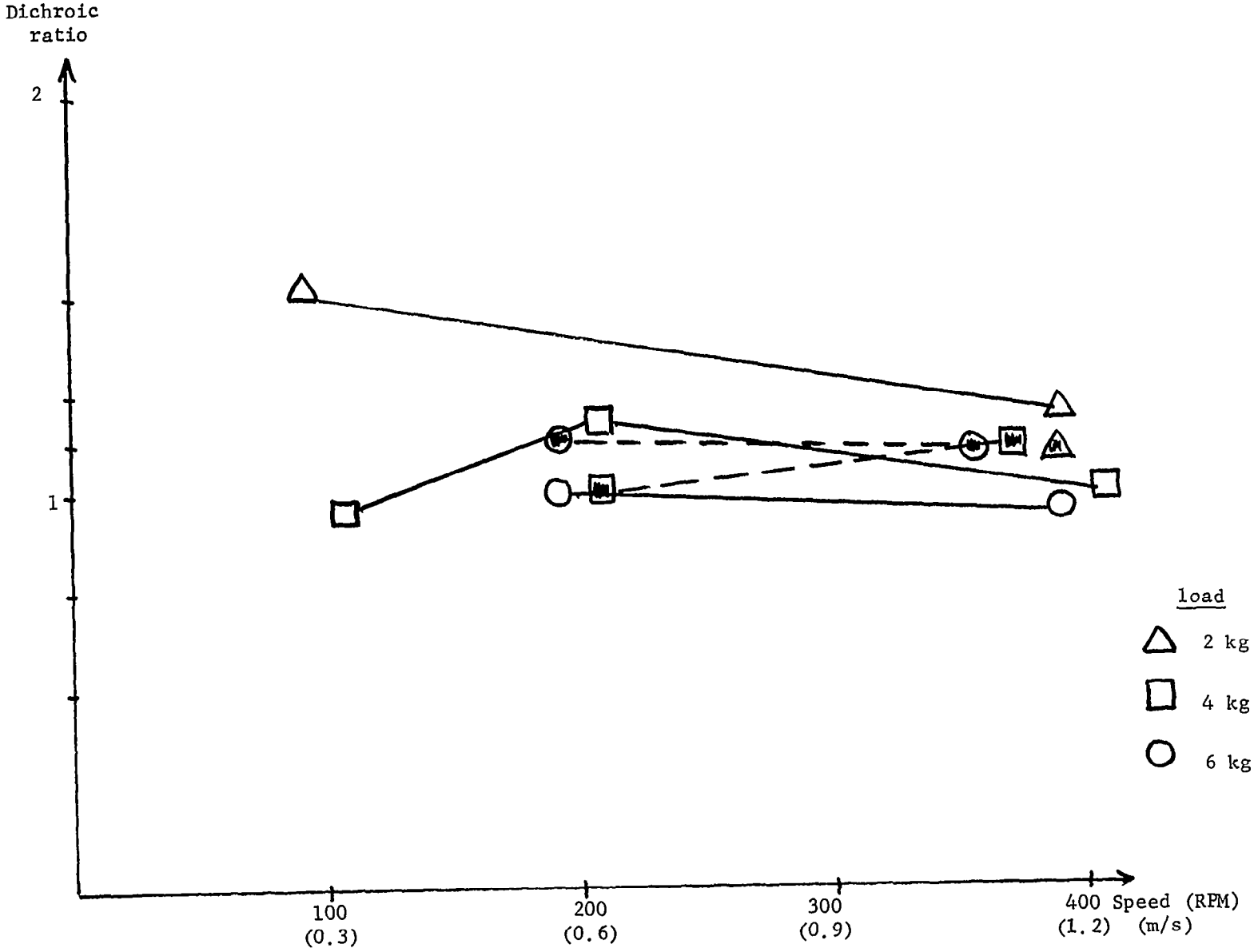

Figure 45 Dichroic ratio of the 690 cm^{-1} emission band in the EHD spectrum of 5P4E polyphenyl ether as a function of speed, when a bronze ball was used.

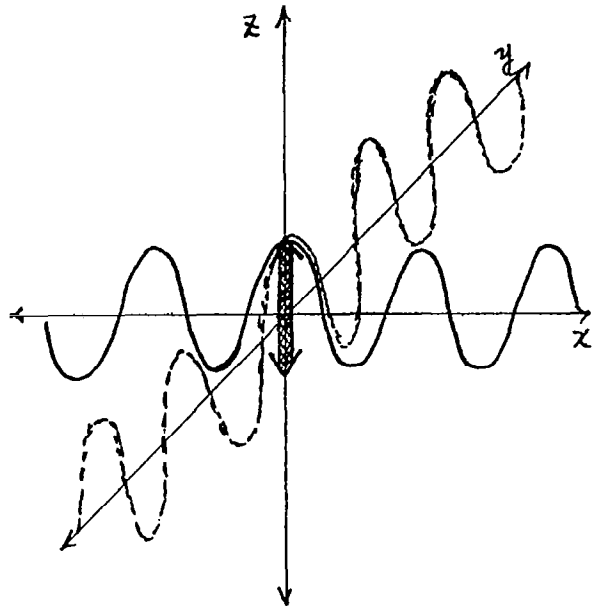

Figure 46 Generation of infrared waves by an oscillating dipole along the z-axis.

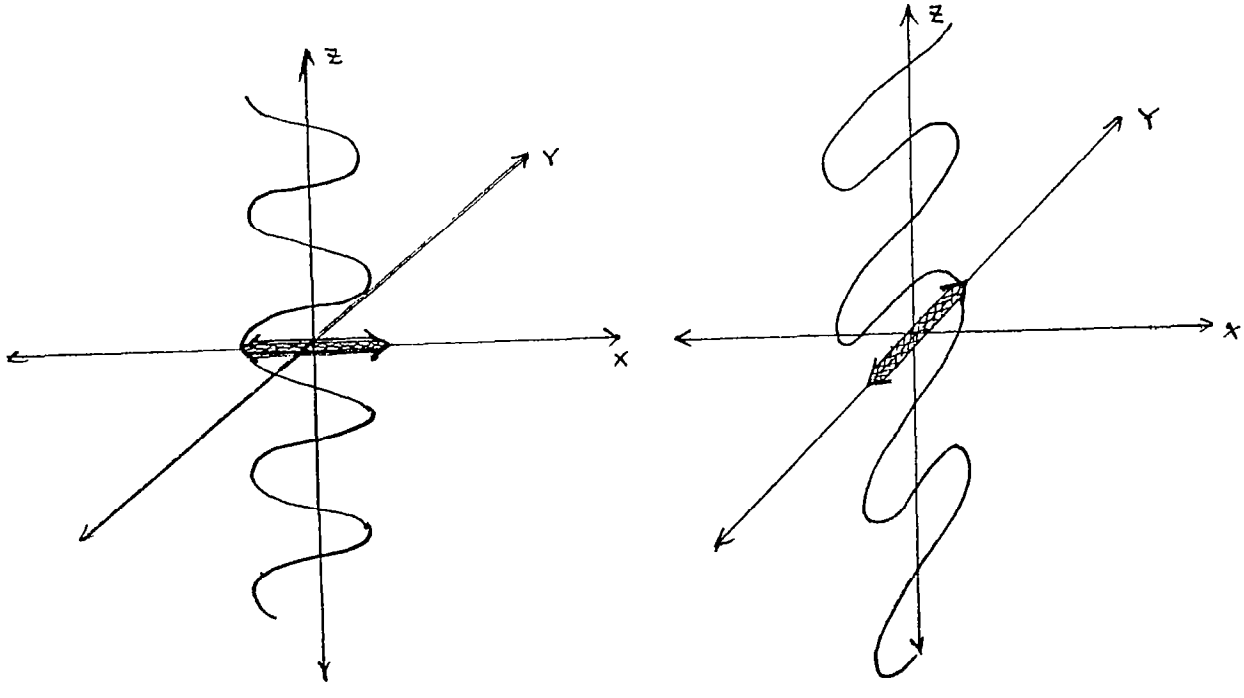

Figure 47 Generation of infrared waves by an oscillating dipole along the x and y axes.

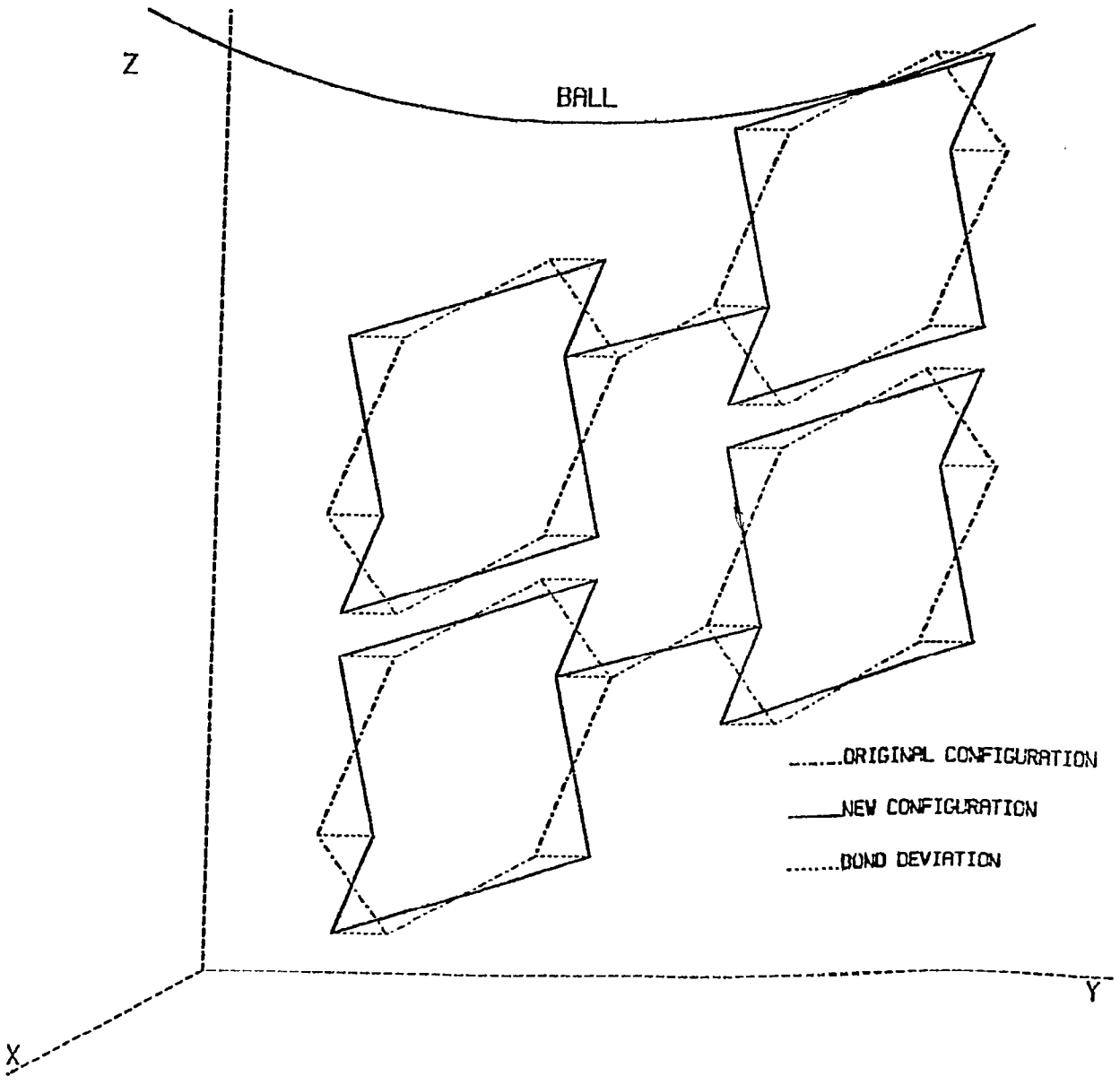

Figure 48 Model of a diphenyl vibrating in the ring-puckering mode, generating a varying dipole moment normal to the phenyl ring plane and to the ball and window surfaces of a ball/plate contact

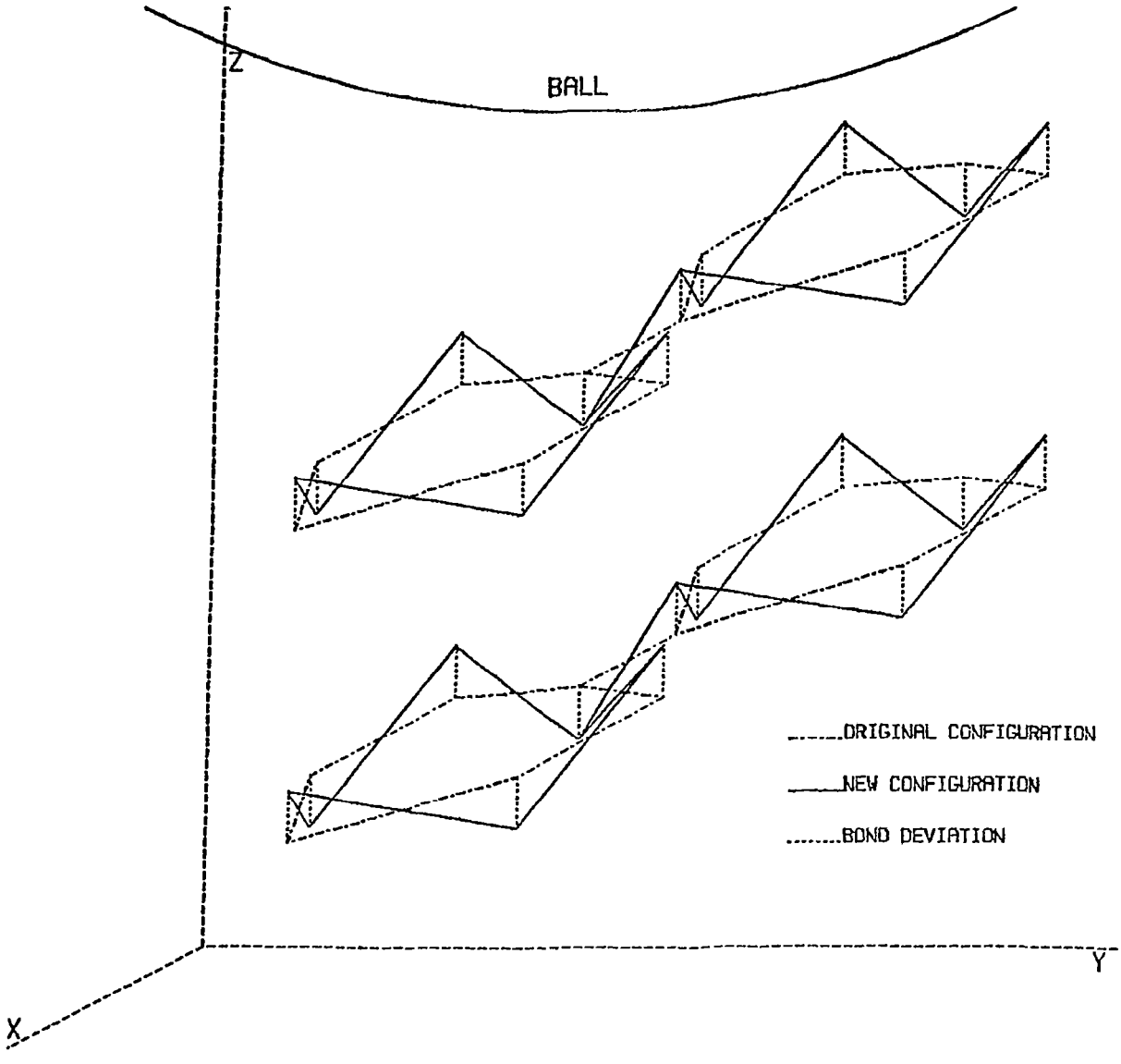

Figure 49 Model of diphenyl vibrating in the ring-puckering mode, generating a varying dipole moment normal to phenyl ring plane and parallel to the ball and window surfaces of a ball/plate contact

1. Report No.	2. Government Accession No.	3. Recipient's Catalog No.
NASA CR-3402		

4. Title and Subtitle	5. Report Date
DETERMINATION OF PHYSICAL AND CHEMICAL STATES OF LUBRICANTS IN CONCENTRATED CONTACTS - PART 2	February 1981
	6. Performing Organization Code

7. Author(s)	8. Performing Organization Report No.
James L. Lauer	None
	10. Work Unit No.

9. Performing Organization Name and Address	11. Contract or Grant No.
Rensselaer Polytechnic Institute Department of Mechanical Engineering Troy, New York 12181	NSG-3170
	13. Type of Report and Period Covered
12. Sponsoring Agency Name and Address	Contractor Report
National Aeronautics and Space Administration Washington, D.C. 20546	14. Sponsoring Agency Code 506-53-22

15. Supplementary Notes

Final report. Project Manager, William R. Jones, Jr., Structures and Mechanical Technologies Division, NASA Lewis Research Center, Cleveland, Ohio 44135.

16. Abstract

Infrared emission spectroscopy through a window in an operating bearing continued to provide most of the information gathered on the state of lubricants subjected to elastohydrodynamic (EHD) conditions. Other measurements were traction, scanning electron microscopy and elemental surface analysis by X-rays. A very significant finding was the decomposition of a naphthenic oil lubricant in the presence of small concentrations of an organic chloride. Olefins and aromatics were formed in ever increasing amounts prior to total lubricant failure. An aromatic fluid also failed in the presence of chloride. A correlation was found between changes of the alignment of lubricant molecules evidenced by infrared polarization and changes of traction under varying EHD stresses.

17. Key Words (Suggested by Author(s))	18. Distribution Statement
Fourier transform spectroscopy Elastohydrodynamics Lubricant degradation Traction	Unclassified - unlimited STAR Category 27

19. Security Classif. (of this report)	20. Security Classif. (of this page)	21. No. of Pages	22. Price*
Unclassified	Unclassified	89	A02

* For sale by the National Technical Information Service, Springfield, Virginia 22161

NASA-Langley, 1981